This is to certify that the

thesis entitled

Prostaglandin Metabolism and Function in Canine
Cortical Collecting Tubule Cells Isolated
Using a Monoclonal Antibody

presented by

Arlyn Garcia-Perez

has been accepted towards fulfillment
of the requirements for

___Ph.D.___ degree in __Biochemistry__

William L. Smith

Major professor
Dr. William L. Smith

Date___May 11, 1984___

PROSTAGLANDIN METABOLISM AND FUNCTION IN CANINE CORTICAL

COLLECTING TUBULE CELLS ISOLATED USING A MONOCLONAL ANTIBODY

By

Arlyn Garcia-Perez

A DISSERTATION

Submitted to
Michigan State University
in partial fulfillment of the requirements
for the degree of

DOCTOR OF PHILOSOPHY

Department of Biochemistry

1984

ABSTRACT

PROSTAGLANDIN METABOLISM AND FUNCTION IN CANINE CORTICAL
COLLECTING TUBULE CELLS ISOLATED USING A MONOCLONAL ANTIBODY

By

Arlyn Garcia-Perez

A hybridoma line (cct-1) secreting a rat immunoglobulin (Ig)
IgG_{2c} that reacts with an ecto-antigen of the canine renal
collecting tubule was selected and cloned. Plastic culture dishes
coated with the purified monoclonal antibody were routinely used to
adsorb 10^7 collecting tubule cells from a mixture of 10^9 renal
cortical cells prepared by treatment of the canine renal cortex with
collagenase. Primary, monolayer cultures of canine cortical collecting
tubule (CCCT) cells were established from the absorbed cells. These
cells exhibited many of the morphological and biochemical properties of
collecting tubule cells in situ. CCCT cells also formed immunoreactive
PGE_2 in response to bradykinin, (Asu[1,6], Arg[8]) vasopressin
(DD-AVP) and AVP.

Confluent monolayers of CCCT cells seeded on Millipore filters
showed characteristics of asymmetry seen with intact collecting
tubules. These monolayers were used in studies designed to determine
if there is an apical-basolateral asymmetry to the release of

prostaglandins by or to the biochemical effects of prostaglandins on the renal collecting tubule.

Although AVP caused cAMP release only when added to the basolateral side of CCCT cells, AVP caused the release of PGE_2 when added to either the apical or basolateral surface. Bradykinin caused PGE_2 release only when added to the apical surface of CCCT cells. PGE_2 was released in comparable amounts on each side of the monolayer in response both to AVP and to bradykinin.

High concentrations ($\geq 10^{-8}$ $\underline{M}$) of PGE_2 added to either side of the monolayer caused the release of cAMP. However, at concentrations (10^{-10}-10^{-12} $\underline{M}$) at which PGE_2 had no independent effect on cAMP release, PGE_2 inhibited the release of cAMP normally occurring in response to AVP. This inhibition occurred with PGE_2 added to either the apical or basolateral surface of the CCCT cell monolayer. PGE_2 (10^{-11} $\underline{M}$) also inhibited the AVP-induced accumulation of intracellular cAMP by CCCT cells seeded on culture dishes. This inhibition was only observed when the cells were preincubated with $PGE_2 \geq 20$ min. The results presented are consistent with the concept that inhibition by prostaglandins of the hydroosmotic effect of AVP is due to inhibition of AVP-induced cAMP production.

A MAMI, PAPI Y EVELYN, POR CREER

iii

ACKNOWLEDGEMENTS

I thank Dr. William L. Smith, advocatus diaboli per excellentia,
for his continued professional guidance and financial support. Most
importantly, I am grateful to him for relentlessly endeavoring to
instill in me the value of the persistent pursuit of excellence.

I thank the members of my guidance committee, Drs. William S.
Spielman, John L. Wang, J. Throck Watson, and William W. Wells, for
their demonstrated interest in this research project and their sincere
encouragement throughout it.

Jeffrey Day, Frank Grenier, Sherry Huey, Yasuhito Tanaka and
Tsuyoshi Watanabe merit individual kudos. They made my experience in
the lab not only intellectually rewarding, but also emotionally
sustaining.

Particular thanks go to my sisters, Maria de Lourdes
Suarez-Villafane and Carol J. Fiol-Lay, who began this voyage with me,
for their constant fidelity and selfless endorsement of all my
enterprises, however impetuous in nature.

I thank my special friends, los verdaderos, los de siempre:
Joaquin Vila-Barreto, Robert Swift, Shawn Farrell, Marco Villanueva,
Theresa Fillwock, Susan Uselton, John Burczak and Paul Boyer. Each one
in their unique style invariably managed to bring out the best in me,
even during the worst of times.

I thank my favorite secretarial staff, especially Betty Brazier, Julie Doll, and Mary Dunn. With humor and affection they brightened every working day.

Above all, I thank my family. They have been my inspiration, my refuge, my strength, mi fabrica de ilusiones, the beginning and end of my own rainbow.

COPYRIGHT ACKNOWLEDGEMENTS

TABLE OF CONTENTS

Page

LIST OF FIGURES

NOMENCLATURE AND ABBREVIATIONS

A terminological convention should be noted. In absorptive
epithelia (e.g., the renal tubule), the basolateral surface of the
cells corresponds to the region facing the capillaries. This surface
is also referred to as the blood or serosal side of the tubule. The
apical surface of the cells corresponds to the region where absorption
occurs. This region is the lumen of the renal tubule and is also known
as the urine or mucosal side.

Abbreviations used are: ADH, antidiuretic hormone; AVP, arginine
vasopressin; BK, bradykinin; cAMP, adenosine-3',5'-cyclic
monophosphate; CCCT, canine cortical collecting tubule; DD-AVP,
$(Asu^{1,6}, Arg^8)$ vasopressin or desmopressin acetate; DMEM,
Dulbecco's modified Eagle's medium; IBMX, isobutylmethylxanthine; MDCK,
Madin-Darby canine kidney; PG, prostaglandin, RPCT, renal papillary
collecting tubule.

INTRODUCTION

It has been recognized for almost twenty years that the kidneys synthesize prostaglandins. The different experimental approaches historically utilized to identify the agents involved in the overall function of the kidney have also been used to study renal prostaglandin metabolism. These approaches include: whole animal clearance methods, perfusion of isolated kidneys, "stop flow" and micropuncture techniques, and the use of kidney slices and homogenates (1,2). These procedures have helped to define that prostaglanins are involved in the modulation of a variety of renal functions. However, only after the development by Burg et al. of techniques for perfusing microdissected tubules (3), has it been possible to study the contributions of prostaglandins to individual functions of discrete nephron segments.

Although the microdissection technique has provided valuable information about prostaglandin metabolism in single nephron segments, it is not practical for detailed biochemical analyses. This procedure is laborious and yields segments only 1-2 mm in length (approximately 10^3 cells). Hundreds of dissected tubules (10^6 cells) would be required to make biochemical measurements (e.g., PGE_2 and cAMP radioimmunoassays) which can be readily performed with cultured cells using one semi-confluent 24-well dish. This problem has been partially circumvented by the development of renal cell lines such as Madin-Darby canine kidney (MDCK) cells (4-6) and LLC-PK$_1$ (7,8), which are

1

apparently derived from the distal and proximal tubules, respectively. These cells retain many, but not all, of the properties of the parent cells. Consequently, it has become important to prepare homogeneous cell populations from different parts of the renal tubule which can be grown and manipulated in monolayer culture in a differentiated state.

Interest in our laboratory in studying prostaglandin metabolism in isolated collecting tubule cells first arose when Smith et al. immunohistochemically localized the prostaglandin-forming enzyme, PGH synthase, in the kidney (9,10). The collecting tubule was the only tubular segment that stained for this enzyme. This observation, in conjunction with the report by Grantham et al. that PGE_1 inhibited the hydroosmotic effect of antidiuretic hormone (ADH) in perfused, microdissected cortical collecting tubules (11), suggested an important role for prostaglandins in the regulation of collecting tubule function. Suspensions and cultures of cells enriched in rabbit papillary collecting tubule (RPCT) cells were subsequently isolated and studied by Grenier et al. in our laboratory (12-14). Although these studies contributed to our understanding of prostaglandin metabolism in the papillary collecting tubule, RPCT cells did not form prostaglandins in response to AVP. Moreover, prostaglandins did not inhibit AVP-induced cAMP accumulation.

The procedure used to isolate RPCT cells (hypotonic lysis of other cells present) could not be used to obtain other tubular cell types in which prostaglandins may play a role. This was especially true of cells present in the cortex, which contains 4-5 different tubular cell types. Therefore, it was necessary to develop a simple and convenient procedure for the selective isolation of homogeneous populations of

renal tubular cells that could be grown and manipulated in monolayer culture. The approach chosen for this undertaking was the development of monoclonal antibodies that interact with cell surface determinants on specific renal tubular cells and the subsequent isolation of cells by immunoaffinity techniques. The isolation of canine cortical collecting tubule (CCCT) cells by immunodissection and studies on the prostaglandin metabolism and function of these cells is the subject of this dissertation.

The prostaglandins are a family of [...] in Figure 1. These compounds share a common set of precursors so that the synthetic pathway for each prostaglandin differs only in the final step. The major precursor of prostaglandins in humans is all cis 5,8,11,14-eicosatetraenoic acid or arachidonic acid, which gives rise to prostaglandins containing two carbon-carbon double bonds in their side chains: PGE_2, $PGF_{2\alpha}$, PGD_2, prostacyclin (PGI_2) and thromboxane A_2 (TxA_2). Arachidonic acid can be obtained from meat or is formed by elongation and desaturation of the essential fatty acid, linoleic acid, present in vegetables (15). Arachidonic acid is found primarily esterified at the sn-2 position of cellular phosphoglycerides (16).

Prostaglandin formation can be conveniently discussed in three stages (Figure 1)(17). In the first stage, a stimulus, usually a hormone, interacts with the cell surface to activate phospholipases which catalyze the hydrolysis of arachidonate from phosphoglycerides. The major control point for prostaglandin formation appears to be at this stage of arachidonic acid release, since the concentrations of free arachidonate in cells are normally quite low (<10^-6 M). The reactions involved in the release of arachidonic acid are still subjects of controversy (17,18). Arachidonate release has been

Prostaglandin Biochemistry. Prostaglandins are oxygenated fatty acid derivatives. The pathway for the biosynthesis of prostaglandins is illustrated in Figure 1. These compounds share a common set of precursors so that the synthetic pathway for each prostaglandin differs only in the final step. The major precursor of prostaglandins in humans is all cis 5,8,11,14-eicosatetraenoic acid or arachidonic acid, which gives rise to prostaglandins containing two carbon-carbon double bonds in their side chains: PGE_2, $PGF_{2\alpha}$, PGD_2, prostacyclin (PGI_2) and thromboxane A_2 (TxA_2). Arachidonic acid can be obtained from meat or is formed by elongation and desaturation of the essential fatty acid, linoleic acid, present in vegetables (15). Arachidonic acid is found primarily esterified at the sn-2 position of cellular phosphoglycerides (16).

Prostaglandin formation can be conveniently discussed in three stages (Figure 1)(17). In the first stage, a stimulus, usually a hormone, interacts with the cell surface to activate phospholipases which catalyze the hydrolysis of arachidonate from phosphoglycerides. The major control point for prostaglandin formation appears to be at this stage of arachidonic acid release, since the concentrations of free arachidonate in cells are normally quite low ($<10^{-6}$ M). The reactions involved in the release of arachidonic acid are still subjects of controversy (17,18). Arachidonate release has been

Figure 1. Prostaglandin biosynthetic pathway.

Figure 1

Figure 1. Prostaglandin biosynthetic pathway.

studied most extensively in platelets, which form TxA2 as their major

prostaglandin (17). Arachidonate is released mainly from two

phospholipids, phosphatidylinositol (PI) and phosphatidylcholine (PC).

In the current view of arachidonate ...

phosphatidylinositol (PI)-specific phospholipase C cleaves PI to yield

diglyceride and inositol phosphate ... diglyceride ...

seems to have a dual purpose (27). ... lipase ... hydrolyzes

some diglyceride to yield arachidonate ...

1-stearoyl-2-arachidonyl PI)(28). ... the ... resulting

diglyceride serves to activate a ... protein kinase

C, which in turn activates a phospholipase A2 ... which

cleaves arachidonate from PC (18-29). Phospholipase ...

have been found in cells and tissues that ...

generate TxA2, as platelets, neutrophils, ...

macrophages (2...).

The second step in prostaglandin formation involves the

conversion of arachidonic acid to endoperoxide PGH2 by PGH

synthase. This enzyme was ... first of the ... arachidonate

enzymes to be extensively purified and characterized ... It

catalyzes two distinct and sequential events: ... and

cyclization of arachidonic acid to form ... PGG2, and reduction of

the hydroperoxy group at C-15 of PGG2 to produce ... (30). ...

activity that catalyzes PGG2 formation is commonly referred to as a

cyclooxygenase. It is this activity which is inhibited by nonsteroidal

antiinflammatory drugs like aspirin. The reduction of PGG2 is

catalyzed by a hydroperoxidase activity. Both activities ... (30,32). PGH synthase is membrane-bound (28). ... PGH synthase

Figure 1

studied most extensively in platelets, which form TxA_2 as their major prostaglandin (17). Arachidonate is released mainly from two phospholipids, phosphatidylinositol (PI) and phosphatidylcholine (PC). In the current view of arachidonate release, a cytosolic phosphatidylinositol (PI)-specific phospholipase C cleaves PI to yield diglyceride and inositol phosphate (19-22). The diglyceride formed seems to have a dual purpose. Diglyceride lipase(s) (23,24) hydrolyzes some diglyceride to yield arachidonate (90% of platelets' PI is 1-stearoyl-2-arachidonoyl PI)(25) and a 1-monoglyceride. Remaining diglyceride serves to activate a diglyceride-dependent protein kinase C, which in turn activates a phospholipase A_2 that specifically cleaves arachidonate from PC (26-29). Phospholipase A_2 activities have been found in cells and tissues that are active in prostaglandin generation, such as platelets, neutrophils, fetal membranes and macrophages (27).

The second stage of prostaglandin formation involves the conversion of arachidonic acid to the endoperoxide PGH_2 by PGH synthase. This enzyme was the first of the prostaglandin biosynthetic enzymes to be extensively purified and characterized (30,31). It catalyzes two distinct and sequential events: (a) oxygenative cyclization of arachidonic acid to produce PGG_2 and (b) reduction of the hydroperoxy group at C-15 of PGG_2 to produce PGH_2 (18). The activity that catalyzes PGG_2 formation is commonly referred to as the cyclooxygenase. It is this activity which is inhibited by nonsteroidal antiinflammatory drugs like aspirin. The reduction of PGG_2 is catalyzed by a hydroperoxidase activity. Both activities require heme (30,32). PGH synthase is membrane-bound (18). Purified PGH synthase

has a subunit molecular weight of approximately 70,000 daltons (31).
Cyclooxygenase and hydroperoxidase activities copurify (32,33).
Furthermore, both activities are precipitated by monoclonal antibodies
directed against the purified PGH synthase (34). Thus, it has been
concluded that both cyclooxygenase and hydroperoxidase activities
reside in the same protein chain (18).

In the third stage of biosynthesis, PGH_2 is converted to what
are considered to be the biologically active forms of prostaglandins--
PGE_2, $PGF_{2\alpha}$, PGD_2, TxA_2 and PGI_2. Each of these deriva-
tives, with the possible exception of $PGF_{2\alpha}$, can be formed from
PGH_2 in a single enzymatic step (18). Synthesis of PGE_2 and PGD_2
is catalyzed, respectively, by PGH-PGE isomerase (35,36) and PGH-PGD
isomerase (37,38). Conversions of PGH_2 to PGI_2 and TxA_2 are
catalyzed by PGI_2 synthase and TxA_2 synthase, respectively (39,40).
It is unclear whether $PGF_{2\alpha}$ is formed directly from PGH_2 by a
$PGF_{2\alpha}$ reductase (18). No heat-labile activity involved in this
conversion has ever been detected (41,42). Two alternative pathways
for the synthesis of $PGF_{2\alpha}$ have been proposed (18). One involves
the reduction of PGD_2 mediated by an 11-keto-PGD_2 reductase (not
shown in Figure 1)(43-45). This enzyme has been purified to apparent
homogeneity from rabbit liver (43). The second pathway involves
reduction of PGE_2 catalyzed by a 9-keto-PGE_2 reductase (46).

PGH-PGD isomerase and 9-keto-PGE_2 reductase are soluble enzymes
(17). Two different PGH-PGD isomerases have been purified to
electrophoretic homogeneity from rat spleen (37,47) and rat brain
(38,48). These are the only known isoenzymes in prostaglandin
biosynthesis. Both are composed of a single polypeptide chain (18).

The spleen isomerase is cytosolic and has a subunit molecular weight of 26,000-34,000 and an absolute requirement for reduced glutathione (37,47). The brain enzyme is also cytosolic, but has a subunit molecular weight of 80,000-85,000 and no requirement for reduced glutathione (38,48).

All other enzymes that utilize PGH_2 as substrate are integral membrane proteins. PGH-PGE isomerase has only been partially purified (35,50) and little is known of its physical or chemical properties. PGI_2 synthase has been solubilized and purified to electrophoretic homogeneity from bovine aorta (51,52) and porcine aorta (53). Studies with both preparations indicate that the enzyme is a hemoprotein with a subunit molecular weight of approximately 50,000. TxA_2 synthase has not been purified to homogeneity (18).

Biologically active prostaglandins are inactivated by several types of chemical modifications depending on the prostaglandin. Catabolism can be enzymatic or nonenzymatic (54). TxA_2 is hydrolyzed nonenzymically to TxB_2. The $t_{1/2}$ of TxA_2 in aqueous solution at pH 7.4 and 37° is 30 sec (55). TxB_2 has no appreciable biological activity. Enzymatic inactivation of other prostaglandins is effected via a catabolic cascade (18), the first step of which is oxidation of the 15-hydroxyl substituent by a 15-hyroxyprostaglandin dehydrogenase (15-PGDH). The resulting 15-keto products have less than one tenth the biological activity of the parent molecules (47). Two types of 15-PGDH have been described, differing in their specificities for the pyridine nucleotide cosubstrate. Type I 15-PGDH uses NAD^+ (56), while Type II uses $NADP^+$ (57). In vivo, pulmonary 15-PGDH (Type I) activity is responsible for the rapid (30 sec) inactivation of PGE_2 and $PGF_{2\alpha}$

that enter the circulation (58). PGI_2 and PGD_2, which are not taken up by the lung, are probably inactivated by renal (Type I) 15-PGDH (18). The majority of prostaglandin metabolites found in urine contain a 15-keto group, the apparent result of catabolism by 15-PGDH (59,60).

The second step in catabolism is reduction of the double bond between C-13 and C-14 by 15-ketoprostaglandin Δ^{13} reductase (13-PGR). 13-PGR is coupled metabolically to 15-PGDH; it is found in every tissue that contains 15-PGDH (18). 13-PGR from bovine lung has recently been purified to homogeneity (61). The purified enzyme is specific for 15-ketoprostaglandins, uses $NADH^+$ as cofactor, and has an approximate subunit molecular weight of 39,500 (61).

Another enzyme involved in prostaglandin catabolism is 9-hydroxy-prostaglandin-dehydrogenase (9-PGDH), which catalyzes the oxidation of the 9-hydroxyl substituent of 15-keto-13,14-dihydro-$PGF_{2\alpha}$, the $PGF_{2\alpha}$ catabolic product of 15-PGDH and 13-PGR (62,63). 9-PGDH, a cytosolic enzyme which has been purified to homogeneity, uses NAD^+ as cofactor and has a subunit molecular weight of 34,000 (64). 9-PGDH is not essential for prostaglandin inactivation since it mainly modifies already inactive prostaglandin catabolites.

Prostaglandins are considered to be autocoids, acting on the cells in which they are synthesized or on closely neighboring cells. This concept originated with the observations that circulating PGE_2 and $PGF_{2\alpha}$ are rapidly catabolized in the lung (58) and are present in blood at very low concentrations (65). It was also shown that prostaglandins, unlike classical hormones, are synthesized by virtually

all mammalian tissues (66,67), although not all cells within a given organ synthesize prostaglandins.

Newly formed prostaglandins are not stored, but rather exit cells quickly (68,69). Because biological membranes are not freely permeable to prostaglandins (70-72), carrier mechanisms must exist to transport these newly formed prostaglandins. At the present time nothing is known about the nature or regulation of these putative carriers. Finally, with regards to function, prostaglandins can act through both cAMP-dependent and cAMP-independent pathways to influence biological processes (17).

Renal Structure and Function. The mammalian kidney performs two major functions during the process of urine formation: (a) it excretes all nonessential or noxious products of bodily metabolism and (b) it regulates the volume and composition of body fluids. These actions of the kidney provide for the conservation of water and essential substances and the maintenance of acid-base balance. There are more than one million nephrons in each human kidney and each nephron is capable of forming urine by itself.

The kidney is composed of three general regions (Figure 2): cortex, medulla, and papilla or inner medulla. Most nephrons traverse these three areas. Figure 2 illustrates the basic anatomy of the nephron, which consists of a vascular component (the glomerulus) and a tubular component. Throughout its course, the tubule is composed of a single layer of epithelial cells which differ in structure and function from portion to portion.

Blood enters the glomerulus (G) from the interlobular artery (IA) through the afferent arteriole (AA), forcing fluid to filter into

Figure 2

Figure 2.   Basic nephron structure. G, glomerulus; IA, interlobular
            artery; AA, afferent arteriole; EA, efferent arteriole; PCT,
            proximal convoluted tubule; PR, pars recta; DTL, descending
            thin limb; ATL, ascending thin limb; MTAL, medullary thick
            ascending limb; CTAL, cortical thick ascending limb; DCT,
            distal convoluted tubule; CCT, cortical collecting tubule;
            MCT, medullary collecting tubule; PCT, papillary collecting
            tubule; and IC, interstitial cells.

Bowman's capsule, and leaves through the efferent arteriole (EA). Bowman's capsule opens into the first portion of the tubule, the proximal convoluted tubule (PCT). Along with glomeruli, PCTs lie in the cortical region of the kidney. From the PCT, the fluid passes through the pars recta (PR) to Henle's loop, which is found in both cortical and medullary regions. Henle's loop is subdivided structurally into descending thin limb (DTL), ascending thin limb (ATL), medullary thick ascending limb (MTAL) and cortical thick ascending limb (CTAL). Some DTL ... and ... the ATL, but most is confined to the papillary region ... the ATL. ... the loop ... the fluid flows into the distal convoluted tubule (DCT), which is in the renal cortex. Finally, the fluid flows into a collecting tubule, which traverses all three regions of the kidney: cortical (CCT), medullary (MCT) and papillary (PCT). The fluid from collecting tubules of several nephrons merge into a collecting duct, exclusively found in the papilla, on its way to the renal pelvis ...

Blood filtered in the glomerulus passes into the efferent arteriole. Most of this blood ... into the ... a peritubular capillary network that surrounds the cortical portions of the tubules. The remainder of the blood from the efferent ... straight capillary loops called the vasa recta, which ... downward into the medulla and papilla, enveloping ... before heading back upward to empty into the cortical veins.

As the glomerular filtrate flows through the tubule, most of its water and varying amounts of its solutes are reabsorbed into the surrounding capillaries. Tubular segments are very diverse structurally; consequently, there is great heterogeneity in ...

Figure 2

Bowman's capsule, and leaves through the efferent arteriole (EA). Bowman's capsule opens into the first portion of the tubule, the proximal convoluted tubule (PCT). Along with glomeruli, PCTs lie in the cortical region of the kidney. From the PCT, the fluid passes through the pars recta (PR) into Henle's loop. The PR is found in both cortical and medullary regions. The loop of Henle is subdivided structurally into descending thin limb (DTL), ascending thin limb (ATL), medullary thick ascending limb (MTAL) and cortical thick ascending limb (CTAL). Some DTL is found in the medulla, but most is confined to the papillary region, as is the ATL. From the loop of Henle the fluid flows next into the distal convoluted tubule (DCT), which is in the renal cortex. Finally, the fluid flows into the collecting tubule, which traverses all three regions of the kidney, cortical (CCT), medullary (MCT) and papillary (PCT). The fluid from collecting tubules of several nephrons merge into collecting ducts, exclusively found in the papilla, on its way to the renal pelvis for excretion (73).

Blood filtered in the glomerulus passes into the efferent arteriole. Most of this blood then flows through a peritubular capillary network that surrounds the cortical portions of the tubules. The remainder of the blood from the efferent arterioles flows into straight capillary loops called the vasa recta that extend downward into the medulla and papilla, enveloping the tubules, before looping back upward to empty into the cortical veins.

As the glomerular filtrate flows through the tubule, most of its water and varying amounts of its solutes are reabsorbed into the surrounding capillaries. Tubular segments are very diverse structurally; consequently, there is great heterogeneity in tubular

transport processes. A general observation is that each substance is often transported by more than one segment of the nephron and that the mechanism of transport differs from segment to segment (74).

Prostaglandins and the Kidney. In 1965 Lee et al. (75) reported the isolation from the rabbit renal medulla of two prostaglandin-like compounds which were later identified as PGE_2 and $PGF_{2\alpha}$. The presence of PGH synthase within the renal medulla was first demonstrated by Hamberg (76) by adding tritiated arachidonic acid to medullary homogenates. The bulk of the radioactivity recovered was identified as PGE_2. Smaller amounts of $PGF_{2\alpha}$ were also detected.

It is now well established that all of the biologically active prostaglandin derivatives, with the possible exception of PGD_2, are synthesized in the kidney. As illustrated in Figure 3, the cell types which in the healthy kidney have been shown to form prostaglandins are renomedullary interstitial cells (IC)(9,77,78), cortical and medullary collecting tubule cells (9,10,78,79), endothelial cells of the arterial portion of the renal vasculature (10,80) and glomerular mesangial and epithelial cells (10,81,82). It is not known in all cases which products are formed by which renal cells or the extent to which species differences exist.

At the outset of the research described in this dissertation, it was clear that PGE_2 was the major product of the papillary collecting tubule; however, it was only presumed, not established, that this was also the case for other regions of the collecting tubule. The studies with CCCT cells described in this thesis and additional recent reports by Jackson et al. on isolated rat medullary collecting tubules (83) and by Kirschenbaum et al. on isolated rabbit cortical collecting tubules

Figure 3. Renal sites of prostaglandin synthesis (colored in black).
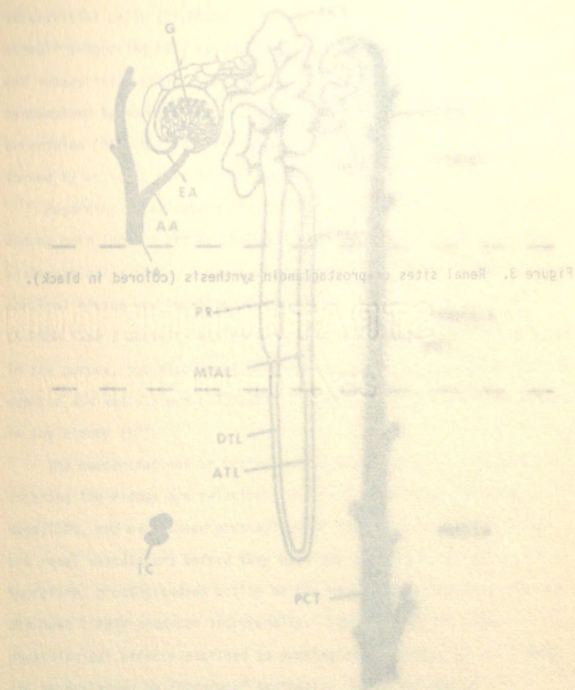
Figure 3

Figure 3. Renal sites of prostaglandin synthesis (colored in black).

(84), strongly suggest that PGE_2 is also the major prostaglandin
product of the cortical and medullary collecting tubules. PGE_2 also
appears to be the major prostaglandin formed by renal medullary
interstitial cells (77,85,86). [...] the nature of the hormonal
stimuli triggering PGE_2 synthesis [...] in collecting tubules
and interstitial [...] principal prostaglandin
synthesized by [...] arterioles (8 [...]) may also be
formed by at lea [...] ain rights in the [...] vasculature.

Regarding [...] catabolism of prostaglandins there exist in the
kidney both Type I and II 15-PGDH [...] studies using
histochemical methods, a prostaglandin dehydrogenase present in
cortical tissue was localized [...] distal convoluted tubule (90).
15-PGDH Type I activity has more recently been [...] to be concentrated
in the cortex, but also [...] appreciable quantities throughout the
nephron and vasculature (47,91,92 [...] 15-PGDH and 15-ketoreductase are also present
in the kidney (17).

The concentrations of arterial prostaglandins in arterial blood
entering the kidney are relatively low (e.g. [...] about two PGE_2 in
dogs)(65), and even these prostaglandins are [...] metabolized by
the renal vasculature before they have any significant effects.
Therefore, prostaglandins acting on the kidney under normal conditions
are most likely produced intrarenally. Furthermore, the [...]
physiological effects ascribed to prostaglandins acting on the kidney
can be explained by intrarenal synthesis. For instance, renin
juxtaglomerular cells can be affected by prostaglandins synthesized
in neighboring glomerular arter [...] (94), increases in renal blood

Figure 3

(84), strongly suggest that PGE_2 is also the major prostaglandin product of the cortical and medullary collecting tubules. PGE_2 also appears to be the major prostaglandin formed by renal medullary interstitial cells (77,85,86). However, the nature of the hormonal stimuli triggering PGE_2 synthesis differs between collecting tubules and interstitial cells (17). PGI_2 is the principal prostaglandin synthesized by homogenates of interlobular arteries and afferent arterioles (80), but PGE_2 and perhaps TxA_2 (87-90) may also be formed by at least certain regions of the vasculature.

Regarding renal catabolism of prostaglanins, there exist in the kidney both Types I and II 15-PGDH (91). In early studies using histochemical methods, a prostaglandin dehydrogenase present in cortical tissue was localized to the distal convoluted tubule (92). 15-PGDH Type I activity has more recently been shown to be concentrated in the cortex, but also found in variable quantities throughout the nephron and vasculature (47,91,92). 13-PGR and 9-PGDH are also present in the kidney (17).

The concentrations of active prostaglandin in arterial blood entering the kidney are relatively low (e.g., <15 pg/ml for PGE_2 in dogs)(65), and even these prostaglandins are probably metabolized by the renal vasculature before they have any significant effects. Therefore, prostaglandins acting on the kidney under normal conditions are most likely produced intrarenally. Furthermore, the major physiological effects ascribed to prostaglandins acting in the kidney can be explained by intrarenal synthesis. Renin release in juxtaglomerular cells can be affected by prostaglandins synthesized in neighboring glomerular arterioles (93,94), decreases in renal blood
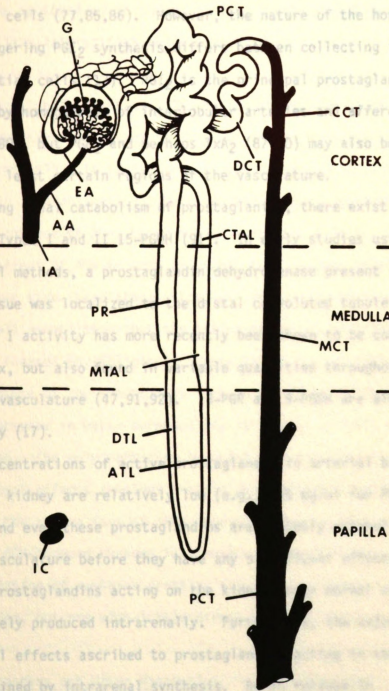
flow occurring in response to vasoconstrictors can be attenuated by prostaglandins formed in the renal vasculature (95), and sodium and water resorption in the collecting tubule can be modulated by prostaglandins synthesized in the collecting tubule itself and possible the renomedullary interstitial cells (10,11,96).

Collecting Tubule Function. The collecting tubule is the site for the final regulation of urinary sodium, potassium, hydrogen ion, and water excretion (97). It is the main target of action for antidiuretic hormone (ADH). The collecting tubule, which is poorly permeable to water in the absence of ADH, becomes highly permeable in its presence (98). This effect of ADH is seen only when this hormone is added to the peritubular side (basolateral side) of the collecting tubule (99).

It is well established that the action of ADH is mediated by cAMP and that ADH induces physiological changes in the luminal cell membrane (99). The nature of the events that link an elevation of intracellular cAMP to an increase in water permeability at the apical cell membrane is ill-defined. The only mechanism by which cAMP has been shown to mediate hormonal effects involves protein phosphorylation (100), catalyzed by the active form of cAMP-dependent protein kinase. That cAMP elicits ADH-induced changes in membrane permeability by activation of phosphorylation of membrane proteins (or other proteins) is an attractive idea, but one with little direct support (101).

Prostaglandins and Water Resorption. A variety of approaches, both in vivo and in vitro, have demonstrated that prostaglandins

antagonize the effect of ADH on water resorption. In several mammals studied, pretreatment with cyclooxygenase inhibitors such as aspirin, indomethacin, and meclofenamate increased urine osmolality in response to arginine vasopressin (AVP), the naturally-occurring form of ADH (102-108). Indomethacin pretreatment also potentiated AVP-stimulated cAMP synthesis, suggesting that prostaglandins may block water resorption by inhibiting cAMP synthesis (108). Using isolated, perfused, rabbit collecting tubules, Grantham et al. (11) showed that AVP-stimulated water resorption is inhibited by 50% with 10^{-9} M PGE_1. The phosphodiesterase inhibitor, theophylline, by itself caused water resorption, an effect that PGE_1 potentiated. PGE_1 alone caused a small increase in water resorption. These results suggested that PGE_1, like AVP, could cause cAMP synthesis in cortical collecting tubules which then leads to water resorption. Grantham further postulated that PGE_1 and AVP may compete for a common receptor coupled to adenylate cyclase and that PGE_1 inhibits AVP-stimulated water resorption when both are present simultaneously. Later, on the basis of similar experiments in toad bladder, other authors concluded that PGE_1 does not alter ADH-receptor binding, but rather 'uncouples' the receptor from adenylate cyclase (109). Most recently, studies have specifically evaluated the effect of prostaglandins on ADH-receptor binding (110,111). These studies were performed in human mononuclear phagocytes, cells which display $AVP-PGE_2$ effects on cAMP metabolism similar to those observed in the collecting tubule (110,111). It was demonstrated that the presence of PGE_2 did not modify AVP specific binding to the cells.

Direct evidence for an inhibition of AVP-induced cAMP synthesis by prostaglandins has been inconsistent at best. One important cause of this problem is the more-recently-apparent biphasic nature of the effect of PGE on cAMP accumulation. Marumo et al. (112) and Beck et al. (113) noted that the inhibitory effect of PGE_1 was apparent at low concentrations (10^{-8} $\underline{M}$), whereas at high concentrations no inhibition was apparent. Studies in which an additive effect was observed (114,115) have used extremely high concentrations of PGE_2 ($>10^{-4}$ $\underline{M}$). PGE_2 used alone at these high concentrations unequivocally stimulates adenylate cyclase activity (115,116), making any inhibitory effect on ADH-stimulated cyclase difficult to detect.

The current hypothesis proposed to explain the relationship between AVP and prostaglandins is that prostaglandins act as negative feedback modulators of the antidiuretic action of AVP on the kidney. If this is so, one would expect AVP to stimulate renal prostaglandin synthesis. Only very recent studies, by Kirschenbaum et al. (84), concurrent with those described in this dissertation, directly demonstrate that ADH does stimulate prostaglandin synthesis in the cortical collecting tubule of the rabbit and the dog, respectively.

CHAPTER II

ISOLATION AND CHARACTERIZATION OF CANINE CORTICAL
COLLECTING TUBULE (CCCT) CELLS: AVP INDUCES PGE$_2$ RELEASE

This chapter describes the preparation of monoclonal antibodies
specific for the canine collecting tubule and the use of these
antibodies to isolate cortical cells. These cells proliferate in
culture and have many of the histochemical and hormonal properties
expected for cortical collecting tubule cells. In addition, the
results of experiments designed to determine the effects of bradykinin,
arginine vasopressin (AVP), and DD-AVP on prostaglandin synthesis by
CCCT cells are presented.

22

MATERIALS AND METHODS

Materials. Hypoxathine, penicillin, streptomycin sulfate, aminopterin, thymidine, bradykinin triacetate, isoproterenol, calcitonin, bovine serum albumin, arginine vasopressin (AVP), 3-isobutyl-1-methylxanthine (IBMX), and trypsin were purchased from Sigma Chemical. Parathyroid hormone (PTH) and $[Asu^{1,6}, Arg^{8}]$ vasopressin (DD-AVP) were obtained from Beckman. Collagenase (CLS II) was obtained from Worthington Biochemicals. Dulbecco's Modified Eagle's Medium (DMEM), antibiotic-antimycotic (100X), and DMEM containing D-glucose (4.5 g/l) and L-glutamine (2 mM) were purchased from KC Biologicals. NCTC 109 medium was from MA Bioproducts, Bethesda, MD. Normal horse serum was from Flow Laboratories. Sea Plaque Agarose was from Marine Colloid Division, FMC. Fluorescein isothiocyanate (FITC)-labeled rabbit antirat immunoglobulin (IgG), goat antirat IgG_{2c}, sheep antirat IgG_1, goat antirat IgG_{2a}, rabbit antirat IgG_{2b}, and rabbit antiprostaglandin (PG) PGE_2 were obtained from Miles Laboratories. $[^{3}H]PGE_2$, $[^{125}I]$adenosine 3',5'-cyclic monophosphate (cAMP), and radioimmunoassay supplies for the cAMP assay were all purchased from New England Nuclear, Boston. PGE_2 was a gift from Dr. John E. Pike of Upjohn, Kalamazoo, MI.

Cell Culture. Madin-Darby canine kidney (MDCK) cells (ATCC CCL34) obtained frm the American Type Culture Collection were grown in DMEM

containing 10% fetal bovine serum, antibiotic-antimycotic (1X) and 2 mM glutamine. Swiss mouse 3T3 fibroblasts (ATCC CCL92) obtained from the American Type Culture Collection were grown in DMEM containing 10% fetal bovine serum. Both cell lines were grown at 37°C under a water-saturated 7% CO_2 atmosphere.

Preparation of Monoclonal Antibodies. Four-week-old female Sprague-Dawley (Spartan Laboratories) rats were immunized two times 2 wk apart (first iv then ip) with 10^7 MDCK cells suspended in 0.2 ml Krebs buffer (composition in mM: 118 NaCl, 25 $NaHCO_3$, 14 glucose, 4.7 KCl, 2.5 $CaCl_2$, 1.8 $MgSO_4$, and 1.8 KH_2PO_4), pH 7.3. Three days after the second inoculation, the rats were killed by cervical dislocation; a blood sample was taken to determine the presence of antitubule antibody activity in the serum; and the spleens were removed under sterile conditions for myeloma-spleen cell fusions.

Fusions were performed by modification of the method of Galfre et al. (118). The spleens were placed in 5 ml of DMEM and cut into pieces that were teased apart with forceps to release the lymphocytes. After the mixture was vortexed, the large tissue fragments were allowed to settle for 1 min, the supernatant was transferred to a new tube, and the splenic lymphocytes were collected by centrifugation at 1,000 g for 5 min. Red blood cells in the pellet were lysed by addition of 5.0 ml of 0.2% saline for 30 s followed by 5.0 ml of 1.6% saline for 30 s. Finally, 10 ml of DMEM containing 20 mM N-2-hydroxyethylpiperazine-N'--2-ethanesulfonic acid (HEPES), pH 7.6, were added, and the spleen cells were again collected by centrifugation, resuspended in DMEM containing 20 mM HEPES, pH 7.6, and counted using a hemacytometer.

The mouse myeloma strain SP2/0-Ag14 (119) obtained from the Cell Distribution Center at the Salk Institute was grown in DMEM (4.5 D-glucose/l) containing 10% fetal bovine serum and 100 µg/ml each of penicillin and streptomycin at 37°C under a water-saturated 7% CO_2 atmosphere. SP2 myeloma cells ($1-5 \times 10^6$), which had been washed and resuspended in DMEM containing 20 mM HEPES, pH 7.6, were mixed with $1-5 \times 10^7$ of the isolated splenic lymphocytes. The cell mixture was collected by centrifugation at 1,000 g for 5 min in a sterile glass centrifuge tube. After the supernatant was removed, the fusion was begun by gently shaking the cell pellet, largely intact, with a solution containing 35% polyethylene glycol 1000 (Baker) and 5% dimethylsulfoxide in DMEM for 1 min. During the ensuing 3 min the fusion solution was diluted with 3 ml of DMEM plus 20 mM HEPES, pH 7.6; then, over a period of 6 min, the fusion mixture was diluted further with 12 ml of HT media [composition: DMEM containing 10% (vol/vol) fetal bovine serum, 10% (vol/vol) horse serum, 10% (vol/vol) NCTC 109 media, 2 mM glutamine, 100 µM hypoxanthine, 16 µM thymidine, 3 µM glycine, 100 mg/l penicillin, and 100 mg/l streptomycin]. Finally, the cells were collected by centrifugation, resuspended in 75 ml of HT media and dispensed into 96-well Costar 3596 tissue-culture plates (100 µl/well). The plates were incubated at 37°C under a water-saturated 7% CO_2 atmosphere. After 36 h, 100 µl of HAT medium (HT media plus 1 µM aminopterin) was added to each well. Half of the media was replaced with fresh HAT media after 2 additional days; 12-20 days after the cell fusion, when the media from those wells with growing hybridomas began to acidify (turn yellow), aliquots of media were removed to test for the presence of anticanine kidney tubule antibody.

Selection of Hybridomas Producing Antibody to Specific Canine Kidney Cell Types. Media from growing hybridomas were screened for antibody activity using an indirect immunocytofluorescence procedure on canine kidney sections. Sections (10 μm) of canine kidney were cut on a Tissue-Tek cryotome essentially as described previously (10) and incubated with media from hybridoma cells (1:2 dilution in phosphate-- buffered saline (PBS, composition in $\underline{mM}$: 151 NaCl, 45 KH_2PO_4, and 2.5 NaOH), pH 7.2, for 30 min. After the sections were washed with PBS, pH 7.2, FITC-labeled rabbit antirat IgG (1:20 dilution in PBS, pH 7.2) was added, and the samples were incubated for 30 min. The sections were then washed, mounted on cover slips, and examined by fluorescence microscopy. Presence of antibody in the medium from hybridoma cells was indicated by the appearance of fluorescence in renal cells compared with the absence of such fluorescence in control samples. HAT media, preimmune rat serum, and PBS, pH 7.2, were all used for control staining. A Leitz Orthoplan microscope equipped with an Orthomat camera was used to visualize fluorescent staining. Photomicroscopy was performed using Kodak Tri-X pan film (ASA 400).

Cells from wells yielding positive responses in the indirect immunofluorescence procedure were cloned once in soft agar using the procedure of Cotton et al. (120), but with Swiss mouse 3T3 cells as a feeder layer (121). 3T3 cells were seeded at a density of 5 x 10^4 cells in a 100-mm culture dish. After the cells had adhered to the dishes, medium was removed and the 3T3 cells were overlayed with 5 ml of Sea Plaque Agarose working solution (6 ml of 5% Sea Plaque Agarose in PBS, pH 7.4, plus 90 ml of HT medium). The dishes were chilled at 4°C to gel the agar layer and then warmed at 37°C for 10-15 min. For

each plate, 2 x 10³ hybridoma cells were resuspended in 1 ml of Sea Plaque Agarose working solution and dripped evenly over the plate. The plates were chilled for 15 min at 4°C and then placed at 37°C under a water-saturated 7% CO_2 atmosphere. After 10-12 days, symmetrically shaped colonies were picked from the agarose-medium suspension using sterile micropipettes. Cells from individual clones were cultured in HT media, and the media was retested for antitubule antibody activity as described above.

Ouchterlony Double-Diffusion Analysis. Media (0.04 ml) from positive hybridoma cultures was tested against sheep antirat IgG_1 (0.04 ml), goat antirat IgG_{2a} (0.04 ml), rabbit antirat IgG_{2b} (0.04 ml), and goat antirat IgG_{2c} (0.04 ml) in 1.5% agar at 24°C for 16-24 h.

Purification of Rat IgG_{2c} from Hybridoma Culture Media. The cct-1 hybridoma line (which secretes antibody to collecting tubule cells) was grown in IgG-free HT medium (121). Antibody-containing medium was decomplemented for 5-10 min at 56°C, adjusted to pH 8.2, and applied to a Protein A-Sepharose CL-4B column (1 x 5 cm). Absorbed material was eluted stepwise using 0.1 $\underline{M}$ buffers of pH 8.0 (sodium phosphate), pH 6.0, pH 4.5, and pH 3.5 (sodium citrate)(121,122). The absorbance at 280 nm of each fraction was measured to determine the location of protein peaks. Anticollecting tubule antibody activity in the peak fractions was detected by the indirect immunofluorescence procedure. IgG (IgG_{2c}) secreted by the cct-1 line was eluted at pH 4.5. Fractions containing IgG_{2c} were pooled, titrated to pH 7.4,

sterilized by filtration using a Millex sterile disposable filter unit (0.45 μm pore size), and stored in glass screw-top tubes at -20°C.

Adsorption of Rat IgG$_{2c}$ to Culture Dishes. Polystyrene culture dishes (100 mm) were coated under sterile conditions with 9 ml of purified IgG$_{2c}$ (cct-1; 10 μg/ml of PBS, pH 7.4) for 3 h at 24°C with intermittent swirling or overnight at 4°C. Unbound antibody was removed by aspiration, and each antibody-coated dish was then washed three times with 3 ml of a 1% solution (wt/vol) of bovine serum albumin in PBS, pH 7.4. The dishes were allowed to dry face down on a layer of sterile absorbing material.

Selective Adsorption of MDCK Cells to Antibody-Coated Culture Plates. MDCK cells (10^6) or 10^6 Swiss mouse 3T3 cells, each suspended in 1 ml of PBS, pH 7.4, were added to different antibody-coated culture dishes. The dishes were then washed five times with PBS, pH 7.4, to remove nonadherent cells. The application procedure was always timed to last less than 3 min to minimize nonspecific binding of the cells to the plates. To test for nonspecific binding of MDCK cells to antibody-coated dishes and untreated dishes. Antibody-coated dishes that had not been washed with 1% bovine serum albumin (BSA) and uncoated dishes that had been washed with 1% BSA were also tested using both 3T3 cells and MDCK cells to determine the effect of the washing procedure on nonspecific binding of cells. Binding was quantitated by detaching the cells from dishes with 0.1% (wt/vol) trypsin containing 0.05% (wt/vol) ethylenediaminetetraacetic acid

(EDTA) in PBS, pH 7.2, and then counting the cells with a hemacytometer.

Isolation of Canine Cortical Collecting Tubule (CCCT) Cells Using Antibody-Coated Plates.

Under sterile conditions, renal cortical tissue (5 g) was carefully dissected from canine kidneys (obtained immediately postmortem from mongrel dogs) and washed gently with 5 ml of PBS, pH 7.4, to remove excess blood. The tissue was minced in a petri dish with a sterile razor blade and transferred to a plastic culture tube containing 24 ml of 0.1% (wt/vol) collagenase (CLS II) in Krebs buffer, pH 7.3. The minced tissue was incubated for 40 min at 37°C under a water-saturated 7% CO_2 atmosphere. The tissue was then gently agitated by drawing it up and down five to ten times in a largebore (10 ml) pipette. The partially dispersed tissue was incubated at 37°C under a 7% CO_2 atmosphere for an additional 20 min. The resulting cell suspension was centrifuged at 1,000 g for 5-10 min. Red blood cells in the pellet were removed by hypotonic lysis with 10.0 ml of 0.2% saline for 30 s followed by 10.0 ml of 1.6% saline for 30 s, and the suspension was filtered through several Gelman stainless steel meshes (0.25 mm pore size). The remaining cortical cells were collected by centrifugation at 800 g for 10 min on a tabletop centrifuge. The cell pellet was resuspended in 10% BSA in PBS, pH 7.2, and centrifuged again for 10 min to collect the cells and remove cell debris (13).

The cells ($\sim 10^9$) were resuspended in 10 ml of PBS, pH 7.4, and overlayed on antibody-coated dishes (1 ml/dish) for 3 min. The dishes were then washed three to five times with 5 ml of PBS, pH 7.4. Bound

cells were detached by treatment with 3 ml of 0.1% (wt/vol) trypsin containing 0.05% (wt/vol) EDTA in PBS, pH 7.2. The sample was centrifuged, the supernatant removed by aspiration, and the cells resuspended in DMEM containing 10% decomplemented fetal bovine serum, antibiotic-antimycotic (1X), and 2 mM glutamine. The cells were then seeded on 100 mm culture dishes, 24-well Costar 3524 tissue culture plates, or sterile glass slips, as required for subsequent experiments.

Incubation of Cells with Effectors. Treatment of monolayer cultures of nonconfluent CCCT cells with effectors (i.e., bradykinin, AVP, DD-AVP, isoproterenol, PTH, calcitonin) was done in triplicate using 24-well culture dishes seeded at a density of 5×10^4 cells/well. All experiments were performed 6-10 days following isolation of the cells. Cells were first rinsed free of media with Krebs buffer, pH 7.3, and then 0.3-0.5 ml of buffer containing an effector was added to the cells. The cells were incubated for the desired time at 37°C under a water-saturated 7% CO_2 atmosphere. Typically, 0.05-0.10 ml of buffer was removed from each well for radioimmunoassays of extracellular cAMP or prostaglandin (PG) E_2. The remaining buffer was removed and discarded, and 0.20 ml of 0.1% (wt/vol) sodium dodecyl sulfate (SDS) was added to each well. The plate was incubated at 37°C for 15 min, and the solubilized protein was assayed by the Lowry procedure (123) using BSA as a standard. All the effectors used were checked to determine whether they had an independent effect on the radioimmunoassays. Catabolism of PGE_2 formed by CCCT cells that could occur during the incubations with

effectors was determined as previously described (126). There was no detectable catabolism.

For intracellular cAMP measurements, the solution in each well was aspirated and 0.5 ml of cold 6% TCA was added to each well. The wells were incubated at -80° for 20 min, thawed at 24° for 25 min and incubated for 2 hrs at 0-4°. The liquid in each well was then transferred to a test tube and extracted four times with 10 volumes of diethyl ether. Residual ether was evaporated in a 60° water-bath for 10 min. The remaining aqueous phase was lyophilized. The lyophilized samples were resuspended in 0.125-0.3 ml of buffer and assayed for cAMP by radioimmunoassay.

Statistical Analysis. All experiments involving an effector-induced response were done using a minimum of three replicates per treatment. A completely random analysis of variance was used to test for differences between sample means at $P < 0.05$ (124). Dunnett's test was used for comparing differences between effector means and the control mean (124).

Enzyme Histochemistry. Histochemical staining for succinate dehydrogenase, glycerol-3-phosphate dehydrogenase, and NADH diaphorase (125) was performed on CCCT cells that had been cultured on glass cover slips and quick frozen in isopentane (-70°C) and on sections (10 μm) of canine kidney cut on Ames Lab-Tek cryotome. Light microscopy was performed on a Leitz Orthoplan microscope.

Electron Microscopy. Samples examined by transmission electron microscopy included canine renal cortical tissue and CCCT cells grown

in monolayers attached to culture dishes. Primary fixation of all samples were performed for 24 h at 4°C with 2% glutaraldehyde in 0.1 M sodium phosphate, pH 7.2. In the case of cortical tissue, cubes (about 1 mm^3) were cut from fresh tissue and immersed in fixative. Cultured CCCT cells were overlayed with the fixative, and the fixation was performed in culture dishes. After fixation in glutaraldehyde all samples were washed for 1 h with frequent changes of 0.1 M sodium phosphate, pH 7.2. The samples were then postfixed overnight at 4°C in 1% OsO_4 for the culture cells and 2% OsO_4 for the cortical tissue. The samples were washed and then dehydrated by sequential exposure to 25, 50, 70, 80, 95, and 100% (3 times each) solutions of ethanol. Infiltration and embedding procedures were slightly different for the two types of samples. After the third treatment with 100% ethanol, CCCT cells were removed from culture dishes by scraping with a rubber policeman, transferred to 4-dram screw-top vials and collected by centrifugation at 500 g for 2 min. Propylene oxide was added to the cell pellet and, after a brief incubation period, mixed with an equivalent volume of Epon-Araldite resin (Epon 812:Araldite 502:dodecenyl succinic anhydride, 25:20:60, vol/vol/vol) and agitated for 4 h at 24°C. Extra resin was then added to provide a ratio of resin to propylene oxide of 2, and the mixture was agitated overnight. The cells were then collected by centrifugation and resuspended in Epon-Araldite resin to which had been added 0.024 volumes of 2,4,6-tri(dimethylaminomethyl)phenol. The samples were placed in Beem capsules and incubated for 72 h at 60°. After the third treatment with 100% ethanol, a gradual transition to acetone was carried out for the cortical tissue by exposing it to a mixture of 100% ethanol:acetone

(2:1) for 15 min, then 100% ethanol:acetone (1:2) for 15 min, and finally two changes of acetone alone, 30 min each change. The cortical tissue in acetone was then mixed with Epon-Araldite resin to a final acetone-to-resin ratio of 3 and agitated for 3 h at 24°C. More resin was then added to a final acetone-to-resin ratio of 1, and the samples were again agitated for 3 h at 24°C. The cortical tissue was then agitated with resin only, overnight at 24°C. The tissue segments were placed in flat embedding molds (1/8 x 1/4 x 1/2 in.) filled with Epon-Araldite resin to which had been added 0.024 volumes of 2,4,6-tri(dimethylaminomethyl)phenol and incubated for 48 h at 65°C. The capsules and blocks were sectioned. The sections were counterstained with 2% uranyl acetate in H_2O and examined and photographed using a Phillips Model 201 transmission electron microscope. Kodak EM 4463 film was used for photography.

RESULTS

Selection and Characterization of Monoclonal Antibodies Against

Canine Collecting Tubule Cells. Spleen cells from rats immunized with

MDCK cells were fused with mouse plasmacytoma cells (SP2/0-Ag14), and

hybridomas were cultured as detailed in MATERIALS AND METHODS. Media

from three of 47 hybridoma-containing wells (from a total of 288 wells)

caused specific staining of collecting tubules and no other tubule

segments when tested by indirect immunofluorescence. No other

antitubule reactions were noted with other hybridomas or with the serum

from the immunized rat. Cells from the hybridoma-containing well that

yielded the most intense fluorescent staining of collecting tubule

cells (Figure 4) were cloned, yielding a hybridoma line designated as

cct-1. This line produced antibody, which when employed in the

immunofluorescence screening procedure, stained cells from both the

cortical and medullary collecting tubules; moreover, all collecting

tubule cells stained with similar intensities, indicating that the

antibody was not directed against a specific subpopulation of

collecting tubules. Identification of the tubular sites of staining

was based on cellular morphology, distribution of staining in the

medullary rays, and coincidence of the fluorescent staining with

histochemical staining for NADH diaphorase activity (125) in both the

cortex and medulla.

34

Figure 4. Photomicrographs of canine collecting tubule immunofluores-
cently stained with cct-1. A: fluorescent photomicrograph
of a section of renal medulla stained sequentially with
media from cct-1 and then with fluorescein isothiocyanate
(FITC)-labeled rabbit antirat immunoglobulin (Ig) IgG. B:
phase contrast photomicrograph of the same tissue shown in
A. Magnification X80.
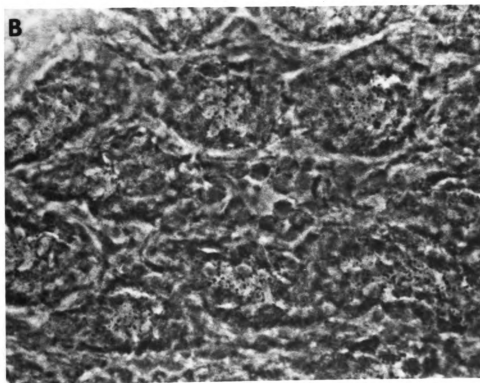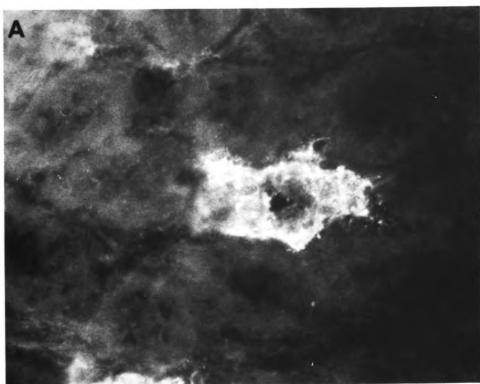
Figure 4

An intense, spackled, fluorescence staining of collecting tubules was observed in cryotome sections of canine kidney treated with IgG secreted by cct-1 and then FITC-labeled rabbit antirat IgG (Fig. 4). Adsorption of medium from cct-1 cells (containing approximately 20 μg of rat IgG) with 10^7 MDCK cells for 1 h at 37°C subsequently eliminated the indirect fluorescent staining of collecting tubules in sections of canine kidney; in contrast, adsorption of the medium with 10^7 Swiss mouse 3T3 cells under the same conditions had no effect on immunocytofluorescence. These data suggest that the antigen that interacts with IgG (cct-1) is located, at least in part, on the cell surface. The IgG secreted by cct-1 cells was identified as belonging to the IgG_{2c} subclass on the basis of 1) Ouchterlony double-diffusion analyses using antirat IgG allotype-specific sera and 2) affinity for Protein A-Sepharose and attenuated Staphylococcus aureus cells (122).

Isolations and Characterization of Canine Cortical Collecting Tubule Cells. Conditions for selective adsorption of CCCT cells were developed by quantitating the binding of MDCK (experimental) and Swiss mouse 3T3 (control) cells to 100 mm culture dishes pretreated with IgG_{2c} (cct-1) (Table 1). The following general observations were made. 1) Maximal binding of MDCK cells occurred with dishes incubated for ≥ 3 h at 4°C with ≥ 90 μg of purified IgG_{2c} (cct-1) per plate; 2) washing the antibody coated dishes three times with 1% BSA in PBS, pH 7.4, eliminated all nonspecific binding of 3T3 cells; and 3) drying the antibody-coated dishes following treatment with the BSA solution enhanced the binding of MDCK cells. Under optimal conditions 15% of

Table 1

Differential Binding of MDCK Cells and Swiss Mouse 3T3 Cells to Culture
Dishes Coated with Rat Anticanine Collecting Tubule Antibody[a]

Cell Type	Treatment of Culture Dish	Cell Bound/Dish
MDCK	PBS wash only	$<10^3$*
3T3	PBS wash only	$<10^3$
MDCK	BSA wash only	ND
3T3	BSA wash only	ND
MDCK	IgG$_{2c}$ (cct-1); no BSA wash	1.3 x 10^5
3T3	IgG$_{2c}$ (cct-1); no BSA wash	$<10^3$
MDCK	IgG$_{2c}$ (cct-1); plus BSA wash	1.4 x 10^5
3T3	IgG$_{2c}$ (cct-1); plus BSA wash	ND

[a]Culture dishes (100 mm) were treated 1) with phosphate-buffered
saline (PBS), pH 7.4; 2) 3 times with PBS, pH 7.4, containing 1%
bovine serum albumin (BSA); 3) with 90 μg of immunoglobulin (Ig)
IgG$_{2c}$ (cct-1) in PBS, pH 7.4, for 3 h at 24°C and then washed 3
times with PBS, pH 7.4; or 4) with 90 μg of IgG2c (cct-1) in PBS, pH
7.4, for 3 h at 24°C and then washed 3 times with PBS, pH 7.4,
containing 1% BSA. Dishes were then dried. MDCK cells (10^6) or 3T3
cells (10^6) in 1 ml of PBS, pH 7.4, were then added to the dish and
incubated for 3 min at 24°C, and dishes were washed 5 times with PBS,
pH 7.4. Binding of cells to the dish was determined as described in
MATERIALS AND METHODS. ND, no cells were detected by microscopic
observation of the culture dish. *A few cells were observed to be
bound to the dish when examined under a microscope but no cells were
seen in the hemacytometer.

10^6 MDCK cells were bound per 100 mm antibody-coated culture dish; under similar conditions less than 0.1% of 10^6 mouse 3T3 cells were bound (Table 1); MDCK cells were not bound to dishes that were not coated with antibody. There was no evidence that the antibody-coated dishes adsorbed only a subpopulation of MDCK cells as approximately 15% of those cells not adsorbed to a first dish could be adsorbed to a second antibody-coated culture dish.

Conditions developed for optimal selectivity in binding MDCK cells to culture dishes were used with minor modifications for isolating CCCT cells (Figure 5). The renal cortex was dissected and then dispersed by a combination of mincing and treatment with collagenase as described in detail in MATERIALS AND METHODS. Dispersed cortical cells (10^8) were added to each of 10 antibody-coated culture dishes and incubated for 1 min prior to washing thoroughly with PBS, pH 7.2, to remove unbound cells. Under these conditions 10^6 cells routinely bound to each dish. Bound cells were removed from dishes by trypsinization and transferred to untreated multiwell culture dishes; approximately 80% of the trypsinized cells adhered to uncoated dishes. Maximal attachment of the trypsinized cells occured within 3-6 h, but 4-5 days were required before the attached cells completely flattened and assumed the typical appearance of the cells in monolayer culture (Figure 6); at about this time the cells entered a proliferative period that continued until they reached confluency (Figure 7). Starting from the density at which the trypsinized cells were seeded ($10/mm^2$), the cells underwent a 40-fold increase in cell number and cell protein prior to reaching confluency (Figure 7). On reaching confluency, the isolated cells remained viable for up to 3 mo on 100 mm culture dishes containing 10

Figure 5. Isolation of canine cortical collecting tubule (CCCT) cells
using polystyrene culture dishes precoated with cct-1.

CULTURE DISH   +   ANTIBODIES

INTACT TISSUE

CELL MIXTURE

TRYPSIN, TRANSFER
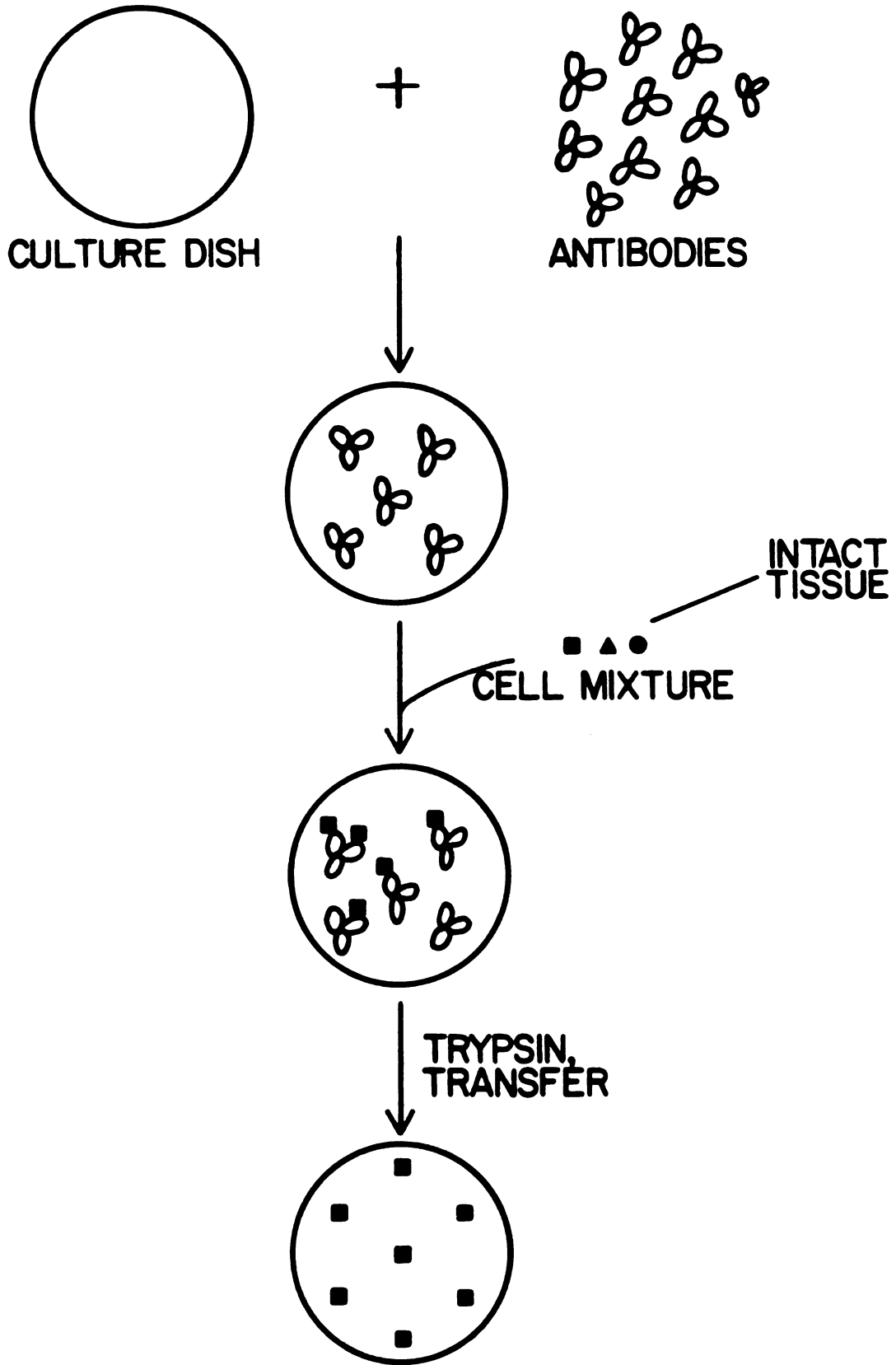
Figure 5

Figure 6.   Photomicrograph of confluent monolayer of CCCT cells.
            Magnification X125.
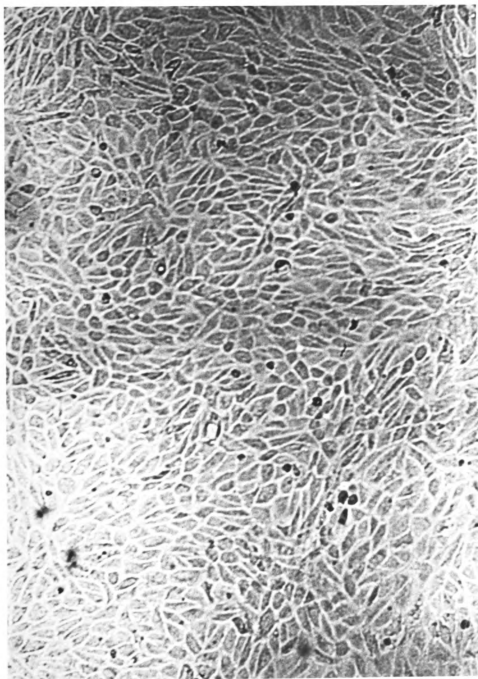
Figure 6

Figure 7. Growth of CCCT cells in monolayer culture. Cells were
seeded at a concentration of 10 cells/mm^2.
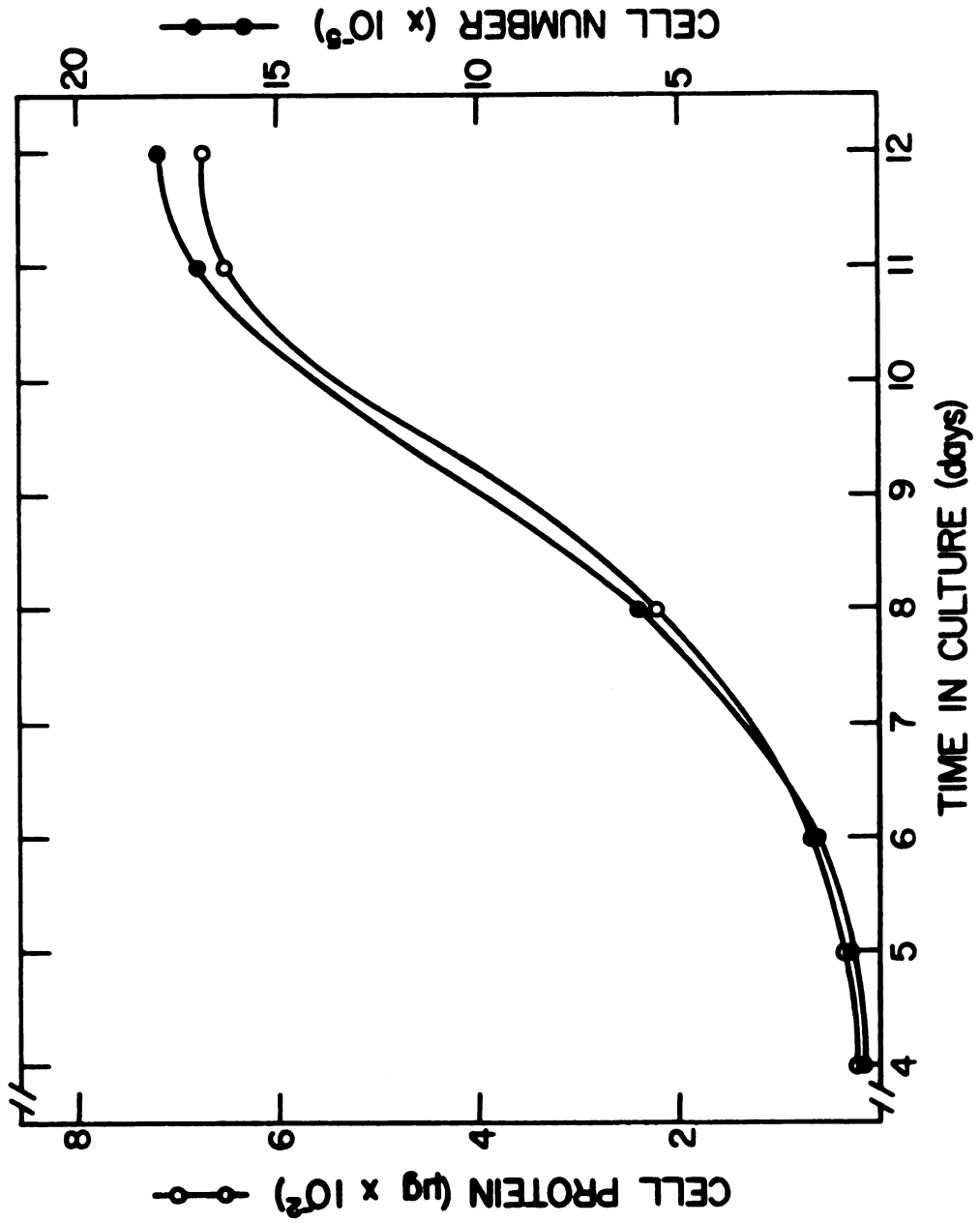
Figure 7

ml of medium with or without changes of culture media. This latter behavior is also exhibited by MDCK cells; in contrast rabbit renal papillary collecting tubule (RPCT) cells (13) detach from the substratum and die shortly after reaching confluency. Confluent CCCT cells formed hemicysts in culture (Figure 8), and hemicyst formation was blocked by the addition of ouabain (10^{-5} M) to the culture medium. When CCCT cells isolated from three different dogs were seeded at confluency on Millipore filters (1-2 x 10^6 cells/cm^2), transepithelial potential differences of 1 ± 0.5 mV (Millipore side positive) developed in each case 7 days after seeding and remained for an additional 7-10 days. In parallel experiments with MDCK cells, a potential difference of approximately 2 mV developed 1 day after seeding and remained for at least 3 wk.

The isolated CCCT cells stained uniformly positive for NADH diaphorase and glycerol-3-phosphate dehydrogenase and uniformly negative for succinate dehydrogenase under reaction conditions in which cortical collecting tubules in cryotome sections of the canine kidney gave a similar pattern of histochemical staining. The uniform response to the histochemical stains given by all cells in the monolayers suggests that the CCCT cell population is relatively homogeneous.

Inspection of primary cultures of CCCT cells from three separate isolations by transmission electron microscopy indicated that two types of collecting tubule cells, principal cells and intercalated cells, were present (126)(Figures 9-11). Of 303 cells examined from both confluent and nonconfluent cultures, 36% were classified as intercalated cells on the basis of their dark, electrondense cytoplasms

Figure 8. Photomicrographs of hemicysts formed by confluent CCCT
           cells. Magnification X140.
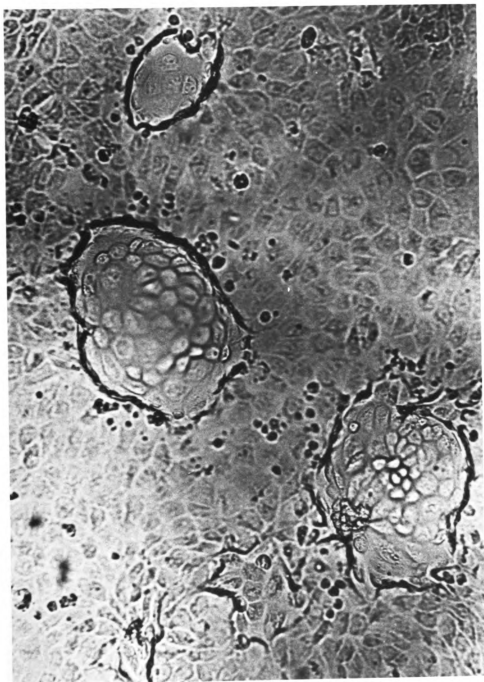
Figure 8

Figure 9. Electron photomicrograph of canine cortical collecting
            tubule in situ. Magnification X10,000. Internal marker is
            1 µm. bm, basement membrane; pc, principal cells; ic,
            intercalated cell; and l, lumen.
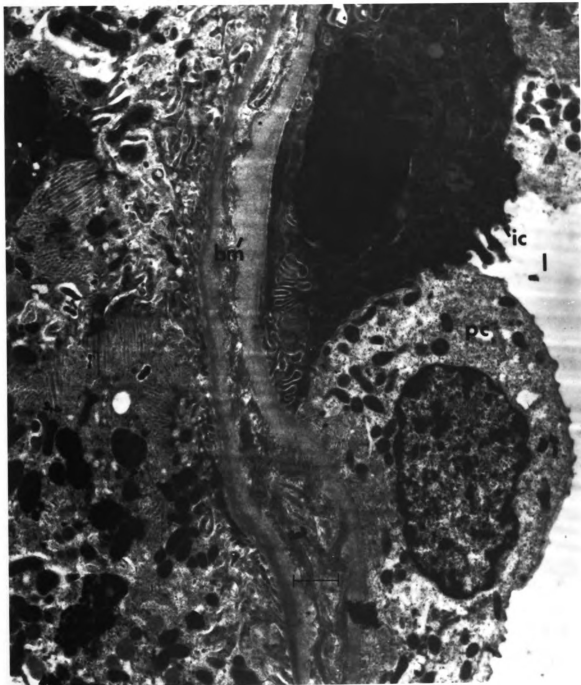
Figure 9

Figure 10. Electron photomicrograph of an isolated intercalated cell. Magnification X17,500. Internal marker is 1 µm. rer, rough endoplasmic reticulum; m, mitochondria; and n, nucleus.

Figure 10

53
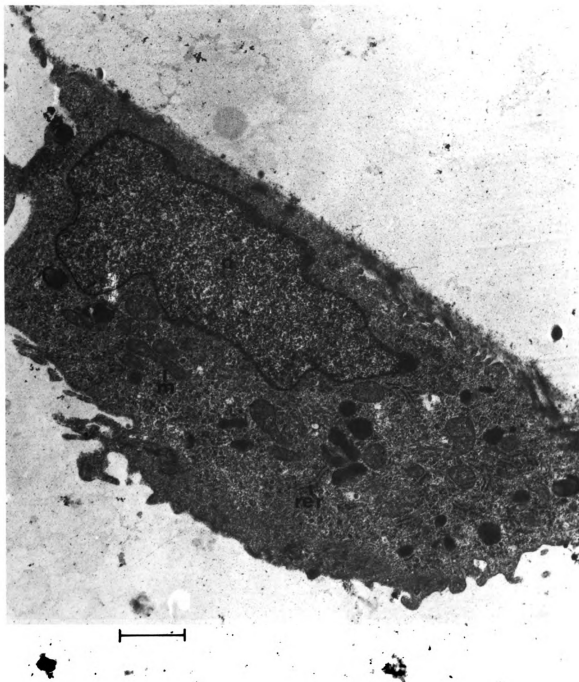
Figure 11. Electron photomicrograph of an isolated principal cell. Magnification X32,000. Internal marker is 1 μm. m, mitochondria; and n, nucleus.
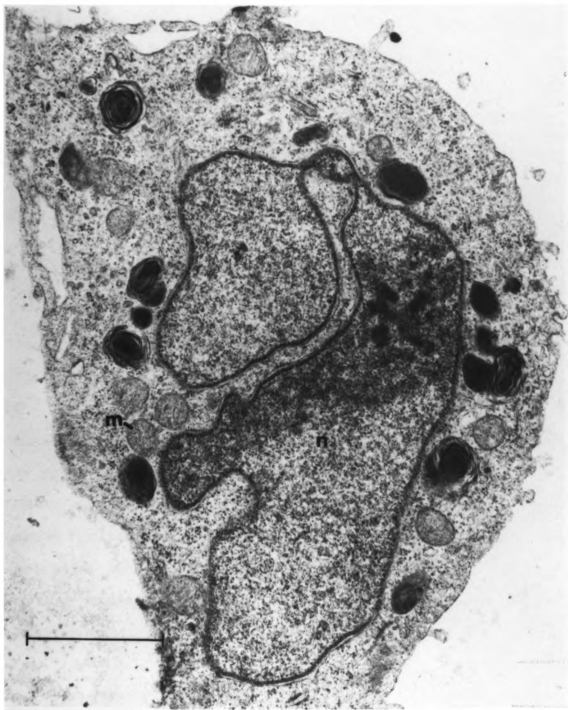
Figure 11

(Figure 10). An abundance of mitochondria and other organelles and a high content of cytoplasmic vesicles were also observed in some of the intercalated cells (126,127). The remainder of the cells (~64%) were classified as principal cells (Figure 11). These latter cells had large nuclei and clear cytoplasms with a moderate content of mitochondria and other organelles (126-128). The number of organelles in these "light" cells was higher than has been observed in the medullary and papillary collecting tubules. The relative numbers of principal and intercalated cells were approximately the same in the three isolates examined. No cells with characteristics (126,127) expected for tubule cells other than collecting tubule cells were observed by electron microscopy.

Primary cultures of CCCT cells were tested for their ability to form cAMP in response to tubule-specific hormonal effectors (Figure 12). Increases in extracellular cAMP were observed in response to AVP, PGE_2, and isoproterenol, but not PTH or calcitonin. Half-maximal increases in cAMP occurred with 10^{-10} $\underline{M}$ AVP, 10^{-8} $\underline{M}$ PGE_2, and 10^{-9} $\underline{M}$ isoproterenol. Thus CCCT cells are more sensitive to AVP and PGE_2 than are MDCK cells (5). Figure 13 illustrates the time courses for the formation of intracellular cAMP in response to supramaximal concentrations of AVP, PGE_2, and isoproterenol. Maximum increases in intracellular cAMP occurred 2-5 min after the addition of each effector.

Prostaglandin Formation by CCCT Cells. Previous immunocytochemical studies had indicated that the cortical collecting tubule has the capacity to synthesize prostaglandins (9,10). Therefore, the ability

Figure 12. Formation of adenosine 3',5'-cyclic monophosphate (cAMP) by CCCT cells in response to hormones. CCCT cells (6-10 days after isolated) were incubated with the indicated concentrations of arginine vasopressin (AVP) (●), isoproterenol (o), PGE_2 (Δ), and parathyroid hormone (PTH) (▲) at 37° for 60 min in the presence of IBMX (10^{-4} $\underline{M}$). Radioimmunoassays for extracellular cAMP were performed as described in MATERIALS AND METHODS. Statistically significant differences from control values (i.e., absence of effector) were observed at $\geq 10^{-10}$ $\underline{M}$ AVP, $\geq 10^{-8}$ $\underline{M}$ PGE_2, and $\geq 10^{-9}$ $\underline{M}$ isoproterenol ($P < 0.05$).
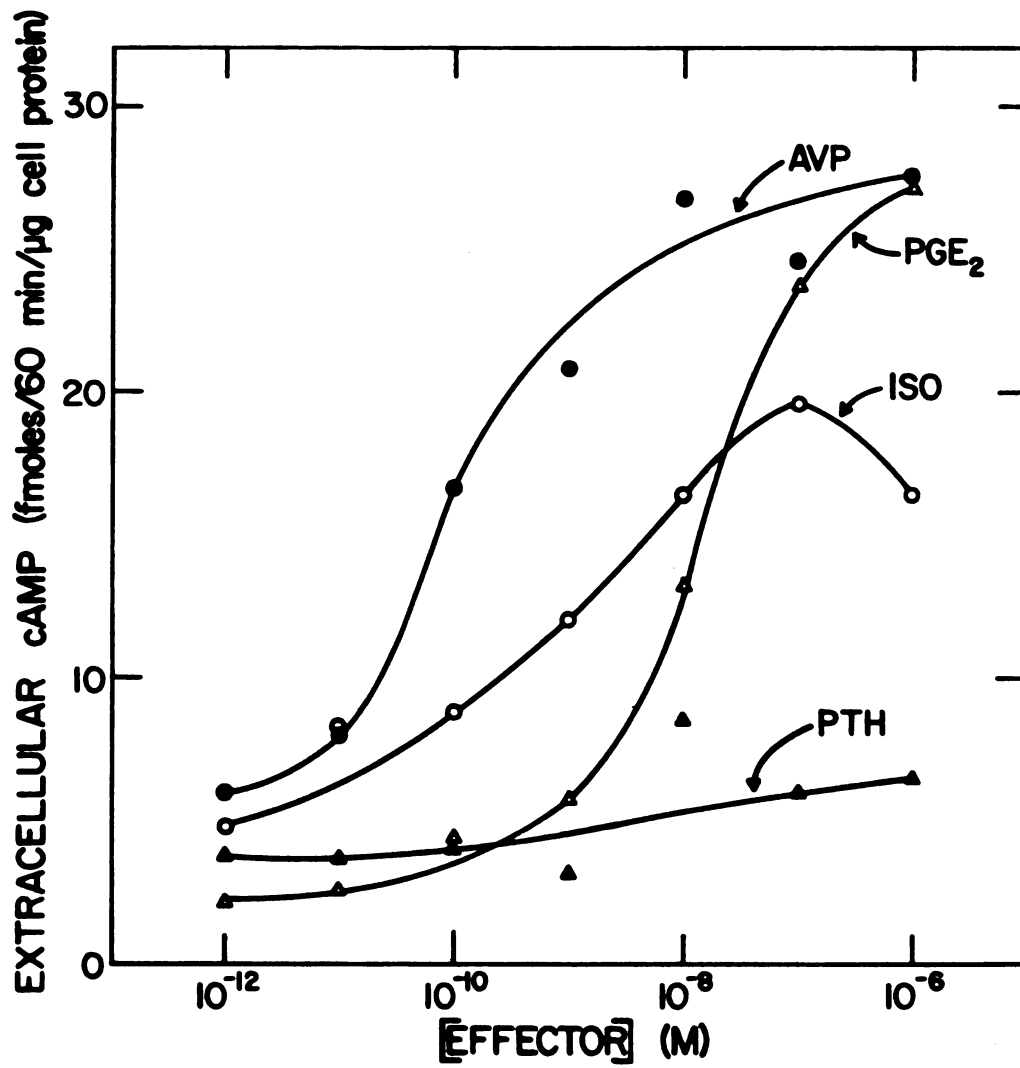
Figure 12

Figure 13. Time course for formation of intracellular cAMP by CCCT cells. CCCT cells (6-10 days after isolated) were incubated for indicated times with 10^{-6} M AVP ($\bullet$), 10^{-6} M isoproterenol (o), 10^{-6} M PGE_2 ($\triangle$), or no effector ($\blacktriangle$). Incubations were performed in the presence of 10^{-4} M IBMX. Intracellular cAMP was measured by radioimmunoassay as described in MATERIALS AND METHODS. Statistically significant differences from control values (0 min) were found at the following times: 2 and 5 min with AVP; 2, 5, and 10 min with isoproterenol; 2, 5, 10, 20, 30, and 45 min with PGE_2. No significant change from the 0-min value was observed with time in the absence of effector (P<0.05).
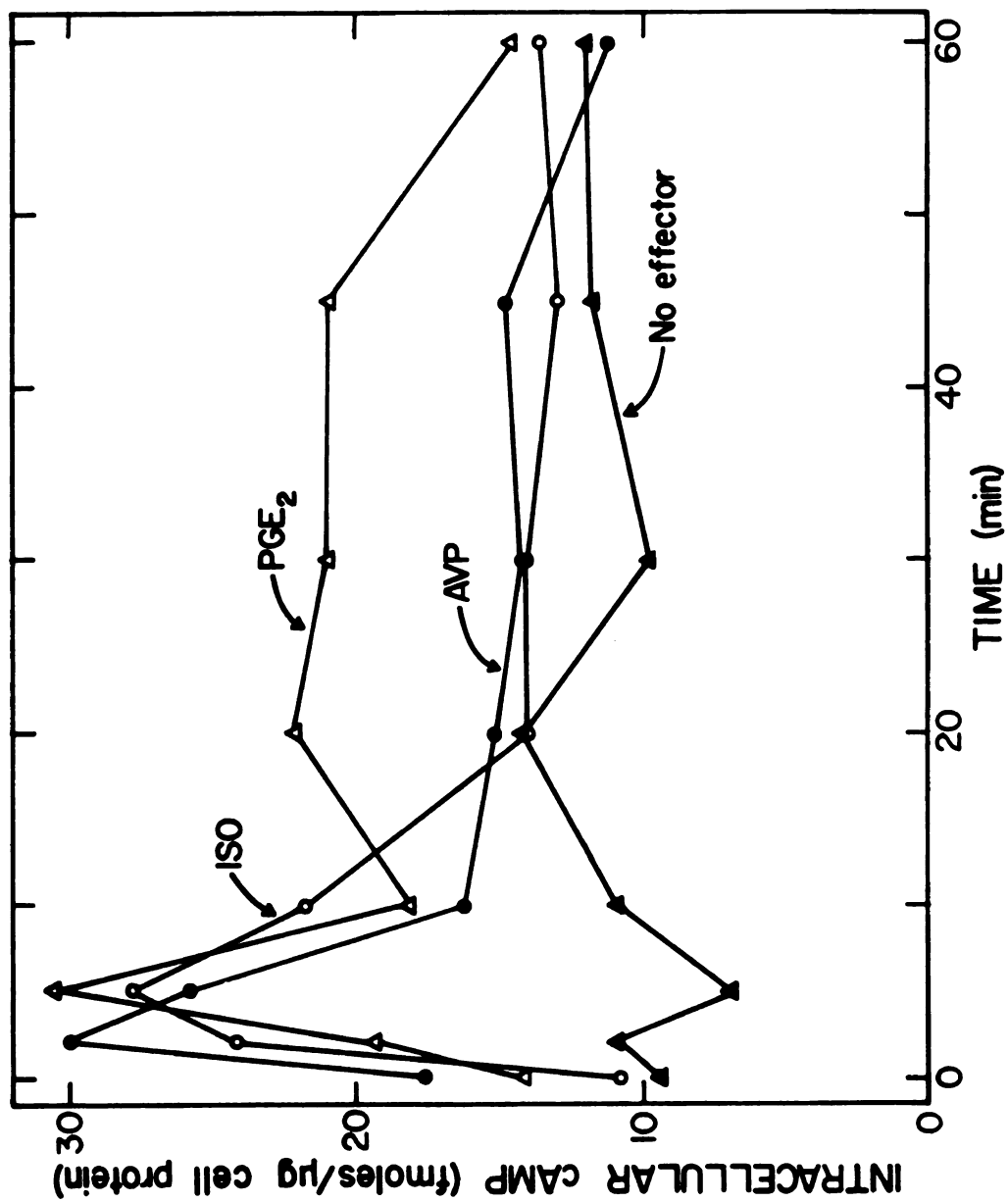
Figure 13

of CCCT cells to synthesize immunoreactive PGE_2 ($iPGE_2$) was examined. As shown in Figure 14, treatment of CCCT cells with bradykinin, AVP, or DD-AVP increased the formation of $iPGE_2$ two-to threefold; moreover, pretreatment of CCCT cells with aspirin (10^{-3} $\underline{M}$ at 37°C for 60 min) blocked the increases in $iPGE_2$ formation brought about by the effectors (Table 2). Half-maximal increases in $iPGE_2$ occurred at approximately 10^{-10} $\underline{M}$ for bradykinin, AVP, and DD-AVP. The half-maximal increases in AVP-induced $iPGE_2$ formation occurred at a concentration of AVP similar to that which caused a half-maximal increase in AVP-induced cAMP formation.

61

Figure 14. Formation of immunoreactive PGE$_2$ (iPGE$_2$) by CCCT cells
in response to bradykinin, AVP, and DD-AVP. CCCT cells
(6-10 days after isolated) were incubated with the indicated
concentrations of AVP (o), DD-AVP (▲), and bradykinin (Δ) at
37° for 60 min. Radioimmunoassays for PGE$_2$ were performed
as described in MATERIALS AND METHODS. Statistically
significant differences from control values (i.e., absence
of effector) were observed at $\geq 10^{-10}$ M for all
effectors tested (P<0.05).
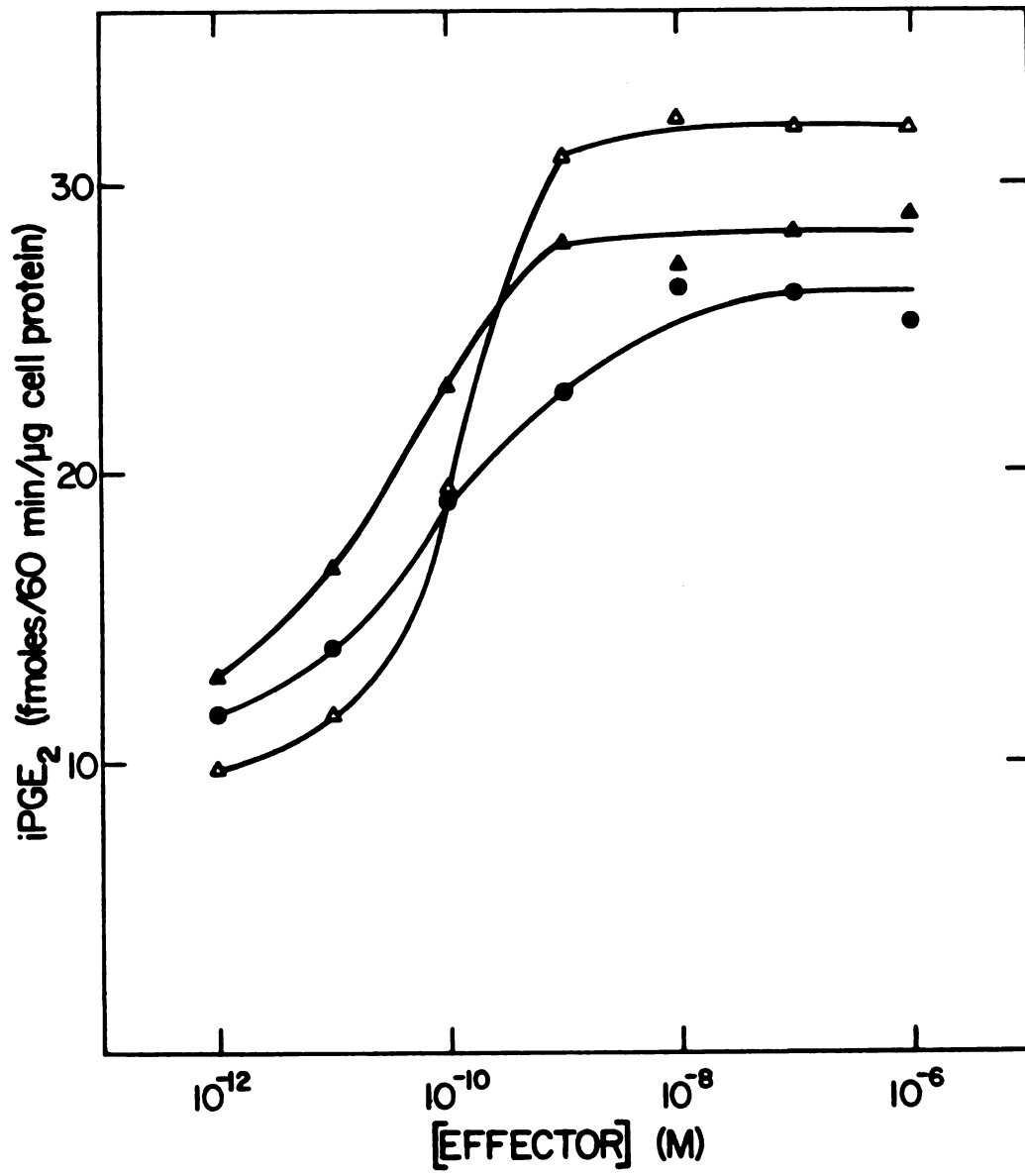
Figure 14

Table 2

Inhibition by Aspirin of Hormone-induced
Synthesis of iPGE$_2$ by CCCT Cells[a]

Hormone	iPGE$_2$, fmol·µg cell protein^{-1}·60 min^{-1}
None	6.0 ± 0.7
None + aspirin	1.8 ± 0.3
Bradykinin	*12.1 ± 1.3
Bradykinin + aspirin	2.5 ± 0.8
AVP	*12.9 ± 0.4
AVP + aspirin	2.9 ± 0.1
DD-AVP	*12.3 ± 0.4
DD-AVP + aspirin	2.7 ± 0.9

[a]Values are means ± SE. Preincubations with aspirin (10^{-3} M) were performed for 60 min at 37°C in Krebs buffer, pH 7.2. Hormone concentrations in all experiments were 10^{-6} M. *Significant change from control (none) values (P<0.05).

DISCUSSION

We have developed a selective immunoadsorption procedure for isolating up to 10^7 collecting tubule cells from a mixture of 10^9 renal cortical cells prepared from a single dog kidney. Evidence that CCCT cells are derived from the collecting tubule is as follows: 1) CCCT cells stain uniformly positive for NADH diaphorase and glycerol-3 phosphate dehydrogenase but not for succinate dehydrogenase activity, a pattern of staining unique for the collecting tubule in the canine renal cortex; 2) when examined by transmission electron microscopy, CCCT cell preparations contained only cells with morphological characteristics of intercalated and principal collecting tubule cells and not of cells derived from other cortical tubule segments; 3) CCCT cells formed hemicysts when grown in culture and exhibited a transepithelial potential difference when seeded on Millipore filters indicating that the isolated cells are transporting epithelia (129); 4) CCCT cells formed cAMP in response to AVP, PGE_2, and isoproterenol but not PTH, responses expected [by analogy to other species (130,131)] for a mixture of cortical collecting tubule cells containing both intercalated and principal cells; 5) CCCT cells formed $iPGE_2$ as anticipated from previous immunocytochemical studies (10); and 6) CCCT cells were adsorbed using antibodies selective for an antigen on the cell surface of collecting tubules. These properties are exhibited by CCCT cells that are grown in primary monolayer

cultures. The data indicate that CCCT cells can be used as a model system to study the biochemistry of cortical collecting tubules. Jefferson et al. (129) have reported the isolation and culture of a distal tubule line (JCK-5) from the canine renal cortex using defined culture media. The properties of JCK-5 cells, especially with respect to hormonal responsiveness, differ considerably from CCCT cells.

We have demonstrated the utility of cell immunoselection (132) in the special case of canine collecting tubule cells. In our studies, homogeneous populations of MDCK cells were used as the immunogen for generating monoclonal antibodies. The broader use of cell immunoselection in renal physiology depends on the generation of monoclonal antibodies specific for each of a variety of different renal cell types. It is not yet known whether this will be possible with all tubule cells. Chan et al. (133) have prepared conventional rabbit antibodies reactive with proximal tubule segments, and Herzlinger et al. (134) have prepared monoclonal antibodies to cell surface determinants of canine thick ascending limb. We have recently been able to prepare two different monoclonal antibodies against ectoantigens found only on rabbit proximal tubules and on rabbit collecting tubules, respectively (135). In related work, Savoy-Moore et al. have used anti-kallikrein monoclonal antibodies in the immunodissection procedure here described to isolate cells that contain kallikrein as an ectoenzyme (136). Most recently, using CCCT cells as immunogen, we have obtained a monoclonal antibody with specificity for a subpopulation of cells of the canine cortical collecting tubule in situ. This antibody may prove to be a useful tool in isolating homogeneous populations of principal cells or intercalated cells.

Studies on the prostaglandin biosynthetic capacity of CCCT cells
indicate that these cells, like rabbit renal papillary collecting
tubule (RPCT) cells (13), form iPGE$_2$ in response to extremely low
concentrations of bradykinin. However, in contrast to RPCT cells (13),
CCCT cells formed iPGE$_2$ in response to AVP and DD-AVP. It is not yet
clear how AVP operates to elicit iPGE$_2$ synthesis, although one would
anticipate that AVP causes the activation of a lipase system capable of
liberating arachidonic acid (19,20,26). The differences between the
AVP responses of CCCT and RPCT cells may be attributable to a segmental
variation in the source of the cells since there is evidence that AVP
also induces prostaglandin formation by cortical collecting tubules
from rabbits (84,137). It will be of considerable interest to
determine if there are other regional differences between the
AVP-prostaglandin responses in the collecting tubule.

CHAPTER III

APICAL-BASOLATERAL MEMBRANE ASYMMETRY IN CANINE CORTICAL COLLECTING

TUBULE (CCCT) CELLS: BRADYKININ, AVP, PGE_2 INTERRELATIONSHIPS

Prostaglandins have been shown to have two potent effects on the

transport properties of isolated collecting tubule segments. One

effect is to inhibit water resorption occurring in response to AVP

(11,138) and the second is to inhibit Na^+ resorption (96,137,138,

140,141). The studies reported in this Chapter were designed to

determine whether there is an apical-basolateral membrane asymmetry

either to the release of prostaglandins by CCCT cells or to the effects

of prostaglandins on cAMP metabolism in CCCT cells. These questions

were prompted in part by a report that PGE_2 acts only from the

basolateral surface of rabbit collecting tubule segments to inhibit

Na^+ resorption (96). This result suggested that PGE_2 is unable to

traverse the collecting tubule and that there is an asymmetry to PGE_2

receptors in the collecting tubule.

MATERIALS AND METHODS

Materials. [^{3}H]Inulin Methoxy (2-3 Ci/mmole), [^{3}H]PGE$_2$ (160 Ci/ mmole), [^{3}H]PGF$_{2\alpha}$ (150 Ci/mmole), [^{3}H]6-keto-PGF$_{1\alpha}$ (150 Ci/mmole), [^{3}H]Thromboxane (Tx) B$_2$ (155 Ci/mmole), [^{125}I]-adenosine 3',5'-cyclic monophosphate (cAMP) (150 Ci/mmole), ^{22}NaCl (20 Ci/mmole), and radioimmunoassay supplies for the cAMP assay were all purchased from New England Nuclear, Boston. Rabbit anti-PGE$_2$ serum was obtained from Miles Laboratories. Rabbit anti-PGF$_{2\alpha}$, rabbit anti-6-keto-PGF$_{1\alpha}$, and rabbit anti-TxB$_2$ sera and radioimmunoassay supplies for these three compounds were purchased from Seragen, Inc. PGE$_2$ was purchased from Upjohn Diagnostics, Kalamazoo, MI. SEP-PAK C$_{18}$ cartridges were purchased from Waters Associates, Milford, MA. Soluble calf skin collagen was obtained from Worthington. Dulbecco's Modified Eagle's Medium (DMEM) containing D-glucose (4.5 g/l), PSN antibiotic mixture (100X), and fetal bovine serum were purchased from GIBCO Laboratories. (Asu^{1,6},Arg^8)vasopressin (DD-AVP) was obtained from Beckman. Desmopressin Acetate (DD-AVP) was purchased from Armour Pharmaceutical Company. Arginine vasopressin (AVP) was obtained from Calbiochem-Behring. Bradykinin triacetate, 3-isobutyl-1-methylxanthine (IBMX), and L-glutamine were purchased from Sigma Chemical. Silica Gel 60 plates were obtained from E. Merck. Flurbiprofen and Ibuprofen were gifts from Dr. Udo Axen of the Upjohn Company.

Isolation and Growth of CCCT Cells on Millipore Filters. CCCT

cells were isolated by immunodissection as described in Chapter II.

The isolated cells were grown on 100 mm culture dishes in DMEM contain-

ing 10% decomplemented fetal bovine serum, PSN antibiotic mixture (1X)

(5 mg Penicillin, 5 mg Streptomycin and 10 mg Neomycin/100 ml) and 2 mM

glutamine under a water-saturated 7% CO_2 atmosphere. CCCT cells that

were to be seeded on Millipore filters were grown 3-6 weeks with weekly

changes of culture medium. Typically 3-10 x 10^6 cells were obtained

from each culture dish. CCCT cells were removed from dishes by

trypsinization and seeded at supraconfluent densities (2 x 10^6

cells/cm^2) on collagen-coated Millipore filters (0.45 um; cat. no.

HAMK 024 12) bonded to hollow polycarbonate cylinders (Figure 15). The

cylinders containing the cells were incubated in 6-well culture dishes

under the culture conditions described above. Cells were tested for

the presence of a transmembrane potential difference beginning four

days after seeding. CCCT cell monolayers were used only after they

exhibited a potential difference and were found to be impermeable to

inulin (see below). Most monolayers were also tested for and found to

exhibit a sidedness in their response to AVP. Other types of cells

used for comparison including Madin-Darby canine kidney (MDCK) cells

and Swiss mouse 3T3 fibroblasts were cultured as described previously

in Chapter II and were seeded on Millipore filters as described above

for CCCT cells.

Permeability of CCCT Cells on Millipore Filters. The permeability

of cell monolayers to inulin, PGE_2, and Na^+ was measured as

described below. All monolayers were tested for their permeability to

inulin. The medium was removed by aspiration from both the inside and outside of the polycarbonate cylinders under sterile conditions, and this chamber was placed in a fresh 6-well culture dish. A solution containing a radioactive solute was added to one side of the cell monolayer, and the same solution without the isotope was added to the other side. Typically the solution was culture medium (DMEM containing 10% decomplemented fetal bovine serum, PSN antibiotic mixture 1X and 2 mM glutamine). There were no appreciable differences in the permeability of CCCT cells to inulin or PGE_2 when comparing the culture medium to the same medium without serum or to Krebs-Ringer buffer (composition in mM: 118 NaCl, 25 $NaHCO_3$, 14 glucose, 4.7 KCl, 2.5 $CaCl_2$, 1.8 $MgSO_4$, and 1.8 KH_2PO_4), pH 7.4. Usually 1 ml was added to the inside of the cylinder (apical side of the monolayer) and 3 ml was added to the culture well in which the chamber was immersed (Figure 15). In most experiments, [^{3}H]inulin, [^{3}H]PGE_2 and $^{22}Na^+$ were used at concentrations of 10^{-7} M. After the desired incubation periods, 0.05 ml aliquots were removed from inside and outside of the cylinders and radioactivity on both sides measured by scintillation counting. Counts for each vial were normalized to the original volumes. Percentages of the total amount of radioactivity added were then calculated for each side at each time period measured. Percentage data could then be transformed, to obtain a normal distribution for further statistical analysis, by utilizing the angular (inverse sine) transformation (124).

Effector-induced cAMP Release. Medium surrounding CCCT cells grown on Millipore filters was removed under sterile conditions. The

Figure 15. CCCT cell monolayer system for studying functional asymmetry of the cortical collecting tubule. CCCT cells ($2 \times 10^6/cm^2$) seeded on a Millipore filter bonded to a hollow polycarbonate cylinder form a confluent cell monolayer with distinct apical and basolateral surfaces. The chamber stands on three legs in a culture dish. The three criteria routinely used to establish the functional polarity of these chambers (i.e., transcellular potential differences, impermeability to inulin, indicated in this figure by the arrow-traversing the chambers, and asymmetry of AVP-induced cAMP formation) are depicted.
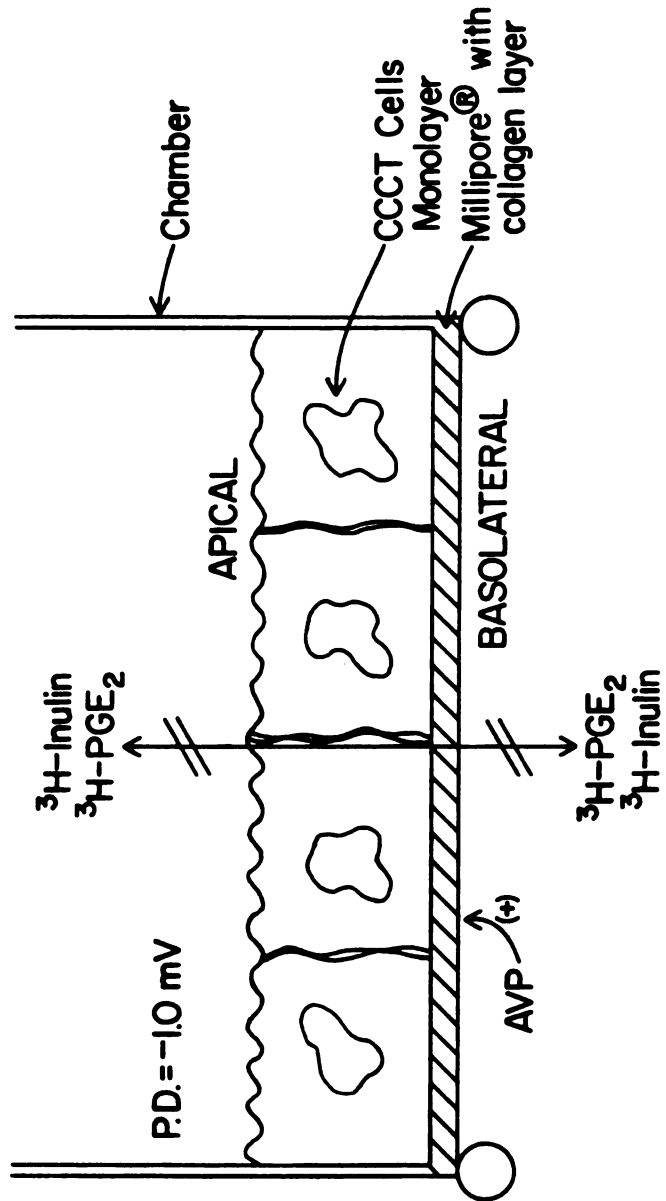
Figure 15

chambers were washed with Krebs-Ringer buffer, pH 7.4 and transferred to 12-well culture dishes (Costar). Each experiment involving only one effector (e.g., AVP) at a single concentration typically consisted of the exposure of each cell monolayer to three treatments: (a) no effector on either side (control), (b) effector present on the apical side and (c) effector on the basolateral side. Because each chamber in a given experiment received all three treatments consecutively, the order of the treatments was randomized. For each treatment an effector in Krebs-Ringer buffer, pH 7.4 containing 10^{-4} $\underline{M}$ IBMX or only buffer with IBMX (no effector) was added to the appropriate sides and incubated at 37° for different times, typically one hour. Volumes were chosen so that the fluid levels were equal on both the inside and outside of the polycarbonate chambers: 0.5 ml for inside the chambers and 1.2 ml for outside the chamber (inside the culture dish). After the desired time, liquid on each side of the monolayer was collected and lyophilized. The lyophilized samples were resuspended in equal volumes (0.3-0.5 ml) of buffer and assayed for cAMP as described previously (13) and in Chapter II. Effector dose-response curves and time courses were performed using only one treatment per chamber. All other procedures were as described above.

Effector-induced PGE$_2$ Release. The incubation procedures described above for measuring cAMP levels were used in experiments designed to measure prostaglandin formation. Krebs-Ringer buffer, pH 7.4 without IBMX was used in these experiments. The fluid containing prostaglandin released by the cells to either side of the cell monolayer was collected in individual tubes. The samples were

immediately acidified to pH 4 with 1 $\underline{M}$ citric acid and extracted twice with two volumes of ethyl ether. The ether was evaporated under a stream of nitrogen, the samples resuspended in an appropriate buffer and analyzed for immunoreactive PGE_2 as described previously (13). In a few instances, simultaneous measurements of effector-induced PGE_2 release and cAMP release were performed to determine whether significant qualitative differences occurred between sets of chambers. All effectors were used in the presence of 10^{-4} $\underline{M}$ IBMX. The fluid containing both released compounds was collected, acidified and extracted as described above for measurements of PGE_2 alone. The aqueous phase of the extracted samples (containing >90% of the cAMP present) was lyophilized and subsequently resuspended as usual for cAMP radioimmunoassays. The organic phase was evaporated under a stream of nitrogen and resuspended for PGE_2 radioimmunoassays.

Characterization of Prostaglandins Released by CCCT Cells. The release of PGE_2, $PGF_{2\alpha}$, 6-keto-$PGF_{1\alpha}$, and thromboxane B_2 by CCCT cells cultured on both Petri dishes and Millipore filters was quantitated. For CCCT cells seeded on culture dishes radioimmunoassays were performed either directly on the medium or after extraction and purification. Analysis of the prostaglandins released by CCCT cells seeded on Millipore filters was performed only on ether extracts of culture media. Purification of prostaglandins was performed as follows: media was extracted using SEP-PAK C_{18} cartridges as described by Powell (142). The methyl formate fractions containing the prostaglandins and thromboxanes were evaporated, and each of the residues was resuspended in chloroform (ca. 100 μl). These samples

were chromatographed on Silica Gel 60 plates (E. Merck). The plates were developed twice in the organic phase of ethyl acetate/trimethyl-pentane/acetic acid/water (55/25/10/50; v/v/v/v)). Prostaglandin standards were visualized with iodine vapor and regions of the plates cochromatographing with the standards were scraped into individual tubes. The silica gel was extracted three times with 2 ml of chloroform/methanol (1/1; v/v). The solvent was evaporated under a stream of nitrogen, and the samples resuspended in buffer and subjected to highly specific radioimmunoassays. The recoveries of all four prostaglandin derivatives were monitored throughout these procedures using tritiated prostaglandins. They averaged 63-65% for PGE_2, $PGF_{2\alpha}$ and TxB_2, and 45-50% for 6-keto-$PGF_{1\alpha}$.

Statistical Analysis. All experiments involving an effector-induced response were done using a minimum of three replicates per treatment. A completely random analysis of variance was used to test for differences between sample means at $P<0.05$ (124). Dunnett's test was used for comparing differences between effector means with the control mean (124). In a few instances, when it was desired to compare all the effector means to each other and not only to the control mean, Student-Newman-Keuls' test for all possible comparisons was used (124). Error bars on the figures are ± SE.

Electron Microscopy. CCCT cells seeded on Millipore filters were examined by transmission electron microscopy. Cells on the monolayers were fixed with 2% glutaraldehyde in 0.1 $\underline{M}$ sodium cacodylate, pH 7.4, for 24 h at 4°. After fixation the chambers were washed thoroughly with 0.1 $\underline{M}$ sodium cacodylate, pH 7.4. The filters containing the fixed

CCCT cells were separated from the polycarbonate cylinders. The filters were washed for 10 minutes in 0.1 $\underline{M}$ sodium cacodylate, pH 7.4 and postfixed in 1% OsO_4 in the same buffer for 4 h at 24° and then overnight at 4°. The filters were washed with sodium cacodylate buffer and dehydrated by sequential exposure to 25, 50, 70, 80, 95 (15 min each) and 100% (15 min then 1 h with a change in between) solutions of ethanol. The filters were exposed to decreasing proportions of ethanol/ acetone: 2/1, 1/2 and finally 100% acetone (twice) for 15 min each. They were carefully cut into small pieces suitable for embedding and placed into glass vials for infiltration. Infiltration was as described previously in Chapter II. The sections obtained from the blocks were counterstained with 2% lead citrate in H_2O and 2% uranyl acetate in H_2O. They were examined and photographed using a Phillips Model 201 transmission electron microscope. Kodak EM 4463 film was used for photography.

RESULTS

Orientation of CCCT Cells on Millipore Filters. In order to use

CCCT cells on Millipore filters as a model to study the sidedness of

the responses of collecting tubules to hormones, we first needed to

determine if CCCT cells, when seeded at confluency on Millipore

filters, were impermeable to small molecules and were morphologically,

electrically, and biochemically asymmetric.

CCCT cells were seeded on Millipore filters at a density of 2 x

10^6 per cm^2. Typically, these cells developed a transepithelial

potential difference of 1 ± 0.2 mV (Millipore filter side positive)

4-13 days after seeding and maintained this potential for up to an

additional 21 days. As has been reported previously for Madin-Darby

canine kidney (MDCK) cells (143), consistent results were obtained only

with cells which had previously been grown and maintained at confluency

on Petri dishes for at least 10 days prior to seeding on Millipore

filters. As shown in Figure 16, CCCT cells grown on Millipore filters

exhibited typical intercellular tight junctions and had microvilli on

their apical surfaces.

Confluent monolayers of CCCT cells on Millipore filters were

relatively impermeable to inulin in comparison to Swiss mouse 3T3

fibroblasts or to filters to which no cells had been added (Figure 17).

MDCK cells exhibited a permeability barrier which was quantitatively

77

Figure 16.   Electron photomicrographs of principal and intercalated
CCCT cells seeded on a Millipore filter in chambers. (A)
One principal and one intercalated cell. The basolateral
sides of the cells show a flattened appearance against the
filter, the presence of basement membrane, and loose
junctional complexes between the cells. At the apical
side, the cells have an abundance of microvilli and are
joined by a tight junction; (B) tight junction between the
two cells shown in (A). BM, basement membrane; PC,
principal cell; IC, intercalated cell; A, apical side; BL,
basolateral side; TJ, tight junction; IS, intercellular
space; MF, Millipore filter. Internal markers are 1 μm for
(A) and 0.1 μm for (B).
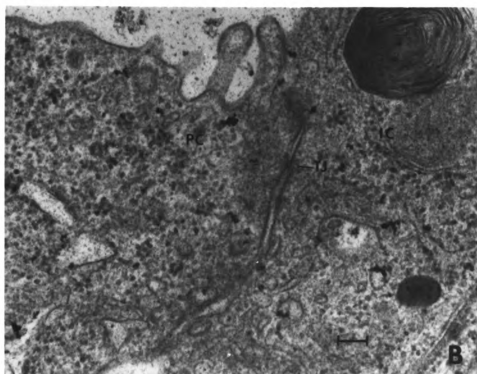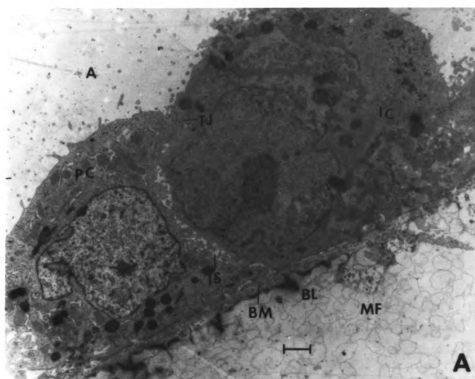
Figure 16

Figure 17. Permeability to [^{3}H]-inulin of Millipore filters seeded with CCCT cells (o), MDCK cells (●), 3T3 cells (Δ), or no cells (▲). All chambers were seeded under identical conditions using 3 x 10^6 cells per chamber (2 x 10^6 cells/cm^2). Points represent the mean values obtained from single experiments on nine different Millipore filters seeded with CCCT cells, and on six filters each seeded with MDCK cells, 3T3 cells, or no cells. [^{3}H]-inulin (100 pmoles) was added initially to the apical side. The amount of radioactivity found on each side of the monolayer at the indicated time periods was determined and used to calculate a percentage value. Identical results were obtained in similar experiments in which [^{3}H]-inulin was added initially to the basolateral side.
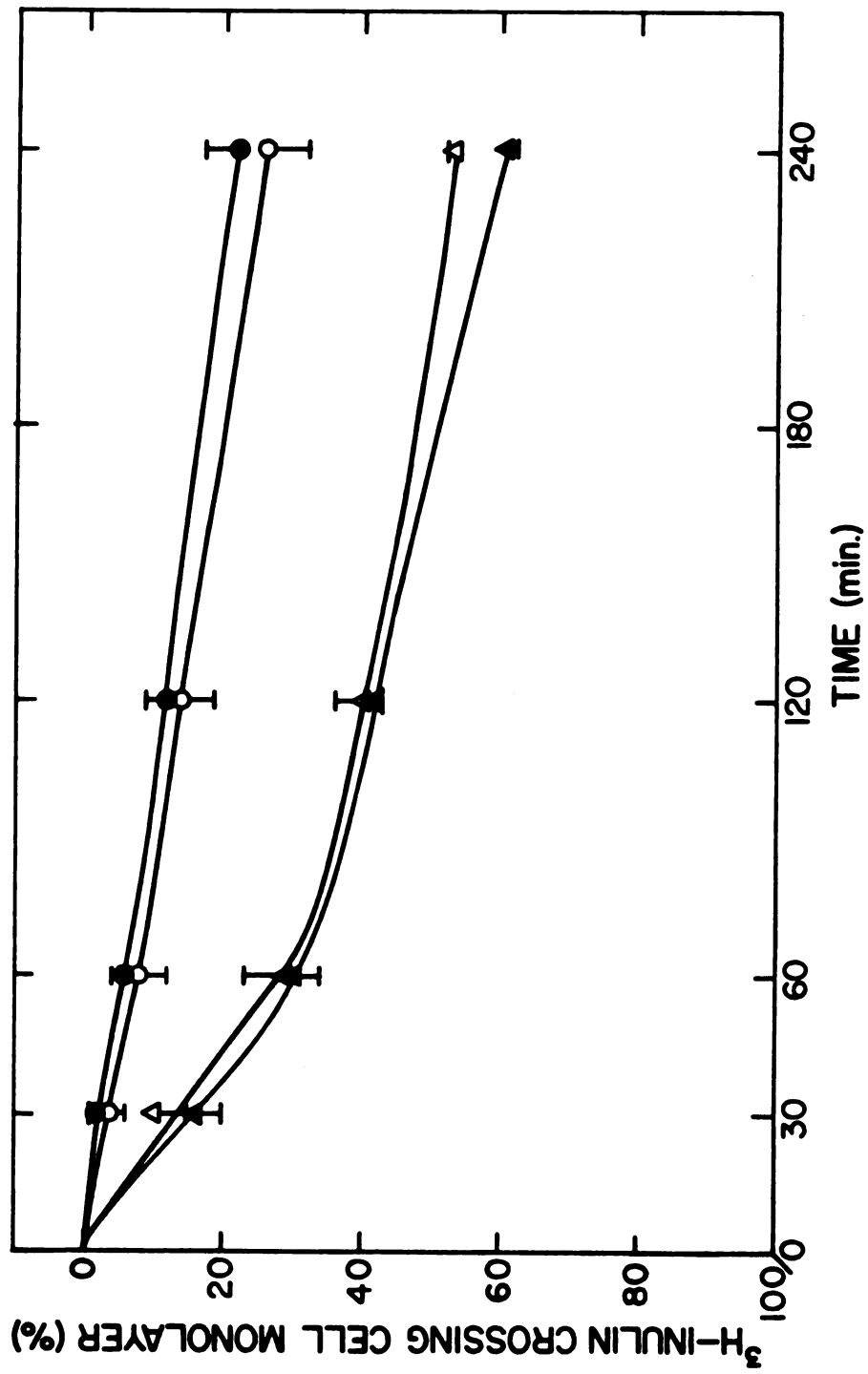
Figure 17

similar to that seen with CCCT cells. The flux of inulin across the monolayer was found to be the same in both directions.

As shown in Figure 18, PGE_2, which is the major prostaglandin product of CCCT cells (see Tables 3, 4 and 5 in this Chapter), crossed the CCCT cell monolayer at the same rate as inulin. This suggests that the only route for the movement of PGE_2 across the monolayer is pericellular. It should also be noted that less than 10% of the PGE_2 added to one side of the CCCT cell monolayer is able to cross the monolayer in 60 min; 60 min was the longest treatment time used in the studies reported below. Neither bradykinin nor AVP affected the rates of inulin (Figure 19) movement across the cell monolayer. PGE_2 movement across the cell monolayer was also unaffected by these effectors (data not shown). (No metabolism of PGE_2 was observed in these experiments.) Our results on the movement of PGE_2 are consistent with the observations of other groups which indicate that prostaglandins do not freely diffuse through cell membranes (70,72).

The sidedness of the effect of AVP on the release of cAMP by CCCT cell monolayers is shown in Figure 20. Extracellular cAMP was measured in all cases because it was impractical to sacrifice a monolayer for a single measurement of intracellular cAMP. AVP added to the basolateral surface of CCCT cells caused the release of cAMP, but even supramaximal concentrations of AVP (10^{-6} $\underline{M}$) added to the apical surface of CCCT cells failed to elicit cAMP release. cAMP was released on both sides of the monolayer, a result consistent with the observation of elevated medullary cAMP levels noted when animals are treated with antidiuretic hormone (108). To determine the time course for cAMP release (Figure 21), CCCT cells were treated for 0, 15, 30, 60, or 120 min with AVP on

83

Figure 18. Permeability of confluent CCCT cell monolayers to [^{3}H]-inulin (o), [^{3}H] PGE$_2$ ($\triangle$), and ^{22}Na+ (●). The same six chambers were used to test the fluxes of each of the solutes. Solute fluxes were measured as described in MATERIALS AND METHODS. Radiolabeled solute (100 pmoles; 10^{-7} M) was added initially to the apical side in the experiments depicted in this figure. The transcellular flux of [^{3}H]-PGE$_2$ was identical when it was added initially to the basolateral side.
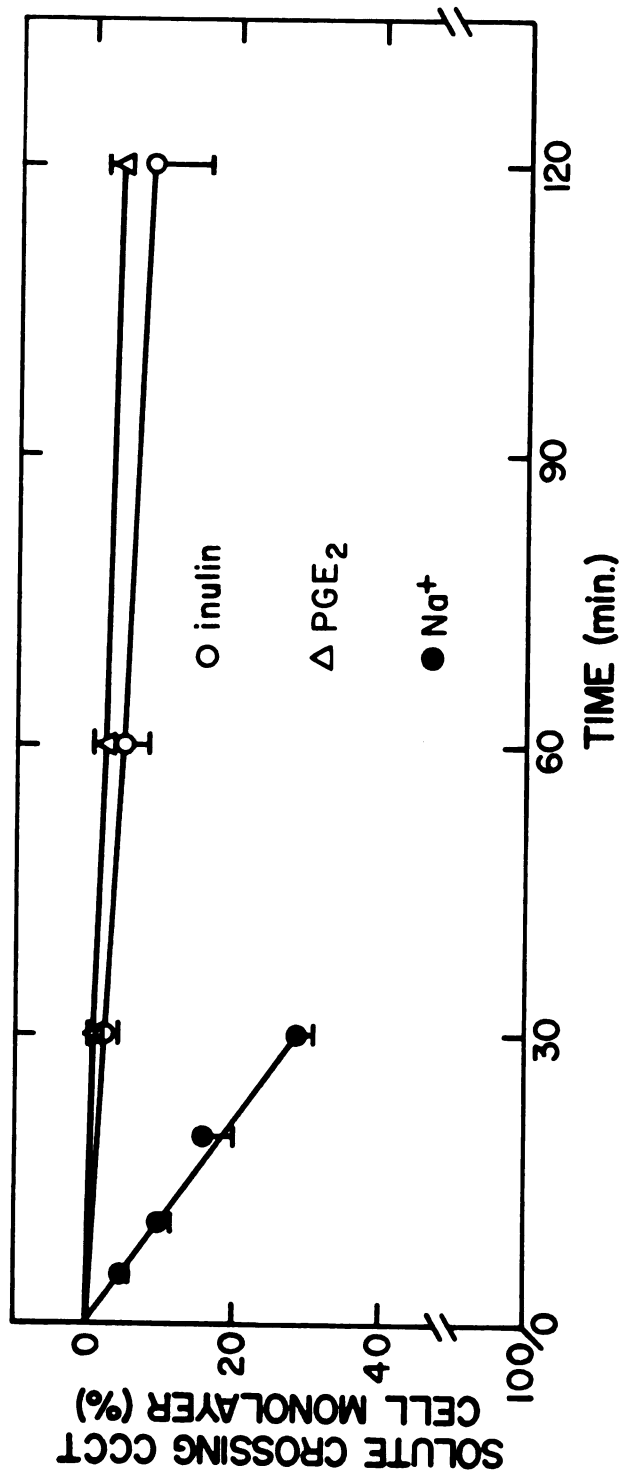
Figure 18

Table 3

Release of Prostaglandins by CCCT Cells on Culture Dishes:
Effect of Flurbiprofen[a]

Treatment	Immunoreactive Prostaglandins Released (fmoles/μg cell protein/60 min)			
	iPGE$_2$	iPGF$_{2\alpha}$	iTxB$_2$	i-6-keto-PGF$_{1\alpha}$
No Effector	5.4 ± 0.2	1.9 ± 0.1	1.4 ± 0.1	0.5 ± 0.2
No Effector + Flurbiprofen	4.3 ± 0.1	1.0 ± 0.1	1.0 ± 0.1	0.4 ± 0.2
Bradykinin	*29.6 ± 1.7	1.9 ± 0.1	1.8 ± 0.1	0.6 ± 0.1
Bradykinin + Flurbiprofen	4.8 ± 0.1	1.2 ± 0.2	1.3 ± 0.3	0.4 ± 0.1
DD-AVP	*15.3 ± 1.8	1.7 ± 0.1	1.4 ± 0.1	0.5 ± 0.2
DD-AVP + Flurbiprofen	5.9 ± 0.2	1.4 ± 0.1	1.2 ± 0.1	0.4 ± 0.1

[a]Nonconfluent CCCT cells (1 x 10^6/60 mm culture dish) were incubated for 60 min in the presence of bradykinin (10^{-6} $\underline{M}$), DD-AVP (10^{-6} $\underline{M}$) or no effector at 37° under a 7% CO$_2$ atmosphere. A 60 min incubation in the presence or absence of Flurbiprofen (10^{-3} $\underline{M}$) was performed prior to incubation with effectors. Prostaglandins were extracted and purified as described in MATERIALS AND METHODS. The data (normalized to 100% recovery for each of the four prostaglandins) are expressed per microgram cell protein and represent the mean of four replicates per treatment. *Significantly different from control values (i.e., absence of effector in the presence or absence of Flurbiprofen) ($P < 0.05$) ± SE.

Table 4

Release of Prostaglandins by CCCT Cells on Culture Dishes: Effect of Aspirin[a]

Treatment	Immunoreactive Prostaglandins Released (fmoles/μg cell protein/60 min)			
	$iPGE_2$	$iPGF_{2\alpha}$	$iTxB_2$	$i-6-keto-PGF_{1\alpha}$
No Effector	5.9 ± 0.1	7.1 ± 0.2	7.1 ± 0.2	4.6 ± 0.1
No Effector + Aspirin	4.6 ± 0.1	8.2 ± 0.2	8.2 ± 0.3	4.6 ± 0.1
Bradykinin	*43.3 ± 0.2	9.7 ± 0.4	9.6 ± 0.4	6.4 ± 2.2
Bradykinin + Aspirin	8.6 ± 0.7	8.7 ± 1.3	9.7 ± 0.6	5.1 ± 1.4
DD-AVP	*22.9 ± 1.6	7.8 ± 0.3	7.7 ± 0.2	5.2 ± 1.2
DD-AVP + Aspirin	8.9 ± 0.6	8.3 ± 1.2	7.6 ± 1.0	4.5 ± 0.1

[a]Nonconfluent CCCT cells (1×10^6/60 mm culture dish) were incubated for 60 min in the presence of bradykinin (10^{-6} $\underline{M}$), DD-AVP (10^{-6} $\underline{M}$) or no effector at 37° under a 7% CO_2 atmosphere. A 60 min incubation in the presence or absence of aspirin (10^{-3} $\underline{M}$) was performed prior to incubation with effectors. Bathing solutions were analyzed by radioimmunoassays without prior purification as described in MATERIALS AND METHODS. The data are expressed per microgram cell protein and represent the mean of six replicates per treatment. *Significantly different from control values (i.e., absence of effector in the presence or absence of aspirin) (P<0.05) ± SE.

Table 5

Release of Prostaglandins by CCCT Cells on Millipore Filters[a]

Treatment	Immunoreactive Prostaglandins Released (pmoles/60 min/chamber)			
	$iPGE_2$	$iPGF_{2\alpha}$	$iTxB_2$	$i\text{-}6\text{-}keto\text{-}PGF_{1\alpha}$
No Effector	3.5 ± 0.1	2.7 ± 0.8	2.8 ± 0.7	1.8 ± 0.3
Bradykinin	$*12.3 \pm 0.4$	3.2 ± 0.3	3.4 ± 0.2	1.3 ± 0.5
DD-AVP	$* 8.6 \pm 0.7$	2.4 ± 0.2	3.1 ± 0.1	2.1 ± 1.1

[a]CCCT cells cultured on chambers were incubated for 60 min in the presence of bradykinin (10^{-6}M), DD-AVP (10^{-6}M) or no effector at 37° under a 7% CO_2 atmosphere. Medium from both sides of the monolayer was pooled and analyzed for immunoreactive prostaglandins without prior purification as described in MATERIALS AND METHODS. The data represent the mean of three replicates per treatment.
*Significantly different from control values (i.e., absence of effector) ($P<0.05$) ± SE.

Figure 19. Permeability to $[^3H]$-inulin of CCCT cell monolayers on Millipore filters in the presence of effectors. $[^3H]$-inulin (100 pmoles) was added initially to the apical side. All effectors were present at 10^{-6} $\underline{M}$ on both sides of the monolayer. Each graph represents the mean of triplicate chambers. No significant difference from the permeability of control chambers (i.e., no effector) was found.
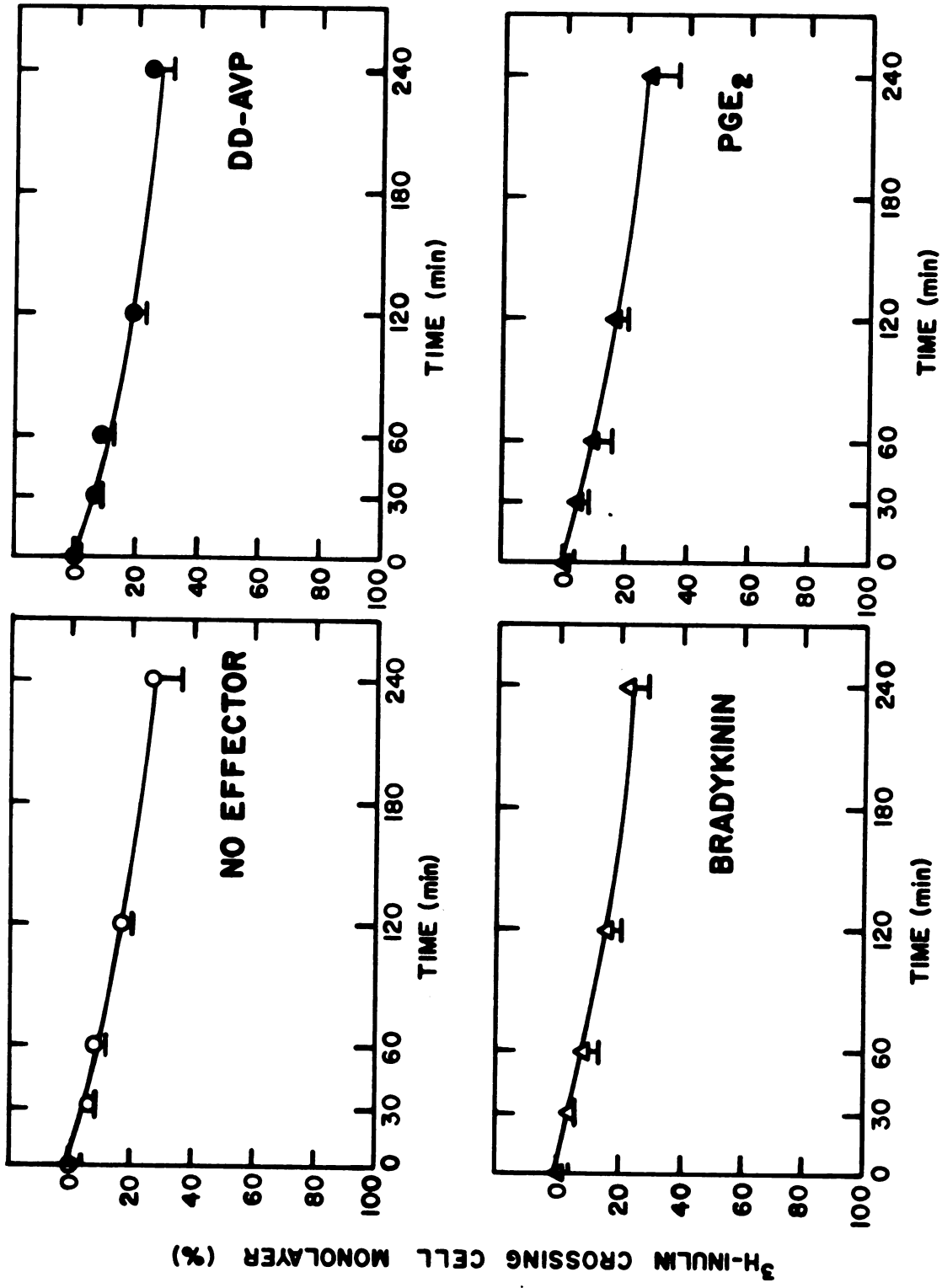
Figure 19

Figure 20. Sidedness of DD-AVP effect on cAMP release from CCCT cell monolayers on Millipore filters. Indicated on the horizontal axis is the side of release of cAMP: A, apical and BL, basolateral. The bars indicate the release in response to no effector or to 10^{-6} M DD-AVP added to either the apical (A) or basolateral (BL) side of the monolayer. The data represent the mean of six chambers. All treatments were at 37° for 60 min in the presence of 10^{-4} M IBMX. Radioimmunoassays for extracellular cAMP were performed as described in MATERIALS AND METHODS. *Significantly different from control values (i.e., absence of DD-AVP) (P<0.05).

Figure 20

92
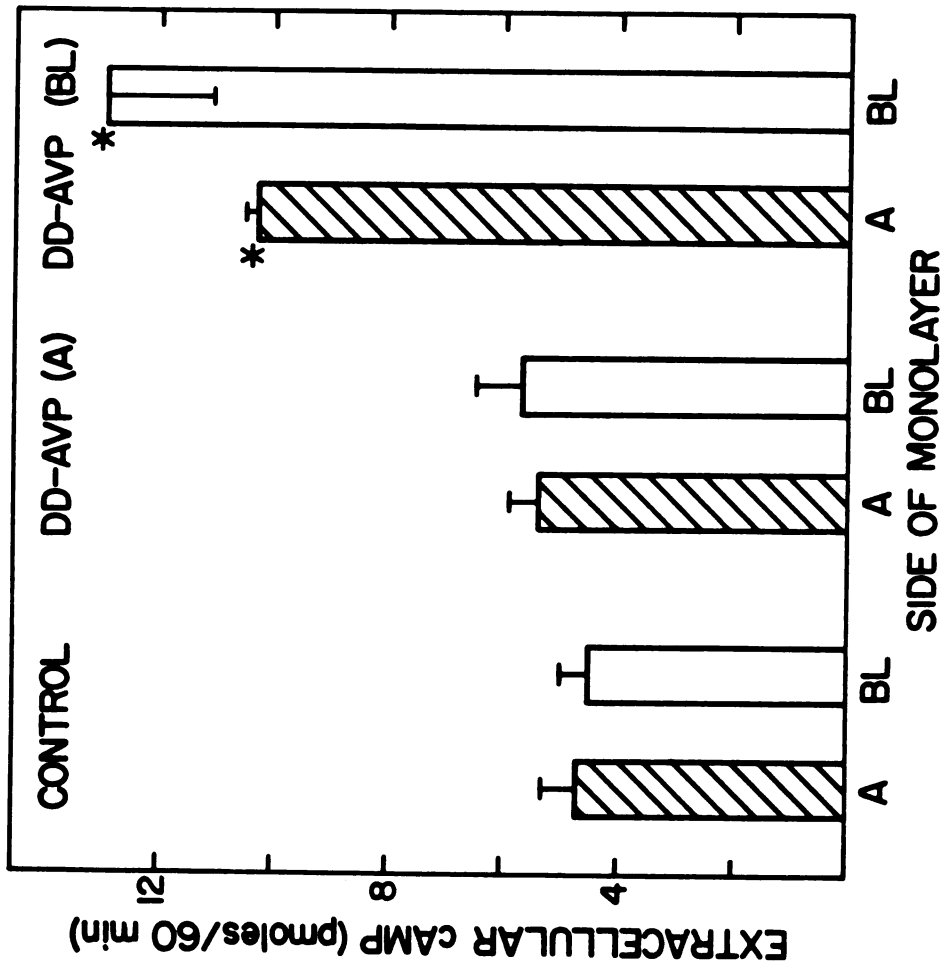
Figure 21. Time course of cAMP release from CCCT cells seeded on Millipore filters. Cell monolayers were incubated at 37° in the presence of 10^{-4} M IBMX for the indicated time periods with no effector (Δ), or with 10^{-6} M DD-AVP added to the basolateral (o) or the apical (●) side. Media from both sides of the monolayer were pooled and analyzed for cAMP as described in MATERIALS AND METHODS. Each point represents the mean of triplicate chambers. *Significantly different from control values (i.e., absence of effector)(P<0.05).
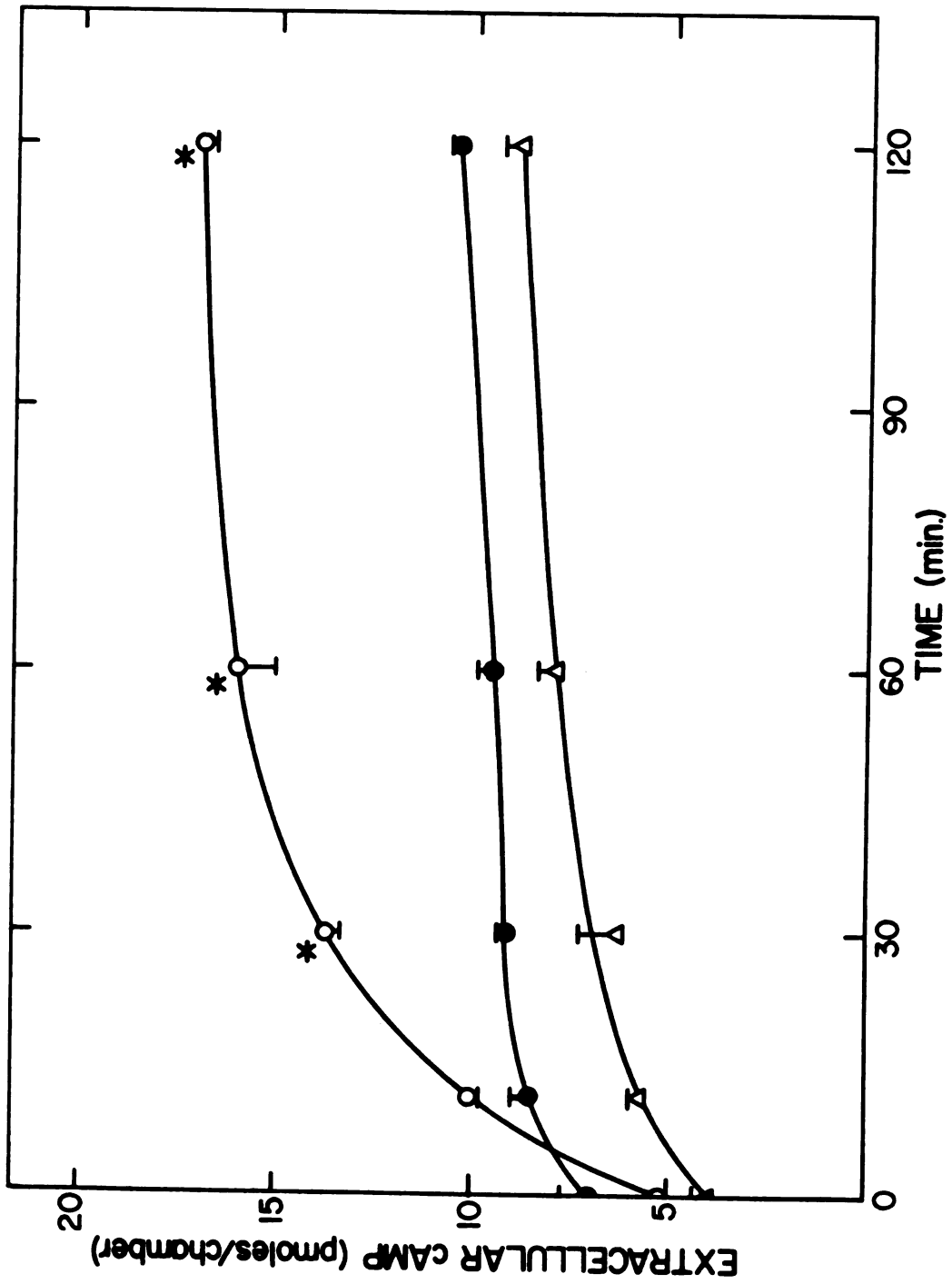
Figure 21

either the apical or basolateral side of the cells. Maximal levels of cAMP in the medium were seen 60 min after addition of AVP to the basolateral surface; AVP added to the apical surface did not increase extracellular cAMP above those levels seen without AVP. Results on the time course of release of cAMP are typical of those observed with cultured epithelial cells (5). Half-maximal release of cAMP occurred at a basolateral AVP concentration of approximately 10^{-10} $\underline{M}$ (Figure 22). This result is quantitatively similar to that seen with CCCT cells grown on plastic culture dishes (Chapter II, Figure 12). These results suggest that AVP can act only from the basolateral surface of CCCT cell monolayers to cause cAMP formation.

Prostaglandin Synthesis by CCCT Cells. It was shown previously that immunoreactive PGE_2 was formed in response to AVP and bradykinin by CCCT cells cultured on Petri dishes (Chapter II, Figure 14 and Table 2). To determine if PGE_2 was the major prostaglandin product, analyses of the prostaglandins formed by CCCT cells were performed. Prostaglandins were extracted from the media surrounding CCCT cells treated with no effector or with AVP or bradykinin. The prostaglandins were separated by thin layer chromatography and the materials in the regions cochromatographing with PGE_2, $PGF_{2\alpha}$, TxB_2 and 6-keto-$PGF_{1\alpha}$ standards were eluted from the silica gel and analyzed by specific radioimmunoassays (Table 3). The results indicate that the major product formed both in the presence and absence of AVP and bradykinin was PGE_2. Small amounts of other prostanoids were also detected but, unlike PGE_2, the amounts of these other products did not increase following treatment of CCCT cells with AVP or bradykinin.

Figure 22. Concentration dependence for the DD-AVP-induced release of cAMP from CCCT cell monolayers on Millipore filters. DD-AVP was added at the indicated concentrations exclusively to the basolateral side of the monolayer. Incubations were performed at 37° for 60 min in the presence of 10^{-4} M IBMX. Media from both sides of the monolayer were pooled and analyzed for cAMP as described in MATERIALS AND METHODS. Each point represents the mean of triplicate chambers. *Significantly different from control values (i.e., absence of DD-AVP) (P<0.05).
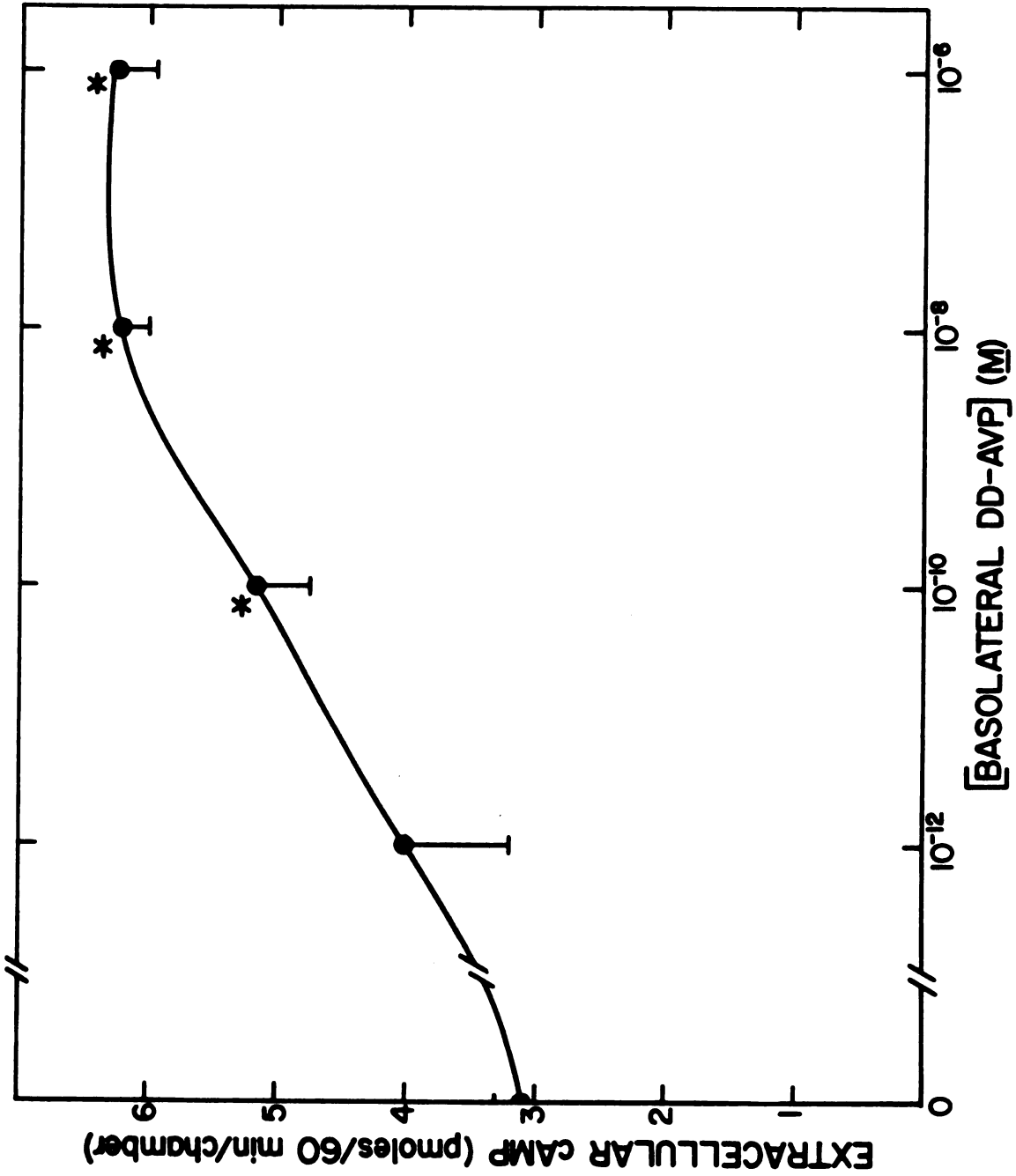
Figure 22

Almost identical data were obtained when medium surrounding the cells was analyzed by radioimmunoassays without prior extraction (Table 4).

Prostaglandin radioimmunoassays were also performed on media pooled from the basolateral and apical surfaces of CCCT cells on Millipore filters following addition of AVP or bradykinin to both sides of the cell monolayer. Again, PGE_2 was found to be the major prostaglandin product (Table 5). PGE_2 has now been found to be the primary prostaglandin formed by preparations of rabbit, canine and rat cortical and papillary collecting tubules (13,84,144).

The effects on PGE_2 release of AVP and of bradykinin added to either the apical or basolateral side of CCCT cells on Millipore filters was examined. As shown in Figure 23, AVP caused an increase in the release of PGE_2 when added to either the apical or basolateral side of the cells. Half-maximal increases in PGE_2 release were observed at approximately 10^{-10} $\underline{M}$ AVP (Figure 23); the half-maximal concentration for AVP-induced PGE_2 release was the same for AVP added to either side of the cell monolayer (Figure 23) and was about the same as that observed for the release of cAMP (occurring when AVP was added to the basolateral side of the cells)(Figure 22). The amounts of PGE_2 found on the apical and on the basolateral side of the cells were comparable both in the case of treatment with no effector or with AVP added to either the apical or basolateral surface (Figure 24). Thus, PGE_2 was released on both sides of the monolayer in response to AVP added to either side of the monolayer.

Although AVP was effective in eliciting PGE_2 release when added to either side of the cell monolayer, bradykinin caused PGE_2 release only when added to the apical surface of the CCCT cell monolayer

Figure 23. Concentration dependence for the DD-AVP-induced release of $iPGE_2$ by CCCT cells on Millipore filters. The chambers were incubated at 37° for 60 min with the indicated concentrations of DD-AVP added to either the basolateral (o) or apical (●) side of the CCCT cell monolayers. Media from both sides of the monolayer were pooled and analyzed for $iPGE_2$ as described in MATERIALS AND METHODS.
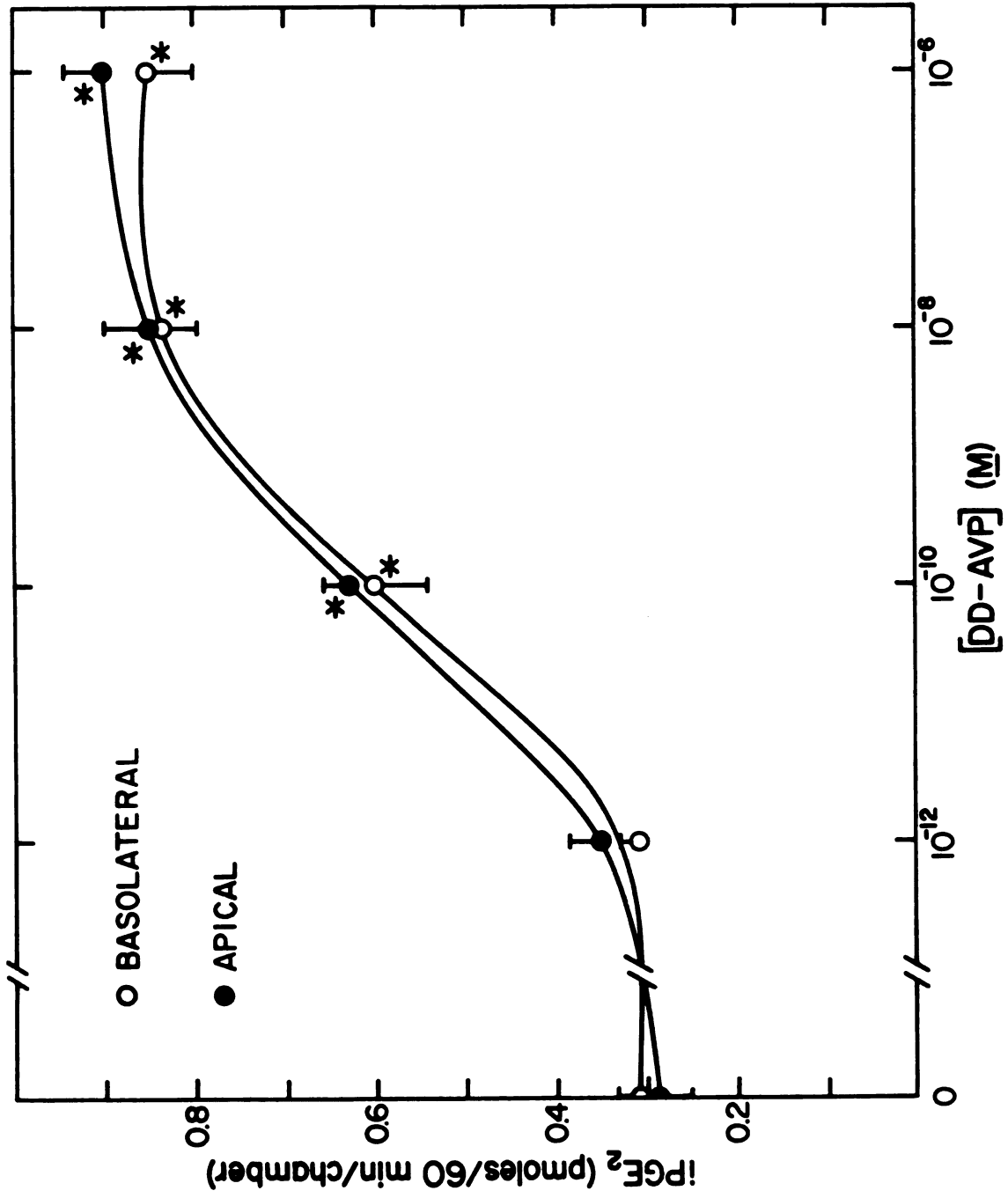
Figure 23

Figure 24. Sidedness of DD-AVP effect on the release of $iPGE_2$ from CCCT cells on Millipore filters. The bars indicate the amount of $iPGE_2$ measured on the apical (A) or basglateral (BL) side of the cell monolayers following treatment with no effector or with 10^{-6} $\underline{M}$ DD-AVP added to the apical (A) or basolateral (BL) side of the cell monolayers. All treatments were performed at 37° for 60 min. Radioimmunoassays for PGE_2 were as described in MATERIALS AND METHODS. *Significantly different from control values ($P<0.05$).
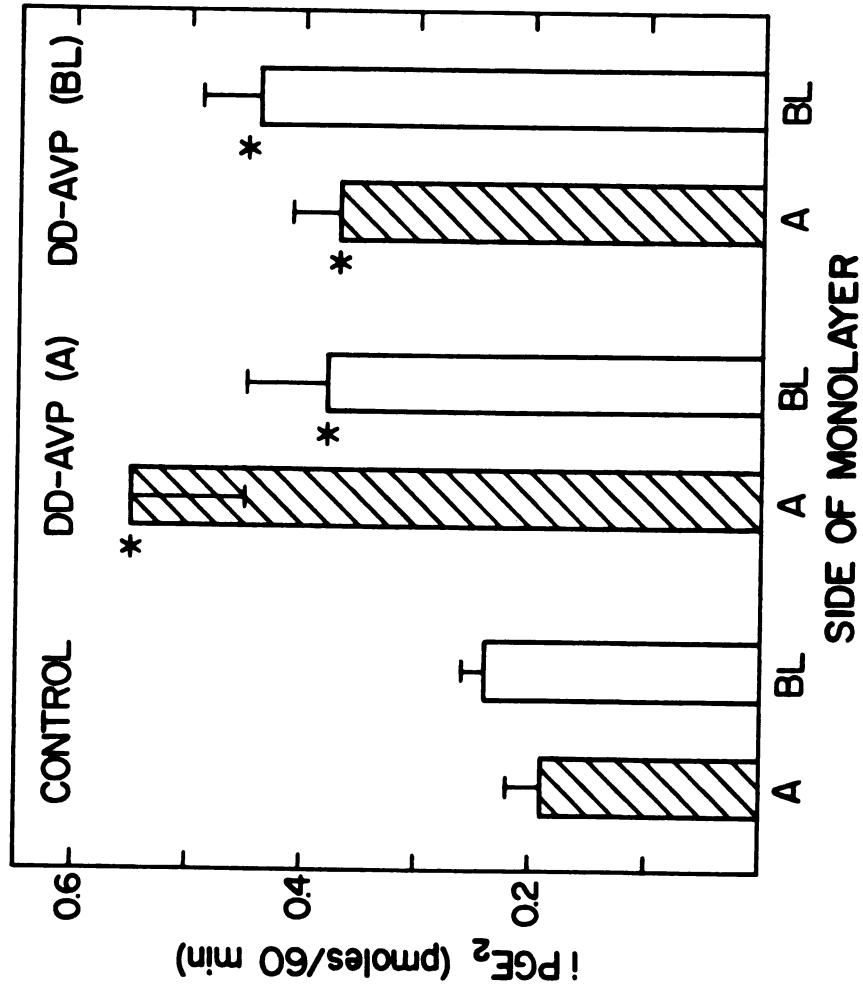
Figure 24

(Figure 25). As shown in Table 6, PGE_2 was found on both sides of the monolayer at different times after the addition of bradykinin to the apical side indicating that PGE_2 was released on both sides of the monolayer. Following bradykinin treatment the amount of PGE_2 found on the basolateral side of the monolayer tended to be 1.5-2 times greater than that found on the apical side (Figure 25); however, this difference was not statistically significant, and the concentration of PGE_2 on each side of the monolayer was the same (ca. 4×10^{-9} $\underline{M}$). In experiments where simultaneous measurements of effector-induced PGE_2 release and cAMP release were performed, qualitatively equivalent results as described above were obtained (Table 7).

PGE_2-induced Release of cAMP from CCCT Cells. PGE_2 was tested at a variety of concentrations and on either side of CCCT cell monolayers for its ability to elicit the release of cAMP. Significant cAMP release was observed with $\geq 10^{-8}$ $\underline{M}$ PGE_2, and there was no difference in the dose-response curves for PGE_2 added to either the basolateral or apical surfaces (Figure 26). Thus, PGE_2, unlike AVP, can act from either side of the CCCT cell to cause cAMP release. As with AVP induction, the cAMP produced was released into both sides of the monolayer (Figure 27).

Figure 25. Sidedness of bradykinin effect on the release of iPGE$_2$
from CCCT cells on Millipore filters. Each bar indicates
the amount of iPGE$_2$ measured on the apical (A) or
basolateral (BL) side of cell monolayers following
treatment with no effector or with bradykinin (10^{-6} M)
added to either the apical (A) or basolateral (BL) side of
the monolayer. The data represent the mean of six
chambers. All treatments were performed at 37° for 60 min.
Radioimmunoassays for PGE$_2$ were as described in MATERIALS
AND METHODS. *Significantly different from control values
(P<0.05).
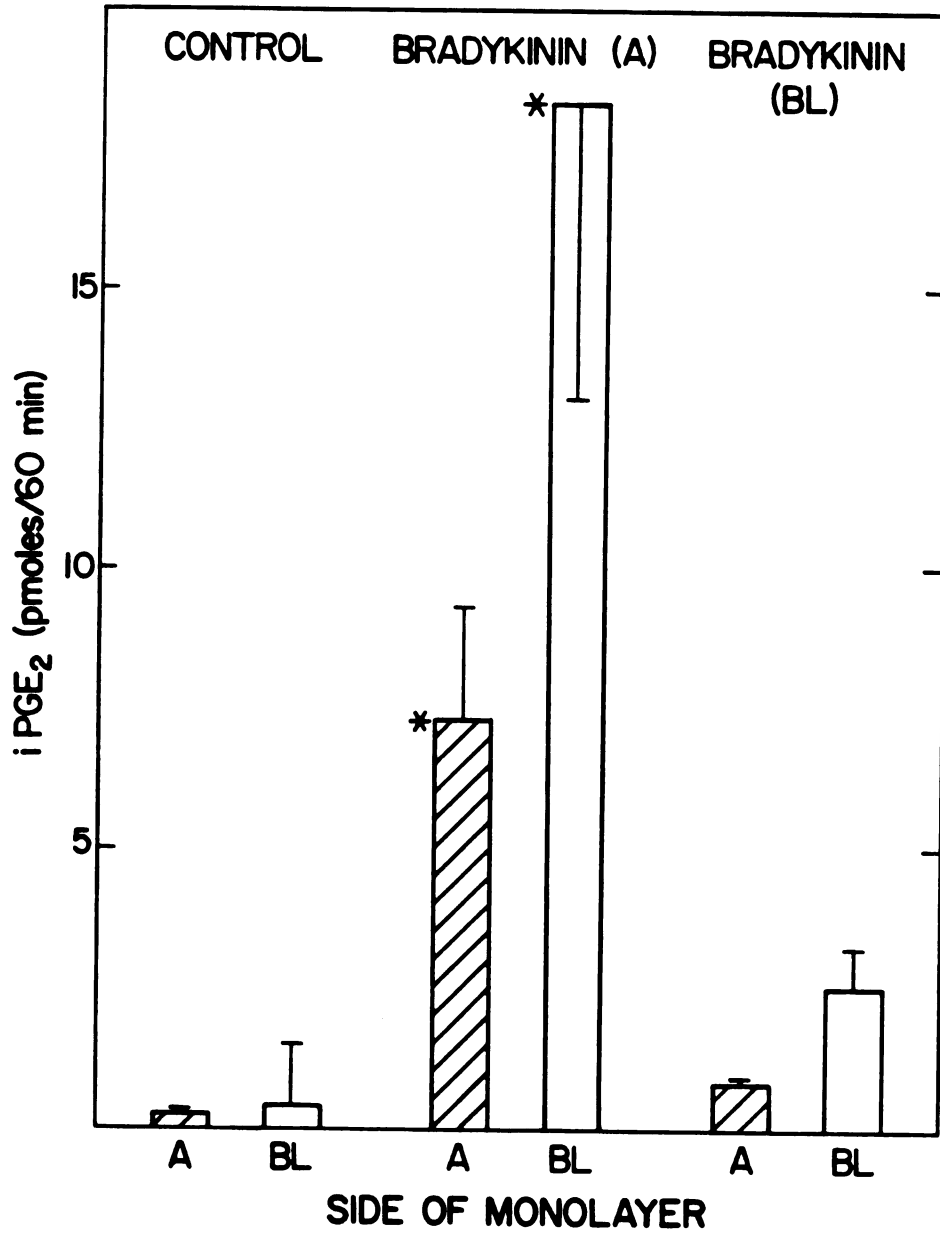
Figure 25

Table 6

Time Course of Bradykinin-Induced Release of PGE_2 by CCCT Cells on Millipores Filters[a]

Treatment	Immunoreactive PGE_2 (pmoles/chamber)	
	Apical Side	Basolateral Side
No Effector, 60 min	2.3 ± 0.2	3.0 ± 0.5
Bradykinin, 0 min	2.3 ± 0.3	2.1 ± 0.2
Bradykinin, 2 min	2.1 ± 0.3	4.3 ± 1.5
Bradykinin, 4 min	$*5.9 \pm 2.0$	$*4.5 \pm 0.5$
Bradykinin, 10 min	$*4.6 \pm 1.2$	$*5.5 \pm 0.7$
Bradykinin, 60 min	$*4.7 \pm 0.7$	$*5.7 \pm 1.2$

[a]Millipore filters seeded with 3×10^6 CCCT cells per chamber (2×10^6 cells/cm^2) were incubated for the indicated times in the presence of bradykinin (10^{-6} $\underline{M}$ on the apical surface) or with no effector at 37° under a 7% CO_2 atmosphere. After the indicated incubation time, medium was removed from each side of the monolayer and assayed for immunoreactive PGE_2 as described in MATERIALS AND METHODS. The data represent the mean of two replicates per treatment. *Significantly different from control values (i.e., after 60 min in the absence of effector) ($P<0.05$) $\pm$ SE.

Table 7

Effector-induced Release of PGE$_2$ and cAMP by CCCT Cells
on Millipore Filters[a]

Treatment	Immunoreactive PGE$_2$ (pmoles/60 min/chamber)		Extracellular cAMP (pmoles/60 min/chamber)	
	Apical Side	Basolateral Side	Apical Side	Basolateral Side
No Effector	1.5 ± 0.2	1.8 ± 0.1	2.3 ± 0.1	2.1 ± 0.3
Bradykinin (A)	*4.8 ± 0.4	*5.7 ± 0.2	3.2 ± 0.2	3.1 ± 0.1
Bradykinin (BL)	2.0 ± 0.1	2.4 ± 0.1	1.9 ± 0.4	2.6 ± 0.1
AVP (A)	*3.5 ± 0.2	*3.4 ± 0.1	2.8 ± 0.3	2.2 ± 0.2
AVP (BL)	*3.2 ± 0.3	*3.8 ± 0.2	*6.6 ± 0.4	*6.9 ± 0.6

[a]CCCT cells cultured on chambers were incubated for 60 min in the presence of bradykinin
(10^{-6} $\underline{M}$) or AVP (10^{-6} $\underline{M}$) on the apical (A) or basolateral (BL) side of the monolayer, or
with no effector, at 37° under a 7% CO_2 atmosphere. All incubations were in the presence of
10^{-4} $\underline{M}$ IBMX. Medium from either side of the monolayer was treated as described in MATERIALS
AND METHODS for final analysis by radioimmunoassays. The data represent the mean of triplicate
chambers per treatment. *Significantly different from control values (i.e., absence of
effector)(P<0.05) ± SE.

107

Figure 26. Concentration dependence for the PGE_2-induced release of cAMP from CCCT cell monolayers on Millipore filters. PGE_2 was added at the indicated concentrations to either the apical (o) or basolateral (●) side of the CCCT cell monolayers. Incubations were performed at 37° for 60 min in the presence of 10^{-4} M IBMX. Media from both sides of the monolayers were pooled and analyzed for cAMP as described in MATERIALS AND METHODS. Each point represents the mean of triplicate chambers. *Significantly different from control values (i.e., absence of PGE_2) (P<0.05).
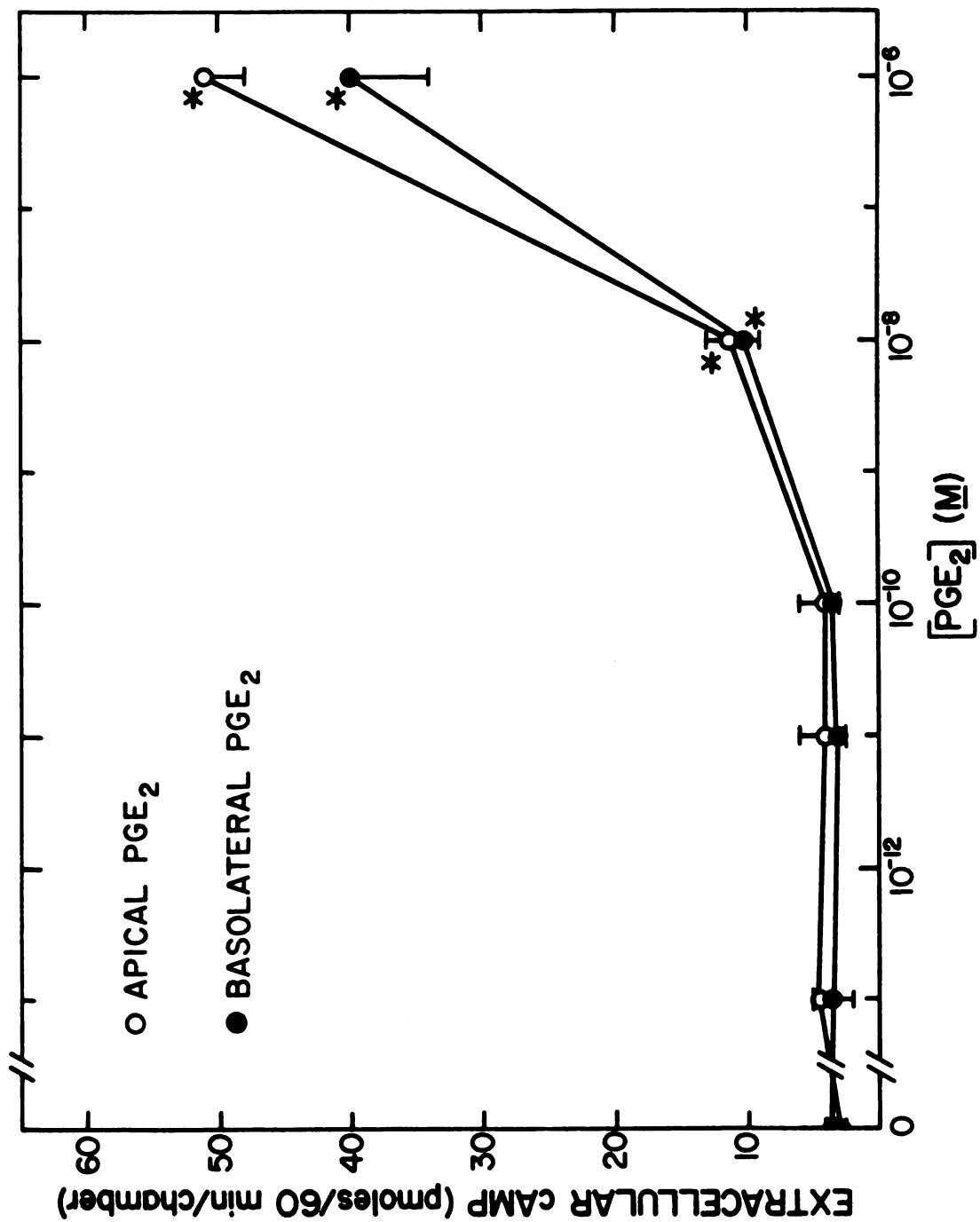
Figure 26

Figure 27. Sidedness of PGE_2 effect on cAMP release from CCCT cell monolayers on Millipore filters. The bars indicate the amount of extracellular cAMP measured on the apical (A) or the basolateral (BL) side of cell monolayers following treatment with no effector or with 10^{-6} M PGE_2 added to the apical (A) or basolateral (BL) side. The data represent the mean of six chambers. All treatments were performed at 37° for 60 min in the presence of 10^{-4} M IBMX. Radioimmunoassays for extracellular cAMP were performed as described in MATERIALS AND METHODS. *Significantly different from control values (i.e., absence of PGE_2) ($P < 0.05$).
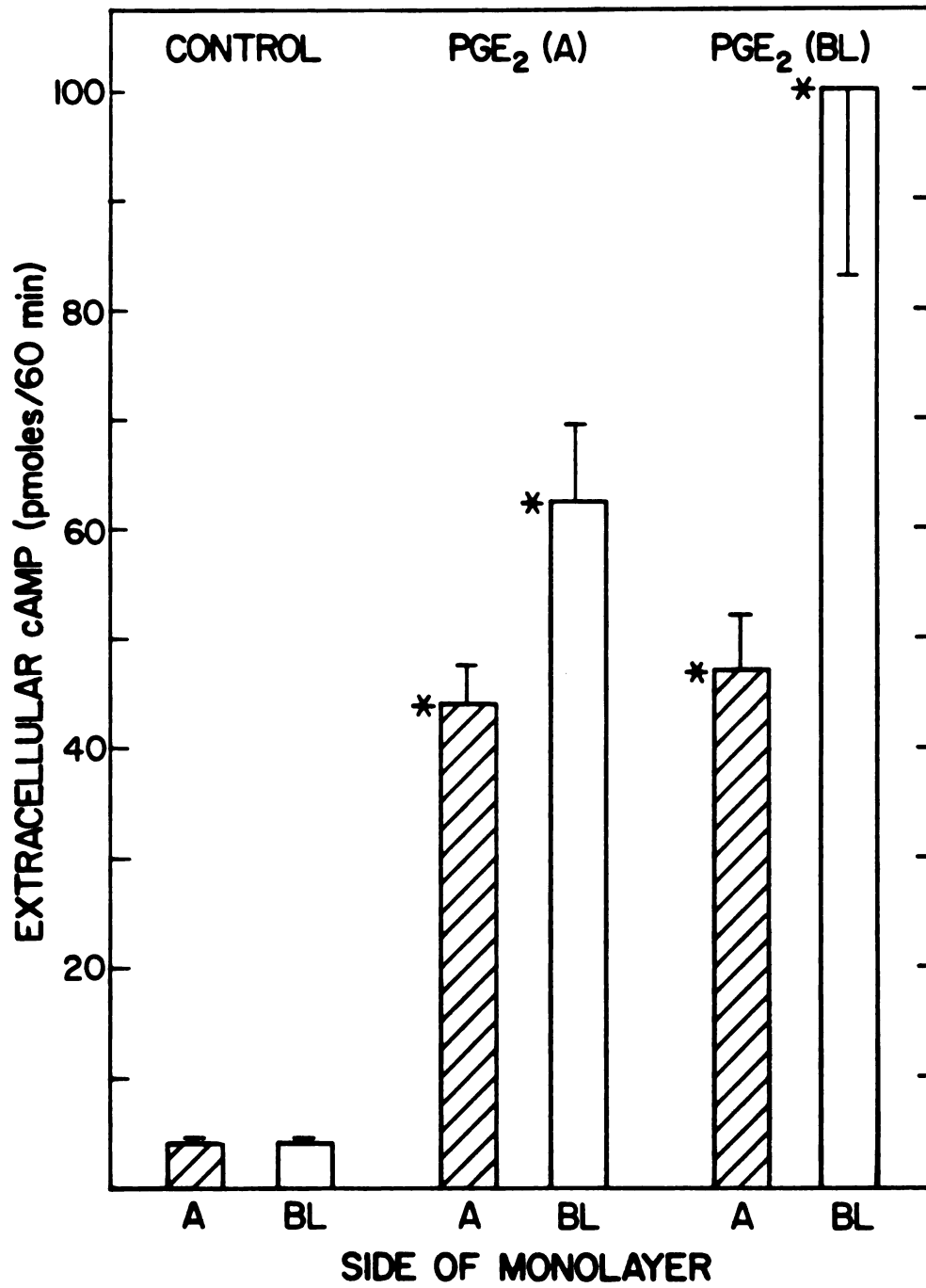
Figure 27

DISCUSSION

CCCT Cells on Millipore Filters. The initial goal of the studies reported here was to test the concept that there is a sidedness to the release of prostaglandins from CCCT cells and to the effects of prostaglandins on cAMP metabolism by CCCT cells. This hypothesis developed from the observations of Stokes and Kokko that PGE_2 inhibited Na^+ resorption when added to the basolateral but not the luminal surface of segments of rabbit cortical collecting tubule (96). The CCCT cell-Millipore filter system was developed to examine the sidedness of prostaglandin biosynthesis and function. The criteria which have qualified this CCCT cell system for use in these studies are as follows: (a) CCCT cells were morphologically asymmetric as determined by TEM; (b) CCCT cells exhibited a transcellular potential difference of the appropriate sign; (c) CCCT cells were impermeable to both inulin and PGE_2 and (d) CCCT cells formed cAMP in response to AVP added to the basolateral but not the apical surface of the cell monolayer. Although MDCK cells also exhibit some of these properties (4,5,143-145), this is the first time that a sidedness to the response of cells on Millipore filters to a hormone (AVP) has been demonstrated.

Functional Asymmetry of CCCT Cells. The major findings on aspects of asymmetry are: (a) that PGE_2 is released from both the

111

basolateral and apical surfaces of CCCT cells, (b) that PGE_2 functions to elevate cAMP in CCCT cells when added to either the basolateral or apical side, (c) that bradykinin acts only from the apical surface of CCCT cells to elicit prostaglandin formation, and (d) that AVP can act from either the apical or basolateral surface to cause prostaglandin production by CCCT cells.

Our studies on the biosynthesis of prostaglandins by CCCT cell monolayers indicate that PGE_2 is the major if not the exclusive prostaglandin product formed both under basal conditions and in response to hormonal stimuli. PGE_2 was found on both sides of the cell monolayer in similar amounts. This result cannot be ascribed to simple transcellular diffusion since the flux of PGE_2 across the monolayer is quite slow. Thus, PGE_2 is released on both sides of the CCCT cell monolayer suggesting, in turn, that PGE_2 is released on both the blood and urine sides of the canine collecting tubule in vivo. A previous report had indicated that the major site of entry of primary prostaglandins into urine occurs at the level of Henle's loop (146). The experiments reported were performed in rat kidneys perfused with angiotensin II, which appears to cause prostaglandin synthesis in glomerular epithelial cells, certain portion of the renal vasculature and in renomedullary interstitial cells (17). Angiotensin II does not elicit prostaglandin formation by collecting tubules (17) or by CCCT cells. In addition, recent studies show that AVP, but not DD-AVP, stimulate PGE_2 synthesis by rat renomedullary interstitial cells in culture (85); yet DD-AVP as well as AVP stimulates renal PGE_2 excretion in the rat in vivo (147-149). These data imply that the increase in urinary PGE_2 excretion in response to AVP or DD-AVP is

due to increased PGE_2 synthesis not by renomedullary cells but rather by the vasopressin-sensitive collecting tubule (149). Our results further suggest that, at least in the dog, PGE_2 can enter the urine at the level of the collecting tubule under conditions where renal bradykinin or AVP concentrations are elevated (150). Our results also indicate that if PGE_2 functions extracellularly to influence collecting tubule metabolism, PGE_2 presumably can affect events from both the apical and basolateral cell surfaces. As will be discussed in more detail in Chapter IV, this concept is consistent with the lack of sidedness to the effects of PGE_2 on cAMP metabolism in CCCT cells.

Although there was no asymmetry to PGE_2 release, there was a sidedness to the effect of bradykinin on prostaglandin synthesis. Bradykinin acted only from the apical surface to cause PGE_2 release (Figure 28). This sidedness of bradykinin action on the prostaglandin biosynthetic system was conceptualized by McGiff and coworkers (151), who proposed that only urinary and not blood-borne kinins are involved in eliciting prostaglandin synthesis by collecting tubules. The sidedness of bradykinin action observed in CCCT cells is also consistent with studies showing that kallikrein may be located on the apical side of the distal tubule (152,153). It should be noted, however, that bradykinin appears to act only from the basolateral surface of rabbit collecting tubules to antagonize the hydroosmotic effect of AVP and that this antagonism appears to be prostaglandin mediated (154).

The lack of a sidedness to the effect of AVP on PGE_2 formation was unexpected (Figure 28). AVP caused the release of PGE_2 when added to either side of CCCT cells even though AVP elicited cAMP

Figure 28. Apical-basolateral asymmetry of effector actions in CCCT cells.
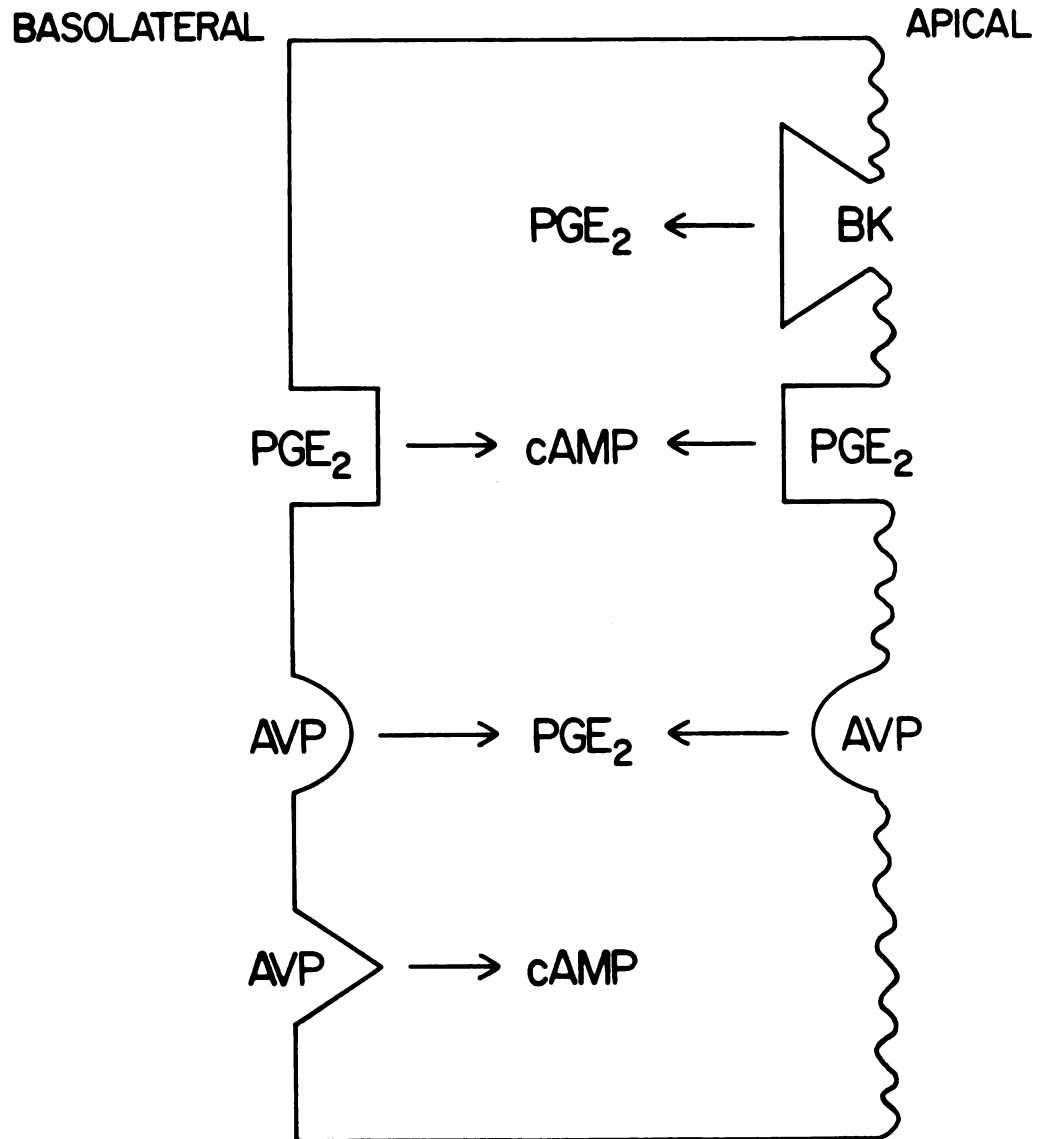
Figure 28

release only when added to the basolateral side of the cells. These data suggest that AVP interacts with different receptor systems in the cases of prostaglandin and cAMP formation.

CHAPTER IV

AVP-PGE2 INTERACTIONS IN CANINE

CORTICAL COLLECTING TUBULE (CCCT) CELLS

There is strong circumstantial evidence that prostaglandins

inhibit the hydroosmotic effect of AVP _in vivo_ as well as _in vitro_

(99,117). For example, indomethacin treatment and essential fatty acid

deficiency, two regimens which inhibit renal prostaglandin production,

increase urine osmolality (103,104,155). Thus, PGE_2 appears to have

a physiological as opposed to simply a pharmacological action on the

collecting tubule.

Recently, PGE_2 has been observed to inhibit AVP-induced cAMP

accumulation in the renal cortical collecting tubule. This action of

PGE_2 accounts for inhibition of the hydroosmotic effect of AVP (156).

However, the molecular mechanisms underlying this inhibition have yet

to be determined.

In performing the studies on the sidedness of hormonal responses

in CCCT cells described in Chapter III, it was noted (a) that extremely

low concentrations of PGE_2 (10^{-12} $\underline{M}$) would inhibit the release

of cAMP that normally occurred in response to AVP and (b) that this

inhibitory effect occurred with PGE_2 added to either side of the CCCT

cell monolayer. In this chapter, experiments on the inhibition by

PGE_2 of AVP-induced cAMP formation by CCCT cells are described.

MATERIALS AND METHODS

Materials. All materials were as described in Chapter III.

Isolation and Growth of CCCT Cells on Millipore Filters. CCCT
cells were isolated by immunodissection as described in Chapter II.
The cells were seeded on Millipore filters and their asymmetrical
functions and permeability characteristics were monitored as described
in Chapter III. Alternatively, CCCT cells were seeded as described in
Chapter II, in multi-well culture dishes for intracellular cAMP
measurements.

Effector-induced cAMP Release. For CCCT cells grown on Millipore
filters, cAMP released into the surrounding media was measured.
Effector dose-response curves and experiments involving more than one
effector (e.g., AVP plus PGE_2) were performed using one treatment per
chamber. All other procedures were as described in Chapter III and
detailed in figure legends and table captions in this chapter.

Effector-induced Intracellular cAMP Formation. Treatment of
monolayer cultures of nonconfluent CCCT cells with effectors (i.e.,
AVP, PGE_2, or both) was done in triplicate using 24-well culture
dishes seeded at a density of 5×10^4 cells/well. Cells were rinsed
free of media with Krebs buffer, pH 7.4 containing 10^{-4} $\underline{M}$ IBMX; 0.3

ml of buffer alone or buffer containing 10^{-11} $\underline{M}$ PGE_2 was then added for a preincubation period of 60 min at 37°. Following this preincubation, the solutions were removed from the wells and 0.3 ml of buffer alone or buffer containing an effector was added to the cells. The monolayers were incubated for the desired time at 37°. The solution in each well was removed and 500 μl of cold 6% TCA was added. The wells were incubated at -80° for 20 min, thawed at 24° for 25 min and incubated for 2 hrs at 0-4°. The liquid in each well was then transferred to a test tube and extracted four times with 10 volumes of diethyl ether. Any remaining ether was evaporated in a 60° water-bath for 10 min. The remaining aqueous phase was lyophilized. The lyophilized samples were resuspended in 0.125-0.2 ml of buffer and assayed for cAMP by radioimmunoassay as described previously (13).

Statistical Analysis. All experiments were done using a minimum of three replicates per treatment. A completely random analysis of variance was used to test for differences between sample means at $P<0.05$ (124). Dunnett's test was used for comparing differences between treatment means with the control mean (124). When it was desired to compare all the treatment means to each other and not only to the control mean, Student-Newman-Keuls' test for all possible comparisons was used (124). Error bars on the figures are ± SE.

RESULTS

Inhibition of AVP-induced cAMP Release by PGE_2. At concentra-
tions of 10^{-10} $\underline{M}$ or less, PGE_2 had no significant effect on

cAMP release (Chapter III, Figure 26). Therefore, we used these con-
centrations to test the effects of PGE_2 on AVP-induced cAMP release

from CCCT cells. In the first experiment, PGE_2 was added to both the

apical and basolateral side of the cell monolayer at a concentration of

$10^{-10}\underline{M}$ on both sides one hour prior to the addition of AVP.

Monolayers used as no effector controls or monolayers treated with AVP

alone were preincubated for 60 min with buffer that did not contain

PGE_2. The preincubation medium was removed after 60 min; then,

following a further one hour incubation in the presence of no effector,

AVP (10^{-8} $\underline{M}$) alone or both AVP (10^{-8} $\underline{M}$) and PGE_2 (10^{-10}

$\underline{M}$), the medium was assayed for cAMP. Under these conditions, PGE_2

completely blocked AVP-induced cAMP release (Figure 29).

Figure 30 shows the sidedness and the concentration dependence for

PGE_2 acting as an antagonist of the release of cAMP occurring in

response to AVP (10^{-8} $\underline{M}$). Significant inhibition of AVP-induced

cAMP release was noted at concentrations of PGE_2 as low as 10^{-12} $\underline{M}$.

Interestingly, the dose-response curves for inhibition of AVP-induced

cAMP release were the same for PGE_2 added to either side of the CCCT

cell monolayer. One cannot ascribe the inhibition obtained with

$10^{-12}\underline{M}$ PGE_2 to diffusion of PGE_2 across the monolayer since a

Figure 29. Inhibition by PGE_2 of DD-AVP-induced cAMP release from CCCT cell monolayers on Millipore filters. Each bar represents the amount of cAMP measured on the apical (A) or basolateral (BL) side of the CCCT cell monolayer following treatment with (a) 10^{-8} M DD-AVP added to the basolateral side; (b) 10^{-8} M DD-AVP (added to the basolateral side) plus 10^{-10} M PGE_2 (added to both sides) or (c) no effector. All samples were preincubated for 60 min at 37°. PGE_2 was added for the duration of the preincubation period to samples that were to be treated with PGE_2. All other samples were preincubated with buffer alone. At the end of the preincubation period the media was removed and the monolayers were incubated for an additional 60 min at 37° with the effectors indicated. Following this incubation period, the media from the two sides were removed and assayed for cAMP as described in MATERIALS AND METHODS. All treatments were performed with triplicate chambers in the presence of 10^{-4} M IBMX. *Significantly different from control values ($P < 0.05$).
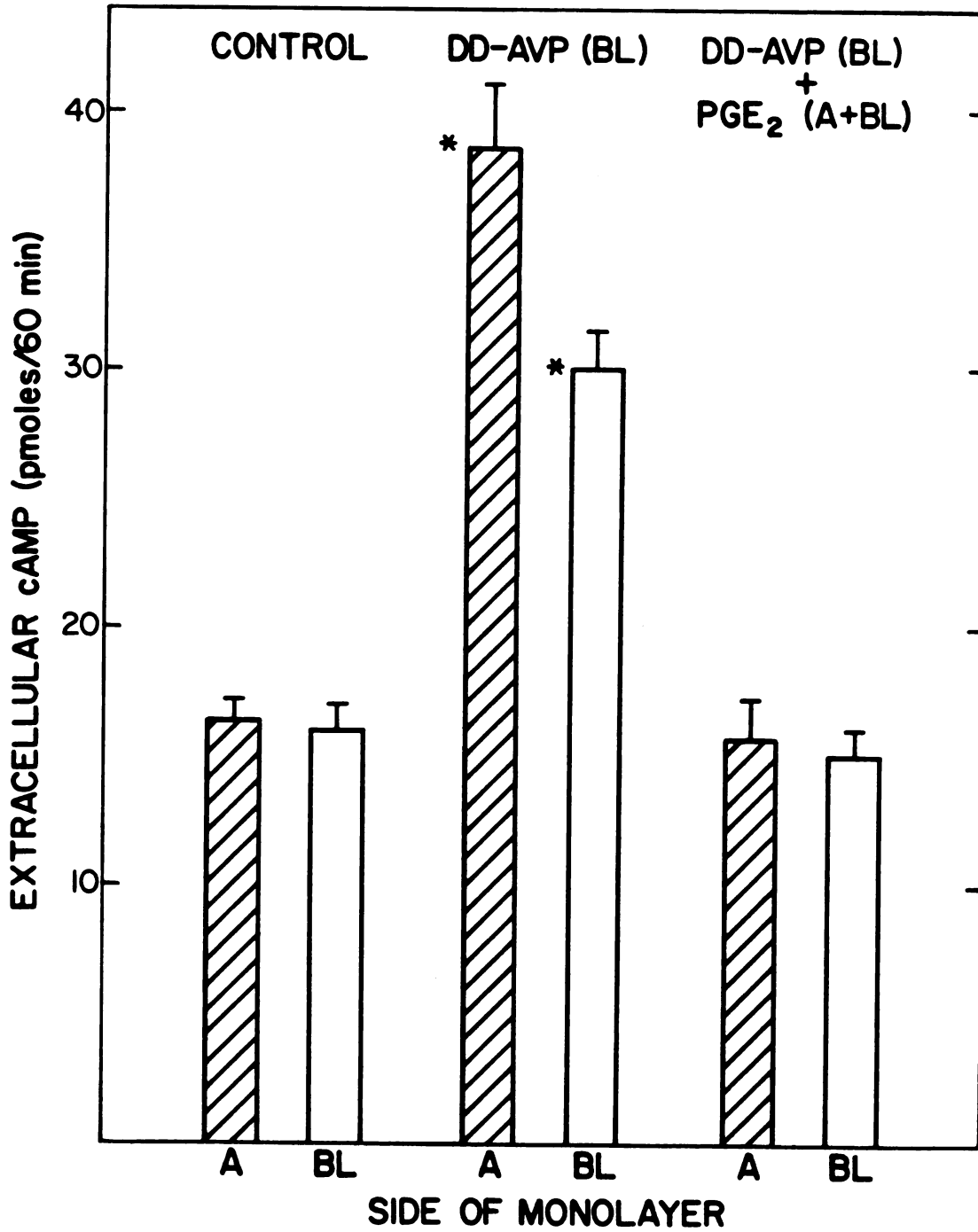
Figure 29

Figure 30. Concentration dependence for the inhibition by PGE_2 of
DD-AVP-induced release of cAMP. CCCT cells on Millipore
filters were preincubated for 60 min at 37° with the
indicated concentrations of PGE_2 on the apical or
basolateral side of the monolayers. The chambers were then
incubated for a second 60 min period at 37° with the same
concentrations of PGE_2 plus DD-AVP (10^{-8} M). DD-AVP
was added only to the basolateral side. Media from both
sides of the monolayer were pooled and assayed for cAMP as
described in MATERIALS AND METHODS. All treatments were
performed in the presence of 10^{-4} M IBMX. Each point
represents the mean of duplicate chambers.
‡Significantly different from control values (i.e., no
effectors; dotted line); *significantly different from
values of samples treated with DD-AVP alone) (P<0.05).
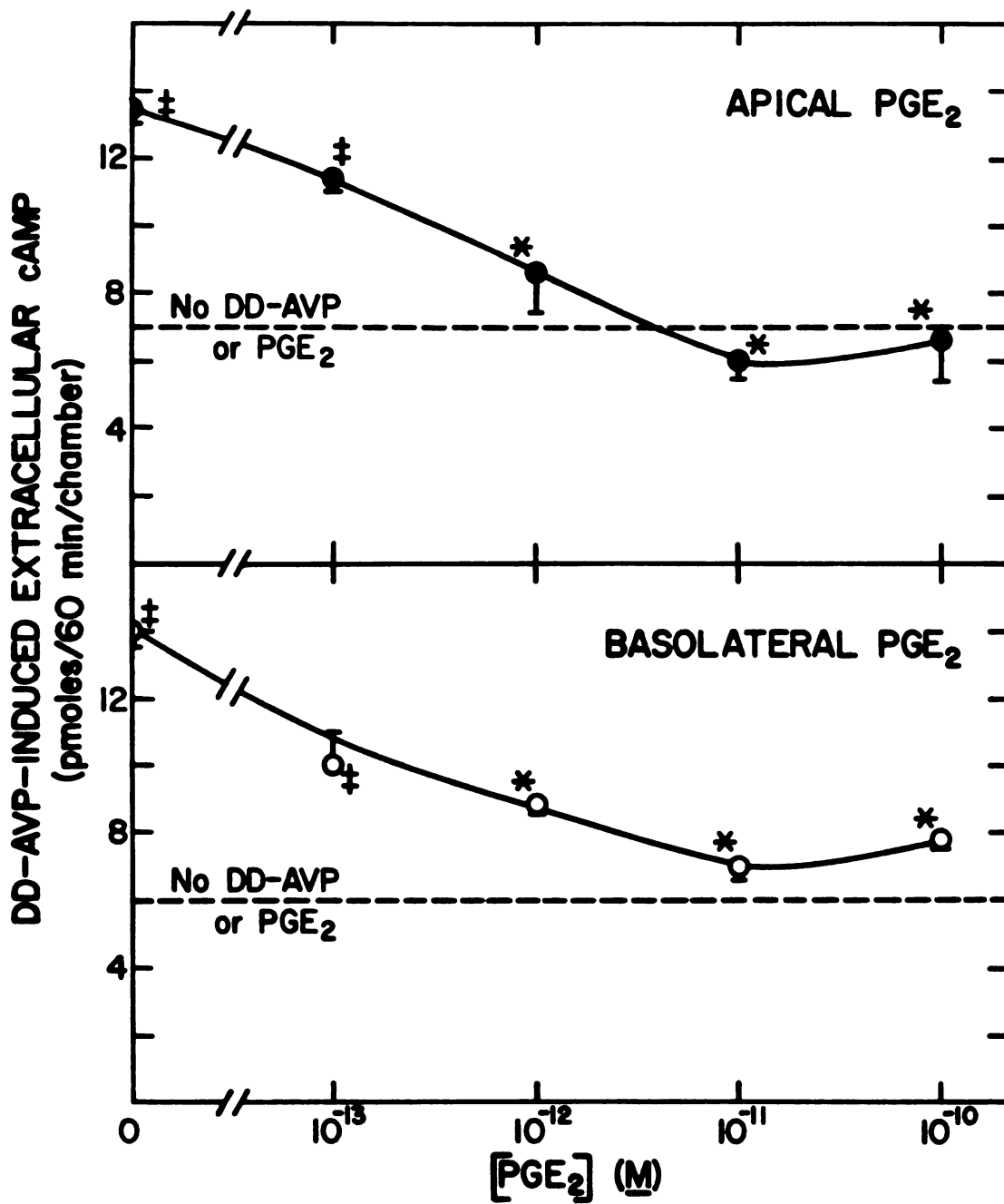
Figure 30

maximum of 10% of the PGE_2 could have crossed the monolayer during the 60 min preincubation period (Chapter III, Figure 18). Thus, PGE_2 apparently can act from either the apical or basolateral surface of CCCT cells to inhibit AVP-induced cAMP release, even though AVP appears to act only from the basolateral surface to cause cAMP formation (Chapter III, Figure 20).

The concentration of PGE_2 surrounding the CCCT cell monolayers after a 60 min preincubation (Figures 23-25) ranges from 10^{-9} to 10^{-10} $\underline{M}$ due to endogenous synthesis of the prostaglandin. When endogenous synthesis was blocked with either Ibuprofen or aspirin, a potentiation of the AVP response was observed (Table 8). Nevertheless, exogenous PGE_2 (10^{-11} $\underline{M}$) completely suppressed AVP-induced cAMP release in the presence or absence of cyclooxygenase inhibitors. Thus, the effect of newly formed prostaglandin, while measureable, does not appear to have an overriding influence on this system. This appears to be due to two factors. First, the inhibitory effect of PGE_2 requires a prolonged incubation with this prostaglandin (see Table 9), and the PGE_2 arising from the cells themselves is not present at elevated concentrations during the entire preincubation period. And second, after the preincubation period, the medium surrounding the cells is removed and replaced with fresh medium to begin the 60 min treatment (e.g., with AVP).

Inhibition of AVP-induced Accumulation of Intracellular cAMP by PGE_2.

In studies on CCCT cells seeded on Millipore filters, only cAMP release was monitored. To determine if PGE_2 inhibits AVP-induced accumulation of intracellular cAMP, experiments were

Table 8

Inhibition by PGE_2 of AVP-induced cAMP Release from CCCT Cell Monolayers on Millipore Filters in the Presence of Inhibitors of Prostaglandin Synthesis[a]

Treatment	Extracellular cAMP (pmoles/60 min/chamber)			
	No Inhibitor	Ibuprofen	No Inhibitor	Aspirin
1. No Effector	6.5 ± 0.1	6.8 ± 1.1	7.1 ± 0.4	6.3 ± 1.3
2. AVP Alone	‡10.8 ± 1.3	‡17.8 ± 1.1	‡11.9 ± 0.5	‡18.2 ± 1.1
3. PGE_2 Alone	6.5 ± 0.5	7.8 ± 0.2	7.2 ± 0.2	7.7 ± 0.3
4. AVP + PGE_2	* 4.4 ± 1.0	* 7.7 ± 0.3	* 7.2 ± 0.3	* 7.5 ± 0.4

[a]CCCT cells on Millipore filters were preincubated for 60 min at 37° with 10^{-11} M PGE_2 (Treatments 3 and 4) or with buffer alone (Treatments 1 and 2) on both sides of the monolayer. At the end of the preincubation period, the media was removed and the monolayers were incubated for an additional 60 min period at 37° with no effector, 10^{-8} M AVP alone, 10^{-11} M PGE_2 alone or 10^{-8} M AVP plus 10^{-11} M PGE_2. AVP was added only to the basolateral side. In the chambers where a prostaglandin synthesis inhibitor (10^{-3} M aspirin or 10^{-4} M Ibuprofen) was used, it was present in the media 30 minutes prior to the preincubation period and then throughout preincubation and treatment periods (i.e., a total of 150 min). Buffer was used for the same time in chambers without such inhibitors. 10^{-4} M IBMX was present in all chambers throughout the 150 min period. Each value represents the mean of duplicate chambers. ‡Significantly different from control value (i.e., no effector); *significantly different from value of treatment with AVP alone (P < 0.05).

Table 9

Effect of Preincubation Time on the Inhibition by PGE$_2$ of AVP-induced
Formation of cAMP by CCCT Cells on Culture Dishes[a]

Preincubation		Treatment	Intracellular cAMP (fmoles/μg cell protein)	
Time with buffer alone (min)	Time with PGE$_2$ (10^{-11} M) (min)		2 min	3 min
1. 60	0	No Effector	2.4 + 0.2	1.7 + 0.2
2. 60	0	AVP Alone	‡8.4 + 0.2	‡5.0 + 0.1
3. 60	0	AVP + PGE$_2$	‡6.8 + 0.4	‡4.5 + 1.3
4. 55	5	AVP + PGE$_2$	‡9.1 + 0.5	‡5.3 + 0.6
5. 50	10	AVP + PGE$_2$	‡7.1 + 1.5	‡4.2 + 0.1
6. 40	20	AVP + PGE$_2$	*2.6 + 0.6	*1.7 + 0.1
7. 20	40	AVP + PGE$_2$	*2.1 + 0.2	*2.2 + 0.3
8. 0	60	AVP + PGE$_2$	*2.3 + 0.5	*2.2 + 0.4

[a]Nonconfluent CCCT cells seeded on culture dishes were preincubated for the indicated time periods at 37°
with 10^{-11} M PGE$_2$ (Treatments 4-8) or with buffer alone (Treatments 1-3). In treatments where the
preincubation with PGE$_2$ was performed for less than 60 min (Treatments 4-7), the cells were preincubated
in buffer alone followed by the preincubation with 10^{-11} M PGE$_2$ (e.g., Treatment 4 included 55 min
of preincubation in buffer alone followed by 5 min of preincubation in the presence of PGE$_2$). At the end
of the full preincubation period, the media was removed and the cells were incubated for 2 min or 3 min
with no effector, 10^{-8} M AVP alone, 10^{-11} M PGE$_2$ alone or 10^{-8} M AVP plus 10^{-11} M PGE$_2$.
Preincubations and incubations were performed in the presence of 10^{-4} M IBMX. Each value represents
the mean of triplicate wells. Intracellular cAMP was measured by radioimmunoassay as described in
MATERIALS AND METHODS. ‡Significantly different from control value (i.e., no effector); *significantly
different from value of treatment with AVP alone (P < 0.05).

performed using CCCT cells grown as nonconfluent monolayers on plastic culture dishes. As shown in Table 10, 10^{-11} $\underline{M}$ PGE$_2$ suppressed the AVP-induced accumulation of intracellular cAMP at 2 and 3 min time points. This inhibition also occurred when endogenous PGE$_2$ formation was blocked (Table 11). Curiously, inhibition was only observed after a 20 min preincubation of PGE$_2$ with the CCCT cells (Table 9). A similar time dependence was observed in the inhibition of AVP-induced cAMP release from CCCT cell monolayers on Millipore filters. This time dependence suggests that PGE$_2$ is causing a chain of metabolic events to occur which prevents AVP-induced cAMP accumulation.

Torikai and Kurokawa suggested that PGE$_2$ may exert its inhibitory effect on AVP-induced cAMP formation by activating cAMP phosphodiesterase activity (156). Were this true in the CCCT cell system, one would expect 10^{-12}-10^{-10} $\underline{M}$ PGE$_2$ to decrease basal levels of intracellular cAMP. However, these concentrations of PGE$_2$ had no effect on intracellular cAMP levels in the presence of 10^{-4} $\underline{M}$ IBMX (Table 12).

A dual receptor mechanism for prostaglandin action was conceived to accomodate the biphasic nature of the effects of PGE$_2$ on cAMP metabolism in CCCT cells. We propose that one class of receptors, displaying a low affinity for the ligand (i.e., PGE$_2$), is involved in the activation of adenylate cyclase. We suggest that another class of receptors, having a high affinity for the ligand, is involved in the suppression of AVP-induced adenylate cyclase activation. In support of this concept were the observations that PGF$_{2\alpha}$ inhibited AVP-induced cAMP formation but PGF$_{2\alpha}$ did not increase cellular cAMP levels.

129

Table 10

Inhibition by PGE_2 of AVP-induced Formation of cAMP by CCCT Cells on Culture Dishes[a]

Treatment	Intracellular cAMP (fmoles/μg cell protein)			
	1 min.	2 min.	3 min.	4 min.
1. No Effector	2.8 ± 0.3	4.1 ± 0.4	4.9 ± 0.1	4.6 ± 0.5
2. AVP Alone	‡4.2 ± 0.3	‡6.6 ± 0.1	‡8.7 ± 1.0	6.2 ± 0.8
3. PGE_2 Alone	3.7 ± 0.1	4.6 ± 0.2	5.2 ± 0.2	4.4 ± 0.3
4. AVP + PGE_2	‡4.6 ± 0.5	*3.7 ± 0.1	*5.5 ± 0.1	5.7 ± 0.1

[a]Nonconfluent CCCT cells seeded on culture dishes were preincubated for 60 min at 37° with 10^{-11} M PGE_2 (Treatments 3 and 4) or with buffer alone (Treatments 1 and 2). At the end of the preincubation period, the media was removed and the cells were incubated for the time periods indicated with no effector, 10^{-8} M AVP alone, 10^{-11} M PGE_2 alone or 10^{-8} M AVP plus 10^{-11} M PGE_2. Preincubation and incubations were performed in the presence of 10^{-4} M IBMX. Each value represents the mean of triplicate wells. Intracellular cAMP was measured by radioimmunoassay as described in MATERIALS AND METHODS. ‡Significantly different from control value (i.e., no effector); *significantly different from value of treatment with AVP alone (P<0.05).

Table 11

Inhibition by PGE_2 of AVP-induced Formation of cAMP by
CCCT Cells in the Presence of Flurbiprofen[a]

Treatment	Intracellular cAMP (fmoles/µg cell protein)	
	No Inhibitor	Flurbiprofen
1. No Effector	1.9 ± 0.3	4.9 ± 0.3
2. AVP Alone	‡3.5 ± 0.3	‡8.5 ± 0.2
3. AVP + PGE_2	*1.4 ± 0.3	*4.6 ± 0.4

[a]Nonconfluent CCCT cells seeded on culture dishes were preincubated
for 60 min at 37° with 10^{-11} M PGE_2 (Treatment 3) or with
buffer alone (Treatments 1 and 2). At the end of the preincubation
period, the media was removed and the cells were incubated for 3 min
with no effector, 10^{-8} M AVP alone, or 10^{-8} M AVP plus
10^{-11} M PGE_2. In the wells where Flurbiprofen (10^{-5} M)
was used, it was present in the media 30 min prior to the preincuba-
tion period and then throughout preincubation and treatment periods
(i.e., a total of 93 min). Buffer was used for the same time in
wells without inhibitor. 10^{-4} M IBMX was present in all wells
throughout the 93 min period. Each value represents the mean of
triplicate wells. Intracellular cAMP was measured by radioimmuno-
assay as described in MATERIALS AND METHODS. ‡Signicicantly
different from control value (i.e., no effector); *significantly
different from value of treatment with AVP alone (P<0.05).

Table 12

Effect of Low Concentrations of PGE$_2$ on Basal Levels
of Intracellular cAMP in CCCT Cells[a]

Treatment	Intracellular cAMP (fmoles/µg cell protein)
1. No Effetor	8.6 ± 0.1
2. 10^{-12} M PGE$_2$	8.5 ± 0.3
3. 10^{-11} M PGE$_2$	8.7 ± 0.1
4. 10^{-10} M PGE$_2$	8.8 ± 0.2

[a]Nonconfluent CCCT cells seeded on culture dishes were preincubated
for 60 min with the indicated concentrations of PGE$_2$ (Treatments
2-4) or with buffer alone (Treatment 1). At the end of the preincu-
bation period, the media was removed and the cells were incubated for
3 min with no effector or the indicated concentrations of PGE$_2$.
Preincubations and incubations were performed in the presence of
10^{-4} M IBMX. Each value represents the mean of triplicate wells.
Intracellular cAMP was measured by radioimmunoassay as described in
MATERIALS AND METHODS. No significant difference was observed
between treatments (P<0.05).

Figure 31 illustrates the effect of a wide range of $PGF_{2\alpha}$ concentrations (10^{-12}-10^{-7} $\underline{M}$) on AVP-induced intracellular cAMP accumulation. All concentrations of $PGF_{2\alpha}$ tested were effective in completely inhibiting the AVP-induced response. In addition and contrary to PGE_2, $PGF_{2\alpha}$ does not induce cAMP increases in CCCT cells or renal papillary collecting tubule cells (14) even at very high concentrations (10^{-7}-10^{-4} $\underline{M}$). In this vane, it is interesting to consider a report on experiments performed in isolated, perfused cortical collecting tubules. It was shown in these studies that PGE_2 inhibited both Na+ resorption and AVP-induced water resorption. $PGF_{2\alpha}$, however, caused only inhibition of AVP-induced water resorption. $PGF_{2\alpha}$ had no apparent effect on Na^+ resorption (138).

133

Figure 31. Concentration dependence for the inhibition by $PGF_{2\alpha}$ of AVP-induced cAMP formation. Nonconfluent CCCT cells seeded on culture dishes were preincubated for 60 min at 37° with the indicated concentrations of $PGF_{2\alpha}$. At the end of the preincubation period, the media was removed and the cells were incubated for 3 min with the same concentrations of $PGF_{2\alpha}$ plus AVP (10^{-8} M). Preincubations and incubations were performed in the presence of 10^{-4} IBMX. Each point represents the mean of triplicate wells. Intracellular cAMP was measured by radioimmunoassay as described in MATERIALS AND METHODS. ‡Significantly different from control values (i.e., no effectors; dotted line); *significantly different from value of treatment with AVP alone ($P<0.05$).
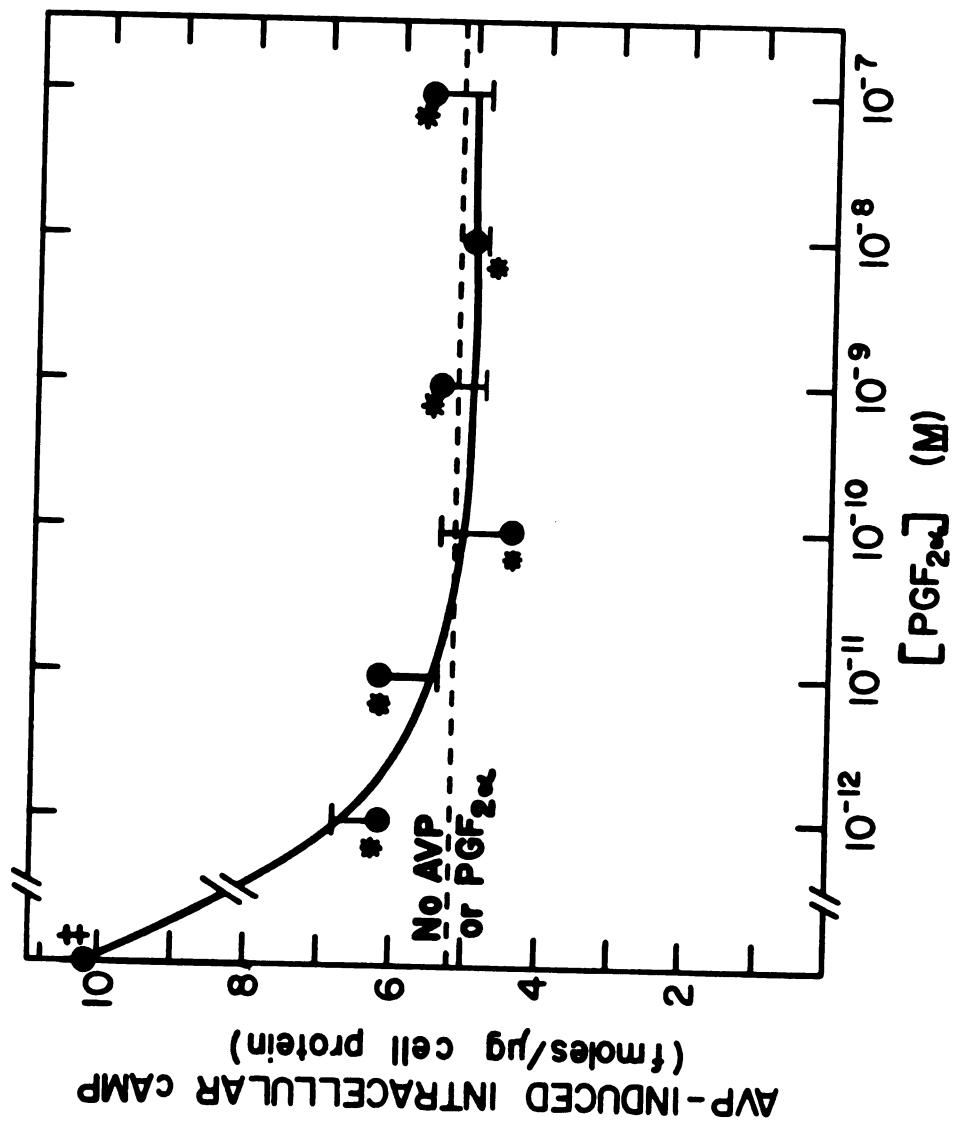
134

Figure 31

DISCUSSION

PGE$_2$-AVP Interactions. The hypothesis that prostaglandins inhibit AVP-induced cAMP formation in the collecting tubule evolved from the classic study of Grantham and Orloff (11). Clear evidence supporting this concept in the collecting tubule system itself has been difficult to obtain (14,112,113,131,144,147). However, there have been two recent reports that, in the absence of phosphodiesterase inhibitors, PGE$_2$ causes partial but significant inhibition of AVP-induced cAMP accumulation in rabbit collecting tubule segments (156,157). We have found that PGE$_2$ inhibits both the release of cAMP normally occurring in response to treatment of confluent CCCT cell monolayers with AVP and the accumulation of intracellular cAMP in nonconfluent CCCT cell monolayers treated with AVP. The effects observed in the CCCT cell system have slightly different characteristics than those reported by Torikai and Kurokawa (156) and Edwards et al. (157) in that inhibition by PGE$_2$ of AVP-induced cAMP release in the CCCT cell system: (a) is quantitative, (b) is time-dependent and (c) involves concentrations of PGE$_2$ which are 5-7 orders of magnitude lower than those reported for the rabbit collecting tubule.

The biochemical mechanism by which PGE$_2$ inhibits AVP-induced cAMP formation is not yet clear. It appears that the effect occurs only with intact cells. For example, the phenomenon is apparent in slices (113), in intact collecting tubules (156,157) and in CCCT cells,

but PGE_2 fails either to activate cAMP phosphodiesterase (157) or to inhibit AVP-independent adenylate cyclase in permeabilized collecting tubule segments (131). This suggests that PGE_2 may be causing production, mobilization or sequestration of an intermediate factor(s) (denoted by an X in Figure 32) which, in turn, modulates cAMP levels in the collecting tubule. Based on the 20 min time requirement (Table 9), this intermediate could be a protein (158). Locher et al. (111) have demonstrated that in human phagocytes there is also a time dependence to the inhibition of AVP-induced cAMP synthesis by PGE_2.

It seems unlikely that PGE_2 is causing its inhibitory effect at the level of cAMP phosphodiesterase because PGE_2 does not decrease basal levels of intracellular cAMP in CCCT cells. More reasonable is an inhibitory effect on the AVP-inducible adenylate cyclase system. PGE_2 does not affect the affinity of binding of AVP to human phago-cytes under conditions in which PGE_2 inhibits AVP-induced cAMP formation (111). Thus, the effect of PGE_2 is probably expressed at a post receptor step. The most applicable precedent for inhibition by PGE_2 of AVP-induced cAMP formation is seen in the heterologous desensitization of adenylate cyclase in human fibroblasts (159,160). In this situation PGE_2 attenuates the coupling of the hormone--receptor complex to the catalytic subunit of adenylate cyclase probably by modifying a GTP binding subunit. Hopefully, the availability of large numbers of CCCT cells in culture will permit the examination of this hypothesis at the biochemical level.

Dual Receptor Concept of Prostaglandin Action. The single experiment performed with $PGF_{2\alpha}$ (Figure 31) provides suggestive

Figure 32. Model for AVP, bradykinin (BK), PGE$_2$ interrelationships in canine cortical collecting tubule (CCCT) cells.
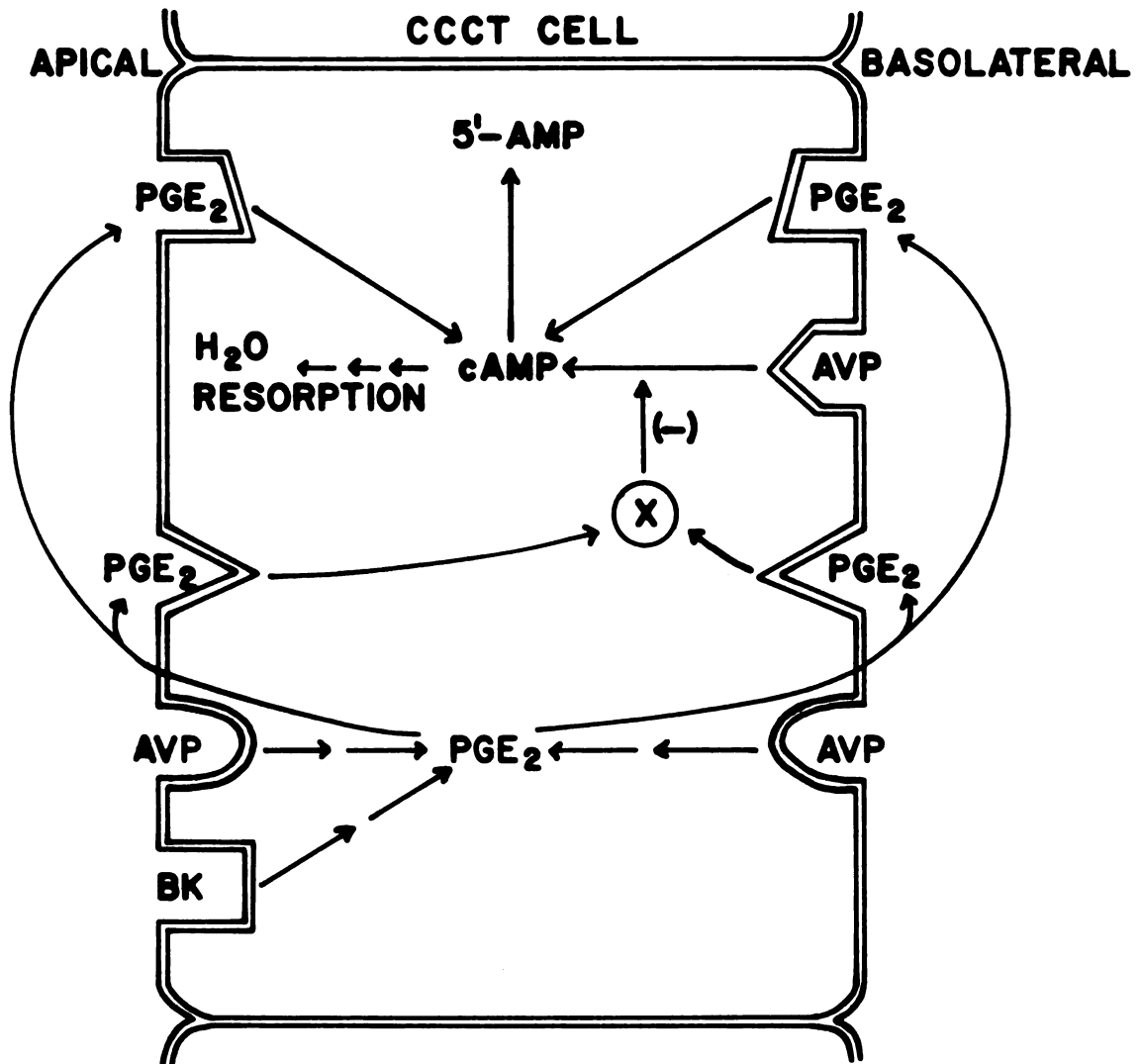
Figure 32

but incomplete evidence for a dual prostaglandin receptor system. However, the existence of dual PGE_2 receptors (Figure 32) would explain the observation that PGE_2 has two actions in the collecting tubule. Binding of PGE_2 to one type of receptor, exhibiting high affinity for the ligand, could initiate desensitization of adenylate cyclase to circulating antidiuretic hormone (ADH). Through this receptor, PGE_2 would act as a negative feedback modulator of the action of ADH on the collecting tubule. The second type of receptor, displaying low affinity for the ligand, would be involved in the activation of adenylate cyclase. This raises the question of the physiological significance for this latter effect. It is pertinent to note that only cells which synthesize prostaglandins exhibit prostaglandin-induced adenylate cyclase activation. This demonstrated tendency, taken together with the recent observation that cAMP inhibits prostaglandin formation in platelets (161,162) and MDCK cells (163), leads to the idea of a feedback mechanism for the regulation of prostaglandin synthesis with cAMP acting as the negative modulator (not shown in Figure 32). Prostaglandin derivatives that elicit activation of adenylate cyclase but not inhibition of AVP-induced cAMP increases could provide additional suggestive evidence for the dual receptor model. Furthermore, such prostaglandins and $PGF_{2\alpha}$ could be used to study the two distinct responses independently.

The identification of heterogeneous classes of PGE_2 receptors in CCCT cells should be pursued. Direct measurements of radiolabeled PGE_2-binding to CCCT cell membranes could provide more direct evidence. The biphasic nature of PGE_2 effects indicates that binding dissociation constants should be detectably different. Analysis of the

data could be complicated by the presence of heterogeneous receptor molecules within a class; a possibility suggested by experiments on RPCT cells (14) and rat hepatocytes (164) for prostaglandin receptors coupled to adenylate cyclase activation. However, prostaglandins with affinity for only one class of receptor (e.g., $PGF_{2\alpha}$) could be used to facilitate distinction between receptor populations in ligand-receptor binding experiments as well as in the ultimate solubilization and characterization of the receptor molecules involved.

SUMMARY

The renal collecting tubule is an attractive system for studying the physiological function and mechanism of action of PGE_2. The collecting tubule is the part of the renal tubule which exhibits the highest cyclooxygenase activity and along with the vasculature, the medullary interstitial cells and the glomeruli constitutes one of the four major sites of prostaglandin synthesis in the kidney. In addition, prostaglandins have been shown to have two potent effects on the transport properties of isolated collecting tubule segments. One effect is to inhibit water resorption occurring in response to arginine vasopressin (AVP), and the second is to inhibit Na^+ resorption.

To facilitate the study of the mechanisms of actions of prostaglandins on the collecting tubule, a culture system of canine cortical collecting tubule (CCCT) cells was developed. These cells were isolated by immunodissection using culture plates coated with a monoclonal antibody which specifically reacts with an ecto-antigen on the canine collecting tubule. CCCT cells, which exhibit many of the morphological and biochemical properties of collecting tubule cells in situ, can be grown and maintained in culture for several months. Confluent monolayers of CCCT cells seeded on Millipore filters, showing characteristics of asymmetry seen with intact collecting tubules, were utilized to examine aspects of apical-basolateral asymmetry related to PGE_2 metabolism and function. PGE_2 is the major prostaglandin

141

derivative synthesized by CCCT cells. Figure 32 incorporates the main concepts progressively developed through the research described in this dissertation. Although AVP caused cAMP release only when added to the basolateral side of CCCT cells, AVP caused the release of PGE_2 when added to either the apical or basolateral surface. This result implies that there are at least two AVP receptor systems, one coupled to cAMP synthesis and one to PGE_2 formation. In contrast to the results observed with AVP, bradykinin caused PGE_2 release only when added to the apical surface of CCCT cells suggesting that urinary but not blood-borne kinins elicit PGE_2 formation by the canine collecting tubule. PGE_2 was released in comparable amounts on each side of the monolayer in response both to AVP and to bradykinin.

High concentrations ($\geq 10^{-8}$ $\underline{M}$) of PGE_2 added to either side of the monolayer caused the release of cAMP. However, at concentrations (10^{-10}-10^{-12} $\underline{M}$) at which PGE_2 had no independent effect on cAMP release, PGE_2 inhibited the release of cAMP normally occurring in response to AVP. This inhibition occurred with PGE_2 added to either the apical or basolateral surface of the CCCT cell monolayer. PGE_2 (10^{-11} $\underline{M}$) also inhibited the AVP-induced accumulation of intracellular cAMP by CCCT cells seeded on culture dishes. This inhibition was only observed when the cells were preincubated with PGE_2 for $\geq$ 20 min. The results are consistent with the concept that inhibition by prostaglandins of the hydroosmotic effect of AVP is due to inhibition of AVP-induced cAMP production. This inhibition does not appear to involve a direct physical interaction of PGE_2 with the AVP receptor which is coupled to adenylate cyclase since (a) CCCT cells must be preincubated with PGE_2 for 20 min for the

inhibition to be observed and (b) PGE_2 added to the apical surface of CCCT cells inhibits cAMP release in response to AVP acting from the basolateral surface. A dual prostaglandin receptor concept, considered in light of the biphasic nature of PGE_2 effects on cAMP metabolism in the collecting tubule, is also briefly discussed in this dissertation.

BIBLIOGRAPHY

1. Morel, F. and DeRouffignac, C. (1973) Ann. Rev. Physiol. 35, 17-54.

2. Grantham, J.J., Irish, J.M. III, and Hall, D.A. (1978) Ann. Rev. Physiol. 40, 249-277.

3. Burg, M., Grantham, J.J., Abramow, M., and Orloff, J. (1966) Am. J. Physiol. 210, 1293-1298.

4. Misfeldt, D.S., Hamamoto, S.T., and Pitelka, D.R. (1976) Proc. Natl. Acad. Sci. USA 73, 1212-1216.

5. Rindler, M.J., Churman, LM., Shaffer, L., and Saier, M.H. Jr. (1979) J. Cell Biol. 81, 635-648.

6. Saier, M.H. Jr. (1981) Am. J. Physiol. 240, C106-C109.

7. Misfeldt, D.S. and Sanders, M.J. (1981) Am. J. Physiol. 240, C92-C95.

8. Mullin, J.M., Cha, C.-J.M., and Kleinzeller, A. (1982) Am. J. Physiol. 242, C41-C45.

9. Smith, W.L. and Wilkin, G.P. (1977) Prostaglandins 13, 873-892.

10. Smith, W.L. and Bell, T.G. (1978) Am. J. Physiol. 235, F451-F457.

11. Grantham, J.J. and Orloff, J. (1968) J. Clin. Invest. 47, 1154-1161.

12. Grenier, F.C. and Smith, W.L. (1978) Prostaglandins 16, 759-772.

13. Grenier, F.C., Rollins, T.E., and Smith, W.L. (1981) Am. J. Physiol. 241, F94-F104.

14. Grenier, F.C., Allen, M.L., and Smith, W.L. (1982) Prostaglandins 24, 547-565.

15. Moncada, S. and Vane, J.R. (1979) New England J. Med. 300, 1142-1147.

16. Lands, W.E.M. and Samuelsson, B. (1968) Biochim. Biophys. Acta 164, 426-429.

17. Smith, W.L. (1981) Mineral Electrolyte Metab. 6, 10-26.

18. Pace-Asciak, C.R. and Smith, W.L. (1983) In The Enzymes (Boyer, P.D., Ed.), Vol. 16, pp. 543-603.

19. Rittenhouse-Simmons, S. (1979) J. Clin. Invest. 63, 580-587.

20. Broekman, M.J., Ward, J.W., and Marcus, A.J. (1980) J. Clin. Invest. 66, 275-283.

21. Mauco, G., Chap, H., and Douste-Blazy, L. (1979) FEBS Lett. 100, 367-370.

22. Broekman, M.J., Ward, J.W., and Marcus, A.J. (1981) J. Biol. Chem. 256, 8271.

23. Bell, R.L., Kennerly, D.A., Stanford, N., and Majerus, S.W. (1979) Proc. Natl. Acad. Sci. USA 76, 3238-3241.

24. Majerus, P.W. and Prescott, S.M. (1982) Meth. Enz. 86, 11-17.

25. Marcus, A.J., Ullman, H.L., and Safier, L.B. (1969) J. Lipid Res. 10, 108-114.

26. Bills, T.K., Smith, J.B., and Silver, M.J. (1977) J. Clin. Invest. 60, 1-6.

27. Dennis, E.A. (1983) In The Enzymes (Boyer, P.D., Ed.), Vol. 16, pp. 307-353.

28. Smith, W.L. (1984) In Biochemistry of Lipids and Membranes (Vance, D., and Vance, J., Eds.), Benjamin/Cummings Publishing Co., in press.

29. Neufeld, E.J. and Majerus, P.W. (1983) J. Biol. Chem. 258, 2461-2467.

30. Miyamoto, T., Ogino, N., Yamamoto, S., and Hayaishi, O. (1976) J. Biol. Chem. 251, 2629-2636.

31. Hemler, M., Lands, W.E.M., and Smith, W.L. (1976) J. Biol. Chem. 251, 5575-5578.

32. Ohki, S., Ogino, N., Yamamoto, S., and Hayaishi, O. (1979) J. Biol. Chem. 254, 829.

33. VanderOuderaa, F.J., Buytenhek, M., Nugteren, D.H., and VanDorp, D.A. (1977) Biochim. Biophys. Acta 487, 315.

34. Pagels, W.R., Marnett, L.J., DeWitt, D.L., and Smith, W.L. (1983) J. Biol. Chem. 258, 6517.

35. Ogino, N., Miyamoto, T., Yamamoto, S., and Hayaishi, O. (1977) J. Biol. Chem. 252, 890-895.

36. Nugteren, D.H. (1982) in Progress in Lipid Research (Holman, R.T., Ed.), Vol. 20, pp. 169-172.

37. Christ-Hazelhof, E. and Nugteren, D.H. (1979) Biochim. Biophys. Acta 572, 43-51.

38. Shimizu, T., Yamamoto, S., and Hayaishi, O. (1979) J. Biol. Chem. 254, 5222-5228.

39. Salmon, J.A., Smith, D.R., Flower, R.J., Moncada, S., and Vane, J.R. (1978) Biochim. Biophys. Acta 523, 250-262.

40. Yoshimoto, T., Yamamoto, S., Okuma, M., and Hayaishi, O. (1977) J. Biol. Chem. 252, 5871-5874.

41. Pace-Asciak, C. and Nashat, M. (1975) Biochim. Biophys. Acta 388, 243.

42. Wlodawer, P., Kindahl, H., and Hamberg, M. (1976) Biochim. Biophys. Acta 431, 603.

43. Wong, P.Y.-K. (1982) Meth. Enz. 86, 117-125.

44. Watanabe, K., Shimizu, T., and Hayaishi, O. (1981) Biochem. Int. 2, 603.

45. Reingold, D.F., Kawasaki, A., and Needleman, P. (1981) Biochem. Biophys. Acta 659, 179.

46. Stone, K.J. and Hart, M. (1975) Prostaglandins 10, 273.

47. Christ-Hazelhof, E. and Nugteren, D.H. (1982) Meth. Enz. 86, 77-84.

48. Shimizu, T., Yamamoto, S., and Hayaishi, O. (1982) Meth. Enz. 86, 73-77.

49. Roth, G.J., Machuga, E.T., and Strittmatter, P. (1981) J. Biol. Chem. 256, 10018.

50. Moonen, P., Buytenhek, M., and Nugteren, D.H. (1982) Meth. Enz. 86, 84-91.

51. Smith, W.L., DeWitt, D.L., and Day, J.S. (1983) In Advances in Prostaglandin, Thromboxane and Leukotriene Research, Vol. 11, 87.

52. DeWitt, D.L. and Smith, W.L. (1983) J. Biol. Chem. 258, 3285.

53. Graf, H., Castle, L., and Ullrich, V. (1983) In Advances in Prostaglandin, Thromboxane and Leukotriene Research, Vol. 11, 105.

54. Stehle, R.G. (1982) Meth. Enz. 86, 436-458.

55. Hamberg, M., Svensson, J., and Samuelsson, B. (1975) Proc. Natl. Acad. Sci. USA 72, 2994.

56. Anggard, E. and Samuelsson, B. (1964) J. Biol. Chem. 239, 4097.

57. Lee, S.C. and Levine, L. (1975) J. Biol. Chem. 250, 548.

58. Ferreira, S. and Vane, J.R. (1967) Nature (London) 216, 868.

59. Granstrom, E. and Samuelsson, B. (1971) J. Biol. Chem. 246, 7470.

60. Hamberg, M. and Samuelsson, B. (1971) J. Biol. Chem. 246, 6713.

61. Hansen, H.S. (1979) Biochim. Biophys. Acta 574, 136.

62. Edwards, N.S. and Pace-Asciak, C.R. (1982) J. Biol. Chem. 257, 6339.

63. Pace-Asciak, C.R. and Domazet, Z. (1975) Biochim. Biophys. Acta 380, 338.

64. Yuan, B., Tai, C.L., and Tai, H.-H. (1980) J. Biol. Chem. 255, 7439.

65. Dunn, M.J., Liard, J.F., and Dray, F. (1978) Kidney Int. 13, 136-143.

66. Christ, E.J. and VanDorp, D.A. (1972) Biochim. Biophys. Acta 270, 537-545.

67. Smith, W.L. (1984) In CRC Handbook of Prostaglandins and Related Lipids, CRC Press, in press.

68. Jouvenaz, G.H., Nugteren, D.H., Beerthuis, R.K., and VanDorp, D.A. (1970) Biochim. Biophys. Acta 202, 231-234.

69. Levine, L., Hinkle, P.M., Voelkel, E.F., and Tashjian, A.H. (1972) Biochem. Biophys. Res. Comm. 47, 888-896.

70. Bito, L.Z. (1975) Prostaglandins 9, 851-855.

71. Bito, L.Z. and Baroody, R.A. (1974) Am. J. Physiol. 229, 1580-1584.

72. Siegl, A.M., Smith, J.B., Silver, M.J., Nicolau, K.C., and Ahern, D. (1979) J. Clin. Invest. 63, 215.

73. Jacobson, H.R. (1981) Am. J. Physiol. 241, F203-F218.

74. Knepper, M. and Burg, M. (1983) Am. J. Physiol. 244, F579-F589.

75. Lee, J.B., Covino, B.G., Takman, B.H., and Smith, E.R. (1965) Circulation Res. 17, 57.

76. Hamberg, M. (1969) FEBS Lett. 5, 127.

77. Zusman, R.M. and Keiser, H.R. (1977) J. Biol. Chem. 252, 2069-2071.

78. Janszen, F.H.A. and Nugteren, D.H. (1973) Adv. Biosci. 1973, 287-292.

79. Bohman, S.O. (1977) Prostaglandins 14, 729-744.

80. McGiff, J.C. and Wong, P.Y.-K. (1979) Federation Proc. 38, 89-93.

81. Sraer, J., Foidart, J., Chansel, D., Mahieu, P., Kouznetzova, B., and Ardaillou, R. (1979) FEBS Lett. 104, 420-424.

82. Hassid, A., Koniecskowski, M., and Dunn, M.J. (1979) Proc. Natl. Acad. Sci. USA 76, 1155-1159.

83. Jackson, B.A., Edwards, R.M., and Dousa, T.P. (1980) J. Lab Clin. Med. 96, 119-128.

84. Kirschenbaum, M.A., Lowe, A.G., Trizna, W., and Fine, L.G. (1982) J. Clin. Invest. 70, 1193-1204.

85. Beck, T.R., Hassid, A., and Dunn, M.J. (1980) J. Pharmacol. Exp. Ther. 215, 15-19.

86. Zusman, R.M. and Keiser, H.R. (1977) J. Clin. Invest. 60, 215-223.

87. Hassid, A. and Dunn, M.J. (1980) J. Biol. Chem. 255, 2472-2475.

88. Needleman, P., Bronson, S.D., Wyche, A., Sivakoff, M., and Nicolaou, K.C. (1978) J. Clin. Invest. 61, 839-849.

89. Ally, A.I. and Horrobin, D.F. (1980) Prostaglandins Med. 4, 431-438.

90. Morrison, A.R., Nishikawa, K., and Needleman, P. (1977) Nature (London) 267, 259-260.

91. Lee, S.C., Pong, S.S., Katzen, D., Wu, K.Y., and Levine, L. (1975) Biochemistry 14, 142-145.

92. Nissen, H.M. and Andersen, H. (1968) Histichemie 14, 189-194.

93. Frolich, J.C., Hollifield, J.W., Michelakis, A.M., Vesper, B.S., Wilson, J.P., Shand, D.G., Seyberth, H.J., Frolich, W.H., and Oates, J.A. (1979) Circulation Res. 44, 781-787.

94. Gerber, J.G., Keller, R.T., and Nies, A.S. (1979) Circulation Res. <u>44</u>, 796-799.

95. Dunn, M.J. and Hood, V.L. (1977) Am. J. Physiol. <u>233</u>, F169-F184.

96. Stokes, J.B. and Kokko, J.P. (1977) J. Clin. Invest. <u>59</u>, 1099-1104.

97. Jamison, R.L., Sonnenberg, H., and Stein, J.H. (1979) Am. J. Physiol. <u>237</u>, F247-F261.

98. Rocha, A.S. and Kokko, J.P. (1974) Kidney Int. <u>6</u>, 379-387.

99. Handler, J.S. and Orloff, J. (1981) Ann. Rev. Physiol. <u>43</u>, 611-624.

100. Nimmo, H.G. and Cohen, P. (1977) Adv. Cyclic Nucleotide Res. <u>8</u>, 145-266.

101. Strewler, G.J. and Orloff, J. (1977) Adv. Cyclic Nucleotide Res. <u>8</u>, 331-361.

102. Zambraski, E. and Dunn, M.J. (1979) Am. J. Physiol. <u>236</u>, F552-F558.

103. Fejes-Toth, G., Magyar, A., and Walter, J. (1977) Am. J. Physiol. <u>232</u>, F416-F423.

104. Anderson, R., Berl, T., McDonald, K., and Schrier, R. (1975) J. Clin. Invest. <u>56</u>, 420-426.

105. Kramer, H., Backer, A., Hinzen, S., and Dusing, R. (1978) Prostaglandins Med. <u>1</u>, 341-349.

106. Berl, T., Ray, A., Wald, H., Horowitz, J., and Czaczkes, W. (1977) Am. J. Physiol. <u>232</u>, F529-F537.

107. Levison, S. and Levison, M. (1978) J. Lab Clin. Med. <u>92</u>, 570-576.

108. Lum, G.M., Aisenberg, G.A., Dunn, M.J., Berl, T., Schrier, R.W., and McDonald, K.M. (1977) J. Clin. Invest. <u>59</u>, 8-13.

109. Ozer, A. and Sharp, G. (1972) Am. J. Physiol. <u>222</u>, 674-680.

110. Block, L.H., Locher, R., Tenschert, W., Siegenthaler, W., Hofmann, T., Mettler, R., and Vetter, W. (1981) J. Clin. Invest. <u>68</u>, 374-381.

111. Locher, R., Vetter, W., and Block, L.H. (1983) J. Clin. Invest. <u>71</u>, 884-891.

150

112. Marumo, F. and Edelman, I. (1971) J. Clin. Invest. 50, 1613-1620.

113. Beck, N., Kaneko, T., Zor, V., Field, J., and Davis, B. (1971) J. Clin. Invest. 50, 2461-2465.

114. Herman, C., Zenser, T., and Davis, B. (1979) Biochim. Biophys. Acta 582, 496-503.

115. Birnbaumer, L. and Yang, P. (1974) J. Biol. Chem. 249, 7848-7856.

116. Zenser, T. and Davis, B. (1977) Prostaglandins 14, 437-447.

117. Beck, T.R. and Dunn, M.J. (1981) Mineral Electrolyte Metab. 6, 46-59.

118. Galfre, G., Howe, S.C., Milstein, C., Butcher, G.W., and Howard, J.C. (1977) Nature (London) 266, 550-552.

119. Shulman, M., Wilde, C.D., and Kohler, G. (1978) Nature (London) 276, 269-270.

120. Cotton, R., Secher, D., and Milstein, C. (1973) Eur. J. Immunol. 3, 135-140.

121. DeWitt, D.L., Rollins, T.E., Day, J.S., Gauger, J.A., and Smith, W.L. (1981) J. Biol. Chem. 256, 10375-10382.

122. Medgyesi, G.A., Fust, G., Gergely, J., and Bazin, H. (1978) Immunochemistry 15, 125-129.

123. Lowry, O.H., Rosebrough, N.H., Farr, A.L., and Randall, R.J. (1951) J. Biol. Chem. 193, 265-275.

124. Steel, R.G.D. and Torrie, J.H. (1980) Principles and Procedures of Statistics, New York, McGraw-Hill.

125. Bancroft, J.D. (1975) Histochemical Techniques, London, Butterworth, pp. 278-290.

126. Kriz, W. (1981) Am. J. Physiol. 241, R3-R16.

127. Spargo, B.H. (1966) The Kidney (Mostofi, F.K. and Smith, D.E., Eds.), Baltimore, Williams and Wilkins, pp. 17-59.

128. Forster, R.P. (1961) In The Cell: Specialized Cells (Brackett, J. and Mirsky, A.E., Eds.), New York, Academic Press, Vol. 5, Part 2, pp. 89-161.

129. Jefferson, D.M., Brown, J.A. Jr., Zadumaisky, J.A., and Scott, W.N. (1982; Abstract). Federation Proc. 41, 1266.

130. Morel, F. (1981) Am. J. Physiol. 240, F159-F164.

131. Torikai, S. and Kurokawa, K. (1981) Prostaglandins 21, 427-438.

132. Wysocki, L.J. and Sato, V.L. (1978) Proc. Natl. Acad. Sci. USA 75, 2844-2848.

133. Chan, S. and Silverman, M. (1977) Kidney Int. 11, 348-356.

134. Herzlinger, D.A., Easton, T.G., and Ojakian, G.K. (1982) J. Cell Biol. 93, 269-277.

135. Allen, M.L., Garcia-Perez, A., and Smith, W.L. (1982; Abstract). Federation Proc. 41, 1693.

136. Savoy-Moore, R.T., Carretero, O.A., and Scicli, A.C. (1984; Abstract). Federation Proc. 43, 359.

137. Holt, W.F. and Lechene, C. (1981) Am. J. Physiol. 241, F452-F460.

138. Stokes, J.B. (1979; Abstract). Kidney Int. 16, 839.

139. Hassid, A. (1981) Prostaglandins 21, 985-1001.

140. Iino, Y. and Imai, M. (1978) Pflugers Arch. 373, 125-132.

141. Iino, Y. and Brenner, B.M. (1981) Prostaglandins 22, 715-721.

142. Powell, W.S. (1982) Meth. Enz. 86, 467-477.

143. Adler, E.M., Fluk, L.J., Mullin, J.M., and Kleinzeller, A. (1982) Science 217, 851-853.

144. Pugliese, F., Sato, M., Williams, S., Aikawa, M., Hassid, A., and Dunn, M.J. (1983) In Advances in Prostaglandin, Thromboxane and Leukotriene Research (Samuelsson, B., Paoletti, R., and Ramwell, P., Eds.), Vol. 11, New York, Raven Press, pp. 517-523.

145. Cereijido, M., Robbins, E.S., Dolan, W.J., Rotrinno, C.A., and Sabatini, D.D. (1978) J. Cell Biol. 77, 853-880.

146. Frolich, J.C., Williams, W.M., Sweetman, B.J., Smigel, M., Carr, K., Hollifield, J.W., Fleischer, S., Nies, A.S., Frisk-Holmberg, M., and Oates, J.A. (1976) In Advances in Prostaglandin and Thromboxane Research (Samuelsson, B. and Paoletti, R., Eds.), Vol. 1, New York, Raven Press, pp. 65-80.

147. Dunn, M.J., Greely, H.P., Valtin, H., Kinter, L.B., and Beeuwkes, R. III (1978) Am. J. Physiol. 235, E624-E627.

148. Dunn, M.J., Kinter, L.B., Shier, D., and Beeuwkes, R. III (1980; Abstract). Clin. Res. <u>27</u>, 496A.

149. Zusman, R.M. (1981) Ann Rev. Med. <u>32</u>, 359-374.

150. Kirschenbaum, M.A. and Serros, E.R. (1980) Am. J. Physiol. <u>238</u>, F107-F111.

151. McGiff, J.C., Itskovitz, H.D., Terragno, A., and Wong, P.Y.-K. (1976) Federation Proc. <u>35</u>, 175-180.

152. Chao, J. and Margolius, H.S. (1979) Biochim. Biophys. Acta <u>570</u>, 330-340.

153. Carretero, O.A. and Scicli, A.G. (1980) Am. J. Physiol. <u>238</u>, F247-F255.

154. Schuster, V.L., Kokko, J.P., and Jacobson, H.R. (!983; Abstract). Proc. Am. Soc. Nephrology, 178A.

155. Hansen, H.S. (1981) Lipids <u>16</u>, 849-854.

156. Torikai, S. and Kurokawa, K. (1983) Am. J. Physiol. <u>245</u>, F58-F66.

157. Edwards, R.M., Jackson, B.A., and Dousa, T.P. (1981) Am. J. Physiol. <u>240</u>, F311-F318.

158. Anderson, W.B., Johnson, G.S., and Pastan, I. (1973) Proc. Natl. Acad. Sci. USA <u>70</u>, 1055-1059.

159. Clark, R.b. and Butcher, R.W. (1979) J. Biol. Chem. <u>254</u>, 9373-9378.

160. Kassis, S. and Fishman, P.H. (1982) J. Biol. Chem. <u>257</u>, 5312-5318.

161. Malmsten, C., Granstrom, E., and Samuelsson, B. (1976) Biochem. Biophys. Res. Commun. <u>68</u>, 569-576.

162. Minkes, M., Stanford, N., Chi, M.M.Y., Roth, G.J., Raz, A., Needleman, P., and Majerus, P.W. (1977) J. Clin. Invest. <u>59</u>, 449-464.

163. Hassid, A. (1983) Am. J. Physiol. <u>244</u>, C369-C376.

164. Garrity, M.J., Westcott, K.R., Eggerman, T.L., Andersen, N.H., Storm, D.R., and Robertson, R.P. (1983) Am. J. Physiol. <u>244</u>, E367-E372.